ABSTRACT

Title of Dissertation: *RV3165C* AND *RV3167C* ARE TWO NOVEL ANTI-APOPTOTIC GENES OF *MYCOBACTERIUM TUBERCULOSIS*

Serdar Abidin Gurses, Doctor of Philosophy, 2012

Dissertation Directed By: Associate Professor Volker Briken
Department of Cell Biology and Molecular Genetics

Tuberculosis continues to kill close to two million people every year. This is due to the ease with which the bacteria spreads, the ineffectiveness of the vaccine currently in use, as well as the long drug regimen that is required for treatment of the disease. In order to develop new vaccines or drugs which require shorter treatment regimens, it is important to understand the interaction of the immune system with *Mycobacterium tuberculosis* (Mtb). One of the mechanisms by which Mtb is thought to survive in the human host is the inhibition of the apoptosis of infected cells. I was able to identify *Rv3165c* and *Rv3167c* as two novel anti-apoptotic genes of Mtb. Mtb knock-outs lacking *Rv3165c* or *Rv3167c* (Δ*Rv3165c*, Δ*Rv3167c*) failed to inhibit apoptosis of infected macrophages and the apoptosis of infected macrophages depended on caspase-8 and 3. Inhibiting reactive oxygen species (ROS) production or scavenging ROS inhibited the

apoptosis of Δ*Rv3165c* or Δ*Rv3167c* infected macrophages. Δ*Rv3165c* and Δ*Rv3167c* failed to upregulate the expression of the only catalase of Mtb, *katG*. Therefore, it seems that Mtb needs to upregulate *katG* expression in order to neutralize host cell produced ROS to inhibit apoptosis. Rv3165c was found to reside mainly in the cell envelope while Rv3167c, which is predicted to be a probable transcriptional regulator, was found exclusively in the cytosol of mycobacteria. *Rv3165c* was required for the upregulation of *Rv3167c* expression. These data led to a working model in which Rv3165c sits in the plasma membrane of Mtb and detects a signal while Mtb is in the phagosome. This signal detection results in upregulation of *Rv3167c* expression. Increased *Rv3167c* expression enables Rv3167c to change the expression of Mtb genes like *katG*. Rv3167c upregulates expression of anti-apoptotic genes and downregulates the expression of pro-apoptotic genes. RNA sequencing and antibody microarray experiments identified the host cell components that are differentially regulated in Δ*Rv3167c* infected cells compared to Mtb infected cells. Validation of these targets will help find the host cell pathways Mtb manipulates to inhibit host cell apoptosis.

RV3165C AND *RV3167C* ARE TWO NOVEL ANTI-APOPTOTIC GENES OF *MYCOBACTERIUM TUBERCULOSIS*

By

Serdar Abidin Gurses

Dissertation submitted to the Faculty of the Graduate School of the
University of Maryland, College Park in partial fulfillment
Of the requirements for the degree of
Doctor of Philosophy
2012

Advisory Committee:

Professor Volker Briken, PhD, Chair
Professor David Mosser, PhD
Professor Kenneth Frauwirth, PhD
Professor Ian Mather, PhD
Professor Philip DeShong, ScD

DEDICATION

I dedicate this dissertation to

My family

ACKNOWLEDGEMENTS

I would like to thank Dr.Volker Briken for entrusting me with my current research project and guiding me through it. I would also like to thank my committee members Dr. David Mosser, Dr. Kenneth Frauwirth, Dr. Ian Mather, and Dr. Philip DeShong for their time and support. I would like to thank the previous members of the Briken lab, especially Dr. Kamalkannan Velmurugan and Dr. Jessica Miller for teaching me so many techniques and methods in the lab. I would like to thank all the current members of the Briken lab: Amro, Ben, Gaya, Hanna, Jeff, Lalitha, Swati for being there when I needed them.

TABLE OF CONTENTS

LIST OF FIGURES

LIST OF ABBREVIATIONS

AP – Alkaline phosphatase
ASK1 – Apoptosis signal-regulating kinase
ATP – Adenosine triphosphate
BAK – Bcl-2 homologous antagonist/killer
BAX – Bcl-2-associated X protein
BCG – Bacillus Calmette-Guérin
BCL-2 – B-cell lymphoma 2 protein
BFL1 - Bcl-2-related gene expressed in fetal liver
BID – BH3-interacting domain death agonist
BMDM – Bone marrow derived macrophage
cAMP – Cyclic adenosine monophosphate
CBA – Cytometric bead array
CCL – C-C motif chemokine
CD – Cluster of differentiation
CD4+ T cells – Helper T cells
CD8+ T cells – Cytotoxic T cells
CE – Cell envelope
CF – Culture filtrate
CFP – Culture filtrate protein
CFU – Colony forming units
CR – Complement receptor
DC – Dendritic cell
DED – Death effector domain
DPI – Diphenylene iodonium
DUOX – Dual oxidase
ELISA – Enzyme linked immunosorbent assay
FADD – Fas-associated death domain
FAP – Fibronectin attachment protein
FCS – Fetal calf serum
FLICA – Fluorescent-Labeled Inhibitor of Caspases
FPKM – Fragment per kilobase of transcript per million mapped reads
IL – Interleukin
iNOS – Inducible nitric oxide synthase
LAM – Lipoarabinomannan
ManLAM – Mannose capped LAM
MAP – Mitogen activated protein
MAPK – MAP kinase
MDR – Multi-drug resistant
MHC – Major histocompatibility complex
MKK – MAP kinase kinase
MNC – Mononuclear cell
MOI – Multiplicity of infection
Mtb – Mycobacterium tuberculosis
Myd88 – Myeloid differentiation primary response protein

NADH – Nicotinamide adenine dinucleotide
NADPH – Nicotinamide adenine dinucleotide phosphate
NF-κB – Nuclear factor-κB
NLR – Nucleotide binding domain, leucine rich repeat containing
NOD – Nucleotide binding oligomerization domain containing
NOX – NADPH oxidase
PAMP – Pathogen associated molecular patterns
PBS – Phosphate buffered saline
PBST – PBS-tween
PknE – Protein kinase E
PknG – Protein kinase G
PMA – Phorbol 12-myristate 13-acetate
pNPP – p-Nitrophenyl Phosphate
RD – Region of difference
ROS – Reactive oxygen species
SECA2 – Protein translocase ATPase
SCID – Severe combined immunodeficiency
SOD – Superoxide dismutase
SODD – Silencer of death domains
TB – Tuberculosis
Th1 – CD4+ T helper cell type 1
Th2 – CD4+ T helper cell type 2
TLR – Toll like receptors
TM – Transmembrane
TMHMM – Transmembrane hidden Markov Model
TNF-α – Tumor necrosis factor alpha
TNFR – TNF-α receptor
TRADD – TNFR-associated death domain
TRAF – TNF-α receptor-associated factor
TUNEL – Terminal deoxynucleotidyl transferase dUTP nick end labeling
WT – Wild type
XDR – Extensively-drug resistant

CHAPTER 1 INTRODUCTION

1.1 TUBERCULOSIS

Tuberculosis (TB) is an infectious disease caused by the bacterium *Mycobacterium tuberculosis* (Mtb). One third of the world's population is currently infected with Mtb, but only 3-15 % of the infected individuals develop the disease in their lifetime (1, 2). There were nearly 8.8 million new cases of tuberculosis and an estimated 1.4 million people died of tuberculosis in 2010 (3) (Figure 1). People who do not develop the disease but still carry live Mtb are said to have latent TB. This latent TB can turn into active TB following a weakening of the immune system (3, 4). Although the tuberculosis death rate and the number of deaths are declining, the rate of this decline is very slow. Another significant statistic is that among women between the ages of 15-44, tuberculosis is among the three major causes of death (3).

TB is spread via aerosols formed when an infected person coughs or sneezes. A single bacterium is thought to be enough to cause an infection. When an uninfected person inhales droplets carrying Mtb the bacteria gain access to the lung where they are phagocytosed by alveolar macrophages through recognition by receptors on their surfaces. While Mtb is replicating in the alveolar macrophages the macrophages move to the underlying epithelial layer (1). Meanwhile Mtb or dendritic cells (DC) containing Mtb antigens move to the lymph nodes in the lung. These DCs can then activate $CD4^+$ T cells in the lymph nodes. Activated $CD4^+$ T cells then move to the sites of infection in the lung to recruit and activate macrophages (5, 6). Blood vessel development increases (via increased vascular endothelial growth factor), which helps macrophage recruitment (7, 8). The recruited macrophages, monocytes and neutrophils surround the infected

	POPULATION	MORTALITY[b]			PREVALENCE			INCIDENCE		
		BEST[c]	LOW	HIGH	BEST	LOW	HIGH	BEST	LOW	HIGH
Afghanistan	31 412	12	8.6	16	110	51	180	59	49	71
Bangladesh	148 692	64	47	85	610	280	1 000	330	270	400
Brazil	194 946	5.0	3.1	8.3	92	34	160	85	70	100
Cambodia	14 138	8.6	6.2	12	93	42	150	62	53	72
China	1 341 335	54	52	56	1 500	1 300	1 700	1 000	910	1 200
DR Congo	65 966	36	27	45	350	160	560	220	190	250
Ethiopia	82 950	29	23	35	330	140	520	220	200	230
India[d]	1 224 614	320	210	470	3 100	2 000	4 600	2 300	2 000	2 500
Indonesia	239 871	64	42	91	690	300	1 200	450	370	540
Kenya	40 513	6.9	4.9	9.4	110	49	180	120	120	130
Mozambique	23 391	11	7.0	17	110	54	200	130	87	170
Myanmar	47 963	20	12	31	250	180	310	180	160	210
Nigeria	158 423	33	11	68	320	110	690	210	99	360
Pakistan	173 593	58	39	84	630	270	1 100	400	330	480
Philippines	93 261	31	21	43	470	410	530	260	210	310
Russian Federation	142 958	26	16	42	190	70	330	150	130	180
South Africa	50 133	25	16	38	400	180	630	490	400	590
Thailand	69 122	11	7.0	16	130	55	210	94	78	110
Uganda	33 425	5.1	3.3	7.3	64	32	100	70	56	85
UR Tanzania	44 841	5.8	4.7	6.9	82	39	130	79	75	85
Viet Nam	87 848	29	19	43	290	130	510	180	130	220
Zimbabwe	12 571	3.4	2.1	5.1	51	23	80	80	61	100
High-burden countries	**4 321 967**	**860**	**730**	**1 000**	**10 000**	**8 500**	**12 000**	**7 200**	**6 800**	**7 500**
AFR	836 970	250	220	280	2 800	2 300	3 300	2 300	2 100	2 500
AMR	933 447	20	17	23	330	260	410	270	250	280
EMR	596 747	95	74	120	1 000	670	1 500	650	580	730
EUR	896 480	61	48	75	560	430	720	420	390	450
SEAR	1 807 594	500	370	640	5 000	3 700	6 500	3 500	3 200	3 700
WPR	1 798 335	130	120	150	2 500	2 200	2 800	1 700	1 500	1 800
Global	**6 869 573**	**1 100**	**920**	**1 200**	**12 000**	**11 000**	**14 000**	**8 800**	**8 500**	**9 200**

Figure 1: Estimated epidemiological burden of TB in 2010.
Numbers in thousands[a].
– indicates no estimate available.
[a] Numbers for mortality, prevalence and incidence shown to two significant figures.
[b] Mortality excludes deaths among HIV-positive TB cases. Deaths among HIV-positive TB cases are classified as HIV deaths.
[c] Best, low and high indicate the point estimate and lower and upper bounds of the 95% uncertainty interval.
[d] Estimates for India have not yet been officially approved by the Ministry of Health & Family Welfare, Government of India and should therefore be considered provisional.
Adapted from (3).

macrophages to form a granuloma. Macrophages can then differentiate into multi-nucleated giant cells, epithelioid cells, and foamy macrophages. Lymphocytes and a fibrous cuff surround the granuloma (1, 8, 9).

Two to three weeks after infection the mycobacteria are contained and the number of mycobacteria stabilizes. The number of blood vessels entering the granuloma decreases. This helps decrease the levels of oxygen in the center of the granuloma in which the mycobacteria are contained, thus helping to prevent their replication (1). If the immune system of the host is compromised during latent TB, (e.g., because of a decrease in TNF-α secretion) the granuloma can exhibit caseous necrosis and will eventually cavitate. The mycobacteria within the granuloma then can enter the airways of the lungs and can be transmitted from the infected person to others (4) (Figure 2). Since formation of the granuloma and its later disintegration provides a mechanism to keep Mtb alive and then to be transmitted, granuloma formation is suggested to be beneficial for the Mtb (10). When TNF-α was neutralized in mice with chronic infection, they could not maintain granulomas, the number of bacteria increased 10 fold and the mice survived less than 120 days while the control mice lived more than 6 months (11). These data show the importance of TNF-α for the survival of the host.

In the mouse model, following infection the number of Mtb increases in a logarithmic fashion until 3-4 weeks and then reaches a stationary level. The leveling of the number of Mtb is thought to be due to the onset of adaptive immunity. However, even the immunocompetent mice strains succumb to TB (4). Mtb that has been delivered to the lungs of the mice can disseminate to the liver and spleen as early as 11 days. The numbers of Mtb in these organs increase and reach a stationary level, which is typically

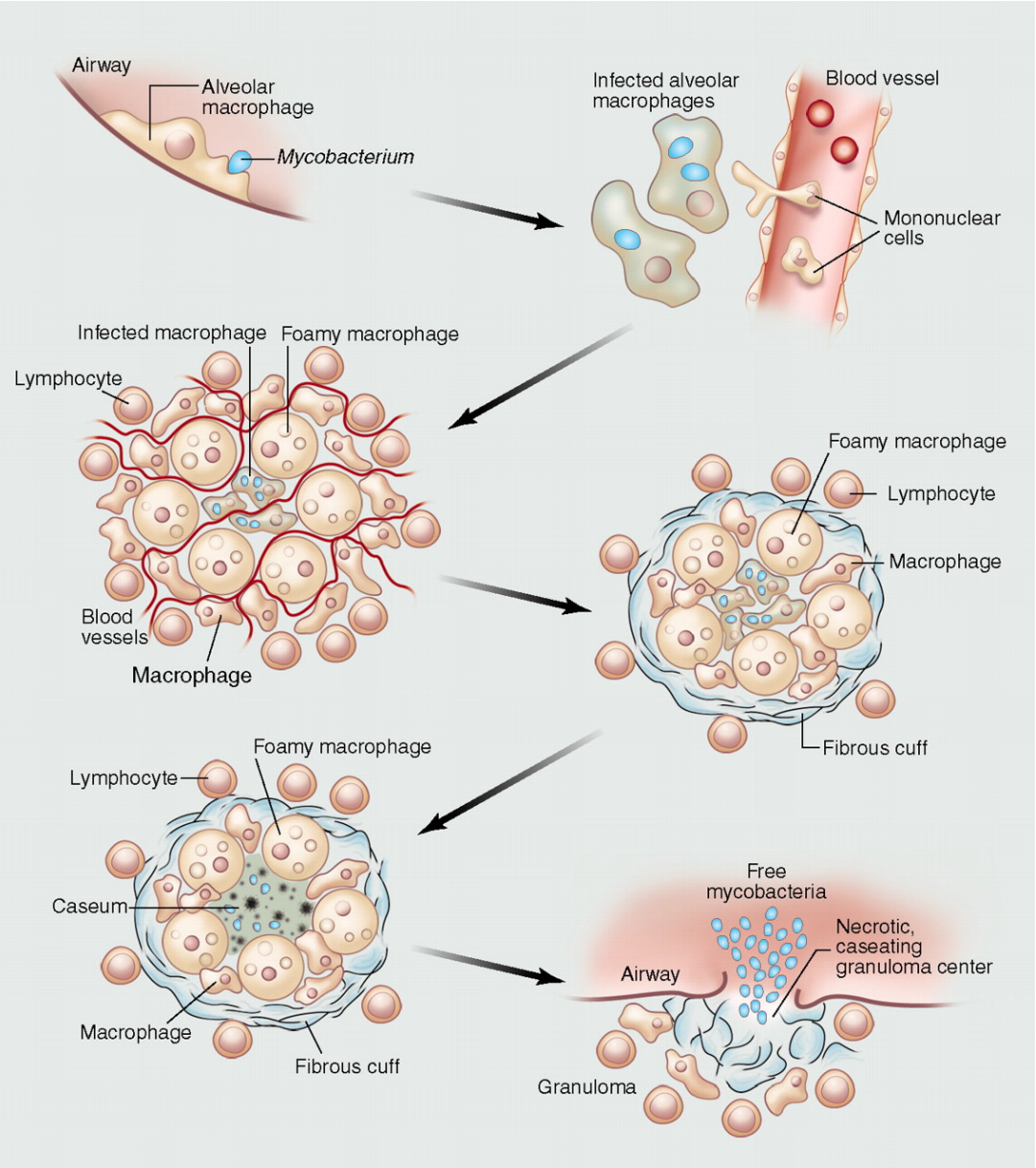

Figure 2: Transmission cycle of Mtb. Live Mtb is inhaled into the lungs where it is phagocytosed by alveolar macrophages. The infected macrophages travel into the epithelial layer. Blood vessels start to develop around the infected cells and more macrophages are recruited. The recruited macrophages, monocytes and neutrophils surround the infected macrophages to form a granuloma. Macrophages can then differentiate into multi-nucleated giant cells, epithelioid cells, and foamy macrophages. Upon weakening of the immune system the granuloma can exhibit caseous necrosis and will eventually cavitate. The mycobacteria within the granuloma then can enter the airways of the lungs and can be transmitted from the infected person to others. Adapted from (1).

lower than the number in the lungs (4, 12). Following aerosol infection of immunocompetent C57BL/6 mice Mtb infects different types of phagocytic cells in the lungs. Although it has been long believed that macrophages are the primary niche for Mtb, it has been reported that the highest percentage of Mtb infected cells in the lungs and the lymphoid nodes were myeloid dendritic cells (DC). The next highest infected cell population comprised recruited interstitial macrophages (6). Interestingly, the myeloid dendritic cells were among the poorest stimulators of Mtb specific $CD4^+$ T cells whereas alveolar macrophages were the best stimulators (6). Therefore not only macrophages but also other phagocytic cell types must be taken into consideration when trying to understand the immune response against Mtb.

1.1.1 Prevention of Tuberculosis

The vaccine currently in use against TB is *Mycobacterium bovis* Bacillus Calmette–Guérin (BCG), which was generated by passaging a strain of *M.bovis* for 13 years (between 1908 and 1921) on potato slices soaked in glycerol (13). After BCG was shown to be useful and safe as a vaccine, it was distributed to other countries which then maintained and passaged their own strains. For many years the reason for attenuation of BCG was not known. When the BCG genome was compared to the genome of parental strain *M.bovis*, several regions of difference were found (14–17) but only "region of difference 1" (RD1) was found to be lacking in all of the BCG strains (18, 19). RD1 contains 9 genes; *Rv3871*, *Rv3872* (*PE35*), *Rv3873* (*PPE68*), *Rv3874* (*esxB*), *Rv3875* (*esxA*), *Rv3876*, *Rv3877*, *Rv3878* and *Rv3879c*. These genes do not have any known functions except *esxB*, which encodes for the 10kDa culture filtrate protein (CFP10) and

esxA, which encodes for the 6kDa early secreted antigenic target (ESAT-6). Deletion of RD1 from Mtb leads to decrease in virulence and produces a phenotype similar to BCG, indicating the involvement of the RD1 genes in virulence of Mtb (20).

BCG is effective against the disseminated form of TB in children (21). However the efficacy of BCG in protecting adults from pulmonary TB varies from 0 - 80% and varies between countries (22). In developing countries the protection efficacy is the lowest. The variability of the protective efficacy of BCG might be due to geographical, environmental and genetic factors (22, 23). Interestingly, the protective efficacy of BCG is lower closer to the equator. One of the reasons for this is thought to be the increased concentration of ultraviolet radiation (UVR) towards the equator. The evidence for this comes from experiments in which exposure to UVR reduced the development of the immune response by BCG in mice (possibly due to increased IL-10 production) and BCG vaccinated guinea pigs had reduced resistance against Mtb if they were exposed to UVR before or after vaccination (24–26). Another reason is thought to be previous or simultaneous infection with parasites leading to a Th2 (Type II helper T cell) immune response that prevents an effective response against Mtb. A Th1 (Type I helper T cell) response is required to achieve immunity against Mtb, but the presence of a Th2 response increases the severity and the onset of the disease (27, 28). Therefore it is suggested that a successful vaccine would have to diminish the Th2 responses in addition to inducing Th1 responses (29). Prior exposure to live environmental mycobacteria greatly decreases the effectiveness of BCG. This is thought to be due to prevention of BCG multiplication and therefore production of a weak immune response (30). Pre-sensitization of guinea pigs

and mice with prior exposure to environmental mycobacteria leads to some protection against Mtb (31–33).

A different explanation for the variable effectiveness of BCG comes from the fact that the strains that each country received from Institut Pasteur were passaged many times. Studies have shown that the various strains that are used around the world have deletions, insertions and SNPs different from each other. On the basis of these differences BCG vaccines were divided into the early strains, represented by BCGs Japan, Birkhaug, Sweden, and Russia and the late strains, including BCGs Pasteur, Danish, Glaxo, and Prague. The major difference between the early and late strains is the lack of RD2 in the late strains (16, 17, 34, 35). A recent study showed that the late strains of BCG had more genetic variability than the early strains, when compared to the late strain BCG Pasteur. Referring to other research done, Brosch et al. suggests that the early BCG vaccine strains might have higher protective efficacy than the late strains (36).

In conclusion, the low efficacy of BCG in preventing tuberculosis has led researchers to try to develop new vaccines. The production of effective and low cost vaccines for use in areas affected most by tuberculosis is much needed and will save many lives. To achieve this goal a better understanding of failure of BCG and new strategies to produce effective vaccines are required.

1.1.2 Treatment of tuberculosis

The treatment of tuberculosis involves a six month minimum drug regimen involving 4 drugs, isoniazid, rifampin, pyrazinamide and ethambutol (37). Unfortunately strains of Mtb that are drug resistant have emerged through the years due to inconsistent

or inappropriate use of drugs. There are multi drug resistant (MDR) Mtb strains that are resistant to more than one of the major drugs against Mtb. The estimated number of MDR tuberculosis cases in 2010 was 650,000 and 150,000 deaths were caused by MDR tuberculosis in 2008 (3). According to estimates, 3.3% of all new tuberculosis cases were MDR tuberculosis in 2009. In 2010 in some areas of the world the percentage of MDR tuberculosis has been reported to be 28% of new tuberculosis cases (3). The patients who have MDR Mtb have to be treated with a second line of drugs that are not only more expensive but also can lead to more side effects in the patients. Treatment of MDR Mtb can last up to two years, which also increases the cost of the treatment. In addition to MDR Mtb, extensively drug resistant (XDR) Mtb strains have emerged. These strains are resistant to the second line of drugs as well as the first line. Fifty eight countries reported XDR tuberculosis cases (3). This evidence shows the requirement for improved and cheaper drugs as well as new vaccine strain(s) (38, 39).

1.1.3 *Mycobacterium tuberculosis*

Mtb is a rod shaped bacillus that has a length between 1-4µm and width between 0.3-0.6µm (40). In terms of replication time, mycobacteria are divided into slow growers (give colonies on solid media in more than 7 days) and fast growers (give colonies on solid media in less than 7 days). *M.tuberculosis* and *M.bovis* are slow growers. *M.fortuitum* and *M.smegmatis* are fast growers (41, 42). The mycobacterial colonies on solid media are usually rough, crinkled and white to cream colored (41). The replication time of Mtb is around 24 hrs *in vitro* and *in vivo* in the lungs of mice (43). The genome of Mtb is 4,411,529 bp and contains an estimated 4,000 genes. The genome has a high G+C

content of 65.6% (44). The Mtb genome contains many repetitive DNA sequences including duplicated housekeeping genes and insertion sequences (44). The cell envelope of Mtb consists of a cell membrane and a complex cell wall. The cell wall contains layers of peptidoglycan, arabinogalactan, mycolic acids and lipids on the outer part. There are lipoarabinomannans and phosphotidylinositol mannosides in the cell wall with their lipid moieties inserted in the cell membrane. Due to this complex cell wall, Mtb is resistant to many chemicals and therapeutic agents (45). Components of the Mtb cell wall are involved in diminishing the immune response (discussed below in 1.2.2). It has been shown that the outer cell wall, consisting of mycolic acids and lipids, actually forms a symmetrical lipid bilayer (46). It is because of this outer membrane that Mtb can not be Gram stained.

1.2 IMMUNE RESPONSE AND MYCOBACTERIA

1.2.1 Immune response to mycobacteria

Upon entering the human host, mycobacteria are phagocytosed by macrophages through recognition by surface receptors. Human monocyte complement receptors CR1 and CR3 are involved in the phagocytosis of Mtb. Complement component C3 in the serum binds to Mtb and is required for adherence of Mtb to human monocytes and heat inactivation of serum significantly reduces Mtb adherence to momocytes (47, 48). Mtb Erdman and H37Rv strains require the presence of mannose receptors on the macrophage surfaces for adherence (49). Lipoarabinomannan (LAM) of Mtb has been discovered as a ligand for the mannose receptor (50). Surfactant protein A (Sp-A), a collectin, increases

Mtb attachment to macrophages and its uptake but it is not required for an effective immune response against Mtb in a murine infection model (51–53).

Humans with active TB produce a Th1 response to Mtb and develop granulomas to contain the bacteria but cannot kill all the bacteria. However the Th1 responses in active TB patients help to restrict the replication and spread of Mtb. In AIDS patients Mtb cannot be contained in granulomas and the bacteria replicate and spread from the lungs to other organs due to decreased number of $CD4^+$ T cells and downregulation of the Th1 response (4, 54, 55).

Toll-like receptors (TLRs) are pattern recognition receptors (PARPs) which detect pathogen-associated molecular patterns (PAMPs). TLRs reside in the cell membrane and inside the cell, detect ligands and induce immune responses through induction of cytokines such as TNF-α, IL-1, IL-6 and IL-12. Upon PAMP recognition, TLRs form dimers. Through adaptors like myeloid differentiation primary response gene 88 (MyD88) and TRIF-related adaptor molecule (TRAM) they activate protein kinases like interleukin-1 receptor-associated kinase 1 (IRAK1), leading to changes in gene expression through NF-κB (56, 57).

TLR2 recognizes 19-kDA lipoprotein, lipomannan and phosphatidyl-myo-inositol mannoside of Mtb while TLR4 recognizes heat-labile components of the cell wall. The 19-kDa lipoprotein of Mtb induces apoptosis in macrophages through TLR2 in a caspase-8 dependent manner (58). Although TLR2 and TLR4 recognize many Mtb components and TLR2 knock-out mice show a 50-75% reduction in TNF-α production while TLR4 knock-out mice show a 30-40% reduction, TLR2 or TLR4 knock-out mice have little enhanced susceptibility to Mtb infection. (59). However mice lacking Myd88 (one of the

signal transducers for TLRs) were highly susceptible to Mtb infection (60). These data indicate potential involvements of other TLRs and/or other Myd88 dependent receptors in the immune response against Mtb.

Intracellular recognition of mycobacteria by host cells depends on intracellular proteins called NLRs (Nucleotide binding domain, leucine rich repeat containing) that include NODs (Nucleotide binding oligomerization domain containing). NLRs are involved in activation of caspase-1 that converts pro-IL-1β and pro-IL-18 to active IL-1β and IL-18 (57). NOD1 recognizes γ-D-glutamyl-meso-diaminopimelic acid (ie-DAP) from peptidoglycans of Gram negative bacteria and NOD2 recognizes muramyl dipeptide (MDP) from peptidoglycans from Gram negative and Gram positive bacteria. When peritoneal macrophages from NOD2 knock-out mice were infected with Mtb there was a 40 to 50% reduction in TNF-α production and a 20 to 25% reduction when peritoneal macrophages from NOD1 knock-out mice were used. Blocking the internalization of Mtb, which prevents its recognition by NODs also leads to a 40 to 50% decrease in TNF-α production. When mononuclear cells (MNCs) from patients defective for NOD2 were infected with Mtb there was a 65 to 80% reduction in TNF-α secretion. As another evidence for the synergistic interaction of TLRs and NLRs, it was shown that addition of TLR2 ligand 19-kDa lipoprotein together with NOD2 ligand MDP increased TNF-α production from MNCs much more than the total of the ligands by themselves (59).

While it was shown that macrophages and DCs lacking NOD2 were impaired in their ability to produce inflammatory cytokines (TNF-α and IL-12) and NO upon infection with Mtb, it was also found that NOD2 deficient mice were no more susceptible to Mtb infection than wild-type mice and had similar bacterial counts in the lungs up to 8

weeks after infection (61). However, it was also reported that NOD2 deficient mice have significantly higher bacterial counts by 6 months and succumb to death earlier than wild-type mice after Mtb infection (62). So, although in vitro NOD2 plays a role in cytokine production, especially synergistically with TLR2 it seems to be dispensable for the immune response against Mtb and the control of infection during the early stages of infection. In the case of TNF-α, depletion of TNF-α by a monoclonal antibody in C57BL/6 mice causes mice to succumb to death faster following infection with Mtb. Similarly, infection of C57BL/6 mice lacking TNF-α receptor with Mtb causes them to succumb to death faster (63). Therefore TNF-α is required for a successful immune response against Mtb in mice. The fact that NOD2 deficient mice are not more susceptible to Mtb during early stages of infection although NOD2 deficient macrophages produced significantly less TNF-α upon Mtb infection *in vitro* suggests two possibilities. One possibility is that even though TNF-α production by macrophages is also decreased *in vivo*, it is still enough for an effective immune response. The other possibility is that the *in vitro* result does not reflect conditions *in vivo* and NOD2 knock-out mice can produce similar levels of TNF-α in response to Mtb, at least during the early stages of infection. It is also possible that TNF-α production by another cell type in NOD2 knock-out mice is not affected and that is enough for the host response.

1.2.2 Prevention of phagosome maturation by Mtb

Mtb prevents the fusion of the phagosome with lysosomes and thus prevents phagosome maturation (64, 65). Pathogenic mycobacteria utilize different strategies to prevent the phagosome maturation in order to survive, replicate in the phagosome, cause

necrosis of the infected cells and disseminate (66, 67). The strategies adapted by pathogenic mycobacteria involve manipulation of the host cell signaling that leads to the fusion of the lysosome with the phagosome.

Coronin 1 is a protein identified in the membranes of phagosomes that contain live mycobacteria after infection of murine macrophages. Coronins are thought to be involved in the regulation of the actin cytosekeleton (68). When macrophages were infected with live mycobacteria, coronin 1 was present on phagosomes but when the macrophages were infected with dead mycobacteria, coronin 1 left the phagosomes, which was followed by the fusion of phagosomes with lysosomes and the degradation of the mycobacteria (69). Coronin 1 is dispensable for regulation of the actin cytoskeleton but activates the Ca^{2+}-dependent phosphatase calcineurin. Active calcineurin then blocks the fusion of phagosomes with lysosomes (70). Kupffer cells in the liver do not express coronin1. Following infection of Kupffer cells all mycobacteria were located in phagolysosomes and were then degraded. Expression of coronin 1 in a nonmacrophage cell line was sufficient to prevent lysosomal fusion of the mycobacterial phagosome, allowing survival of mycobacteria (69). These experiments showed the ability of mycobacteria to recruit coronin 1 to phagosomes to prevent their fusion with lysosomes.

Mannose capped lipoarabinomannan (ManLAM) of Mtb is a glycolipid that is a component of the Mtb cell wall. ManLAM from Mtb prevents phagosome maturation, probably by blocking the generation of phosphatidylinositol 3-phosphate (PI3P) and its recruitment to the phagosomal membrane (71–73). PI3P is involved in the recruitment and functioning of PI3P binding domain containing proteins that are involved in membrane trafficking and phagosome maturation (74). ManLAM also inhibits the

activation of mitogen-activated protein kinases (MAPK) in humans (75). MAPK activation elicits the synthesis of TNF-α and induction of iNOS (inducible nitric oxide synthase) (76–78). By blocking MAPK in monocytes, ManLAM prevents the production of TNF-α and nitric oxide. TNF-α is a major cytokine that promotes apoptosis in mycobacteria infected macrophages (79). These data indicate that the ManLAM of Mtb indirectly inhibits apoptosis. Pathogenic mycobacteria also have strategies to block the bactericidal effects of NO and the recruitment of the iNOS to the phagosome (80). Mtb uses its proteasome to defend itself against the destructive effects of NO and mutants with transposon insertions in proteasome associated genes are susceptible to acidified nitrite (81, 82).

Mycobacteria also have proteins that prevent phagosome maturation. One of them is the mycobacterial protein kinase G (*pknG*). A *pknG* knock-out of *Mycobacterium bovis* BCG colocalized with lysosomes and could not resist destruction by macrophages, unlike wild type *M.bovis* BCG. pknG was present in both the lumen of the phagosomes and the cytosol of the infected macrophages and inhibited phagosome lysosome fusion (83). The presence of pknG in the host cytosol suggests it might interefere with host cell signaling in order to prevent phagosome maturation. pknG autophosphorylates but this does not affect its kinase activity. Autophosphorylation of pknG prevents fusion of Mtb containing phagosomes with lysosomes (84). Expression of *PknG* in *M.smegmatis* increases the persistence of *M.smegmatis* in mice (85). *PknG* mutant of Mtb is less virulent in SCID mice (86). This evidence suggests that by preventing phagosome lysosome fusion, pknG increases the virulence of Mtb.

1.3 APOPTOSIS

Apoptosis is a form of programmed cell death, characterized by shrinkage of cytoplasm, condensation of chromatin, fragmentation of chromosomal DNA, formation of cell membrane blebs and formation of apoptotic bodies (87) (Figure 3). Apoptosis is the predominant method for the removal of unwanted cells in the immune and central nervous systems. Removal of certain cells during embryonic development or upon damage is also achieved through apoptosis (88). Apoptosis is preferred over necrosis in these situations because necrosis can damage other healthy cells and cause inflammation, whereas the apoptotic bodies that are formed are taken up by neighboring phagocytes and thus damage is prevented (89, 90). Certain mutations can lead to decreased levels of apoptosis and therefore promote survival of cancer cells (88). Mutations of caspase genes that inhibit their activity or downregulation of caspase gene expression are common in certain cancers (91, 92). On the other hand, flaws in the removal of apoptotic bodies can lead to autoimmune diseases (93).

Apoptosis is carried out by caspases, which are zymogenic proteases. They cleave various cellular substrates that in turn lead to the phenotypes seen during apoptosis (94, 95). There are two pathways for caspase activation, an extrinsic and an intrinsic pathway (88) (Figure 4). The extrinsic pathway involves the binding of ligands to cell surface receptors, which is followed by recruitment and binding of cellular proteins to the cytoplasmic side of the receptors, thus leading to activation of initiator caspases 2, 8, 9, and 10 and effector caspases 3, 6, and 7 (96, 97). TNF-α and Fas-L are two of the ligands which bind to their receptors, TNF-α receptor-1 (TNFR1) and Fas respectively, in this pathway (98). Both of these receptors have death domains on their cytoplasmic sides,

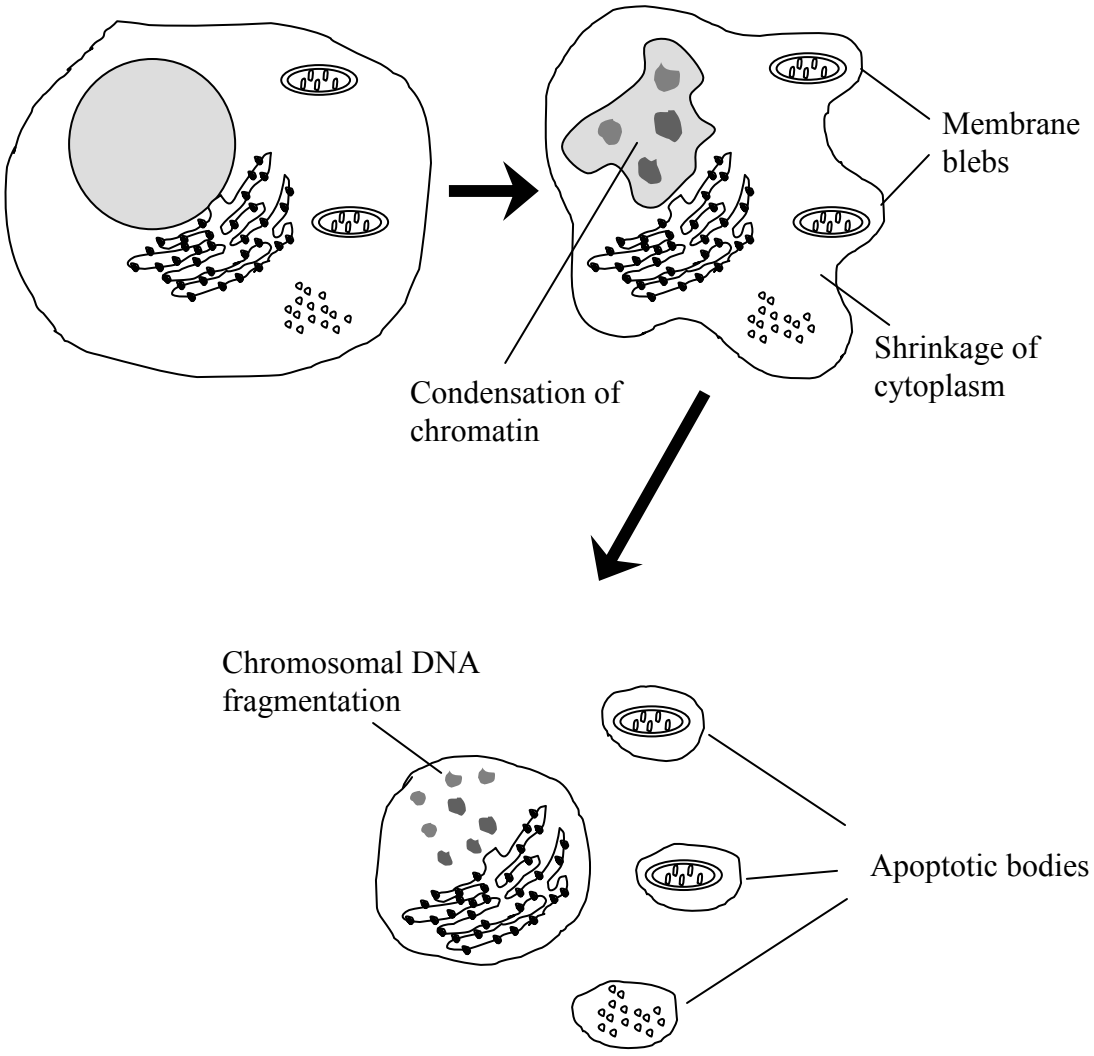

Figure 3: Apoptosis. Progression of apoptosis and its phenotypes.

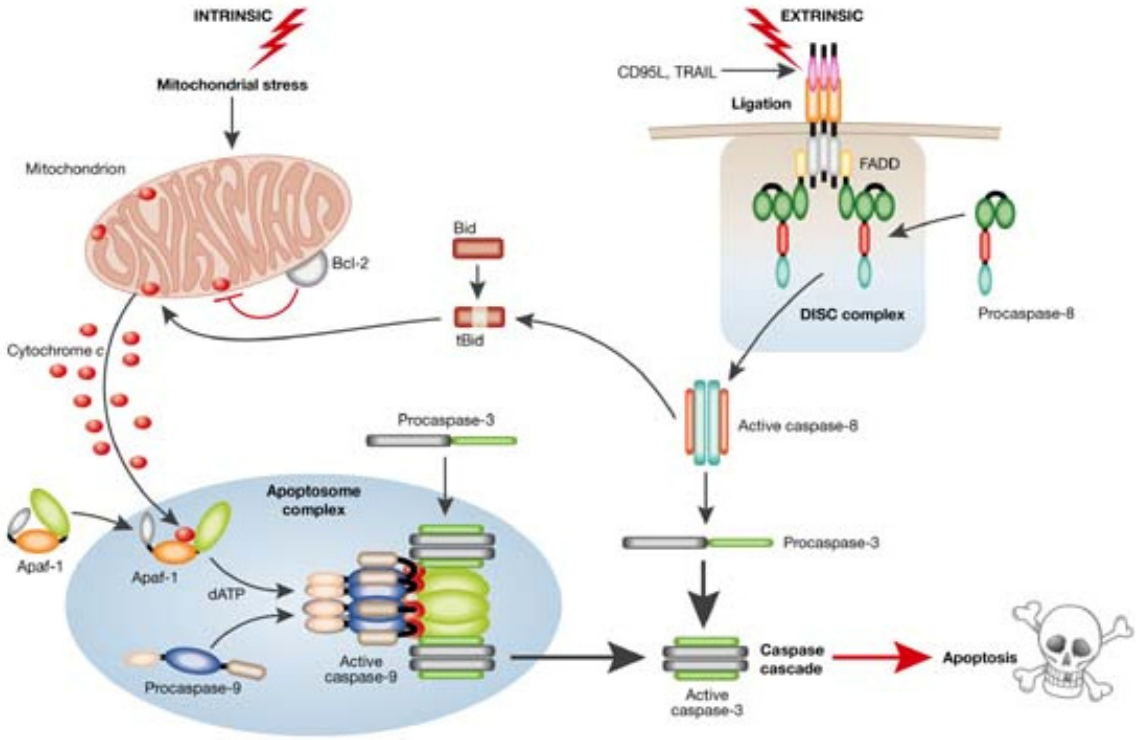

Figure 4: Extrinsic and intrinsic pathways of caspase activation. Adapted from (100).

which allow them to interact with other proteins that have death domains. TNFR1 interacts with TNFR-associated death domain (TRADD) and Fas interacts with Fas-associated death domain (FADD) (98). FADD has another domain called death effector domain (DED), which allows it to interact with caspase-8 (caspase-8 also has DED). This interaction causes the activation of caspase-8 which then leads to the activation of downstream caspases such as caspase-3 (87).

The TRADD that interacts with TNFR1 can also interact with FADD and lead to the activation of caspases (99). TRADD can also interact with RIP1 and TRAF2 to activate anti-apoptotic signals. TNF-α can interact with another receptor, TNFR2 and this interaction leads to activation of NF-κB, which leads to production of anti-apoptotic proteins (101). Fas can also interact with Daxx to activate it, which then activates apoptosis signal-regulating kinase 1 (ASK1). ASK1 is a MAPKKK that activates c-jun N-terminal kinase and p38 MAPK signaling pathways followed by apoptosis (102–104).

The intrinsic pathway of caspase activation involves the release of cytochrome c from the mitochondria after the permeabilization of its outer membrane upon apoptotic stimuli. The release of cytochrome c is regulated by the Bcl-2 protein family, some of which promote and some of which inhibit the release of cytochrome c (105). Depending on the cell type, cytochrome c is usually proapoptotic. The release of cytochrome c in some cases is required for events like cellular differentiation (106). The released cytochrome c, together with Apaf-1 and pro-casspase-9, forms a complex that has been called the apoptosome. The apoptosome then activates the downstream effector caspases (107, 108).

There is crosstalk present between the two caspase activation pathways. Caspase-8, which is a part of the extrinsic pathway can cleave and activate the protein Bid which is a Bcl-2 protein family member. The activation of Bid promotes the release of cytochrome c from mitochondria and activation of caspase-9 (108). Therefore it is possible to observe caspase-9 activation following extrinsic caspase activation.

1.3.1 Role of ROS in apoptosis

Reactive oxygen species (ROS) are used by the cells in both defense against pathogens and regulation of cell signaling (109–111). ROS are produced by mitochondria as well as Nox and Duox enzymes that are on the membrane, using NADPH and oxygen (112–114). As signaling molecules, ROS can induce prolonged JNK activation and TNF-α induced apoptosis in certain cells. As another strategy, NF-κB activation can be blocked by ROS and this prevents transcription of survival genes and promotes cell death (Figure 5) (115). ROS are able to inhibit the activity of some NF-κB activators since they contain specific cysteines that can be oxidized and lose their activity afterwards (110). Thus, increased levels of ROS promote apoptosis by inducing prolonged JNK activation and blocking NF-κB activation.

1.3.2 Apoptotic response to bacterial pathogens

Some pathogens induce apoptosis while others inhibit apoptosis. Pathogens can employ toxins and virulence factors for these purposes (116, 117). Pathogens also affect host cell apoptosis through manipulation of cell survival pathways that include NF-κB and MAPK. One of these pathogens is *Chlamydia pneumoniae*, which can activate NF-

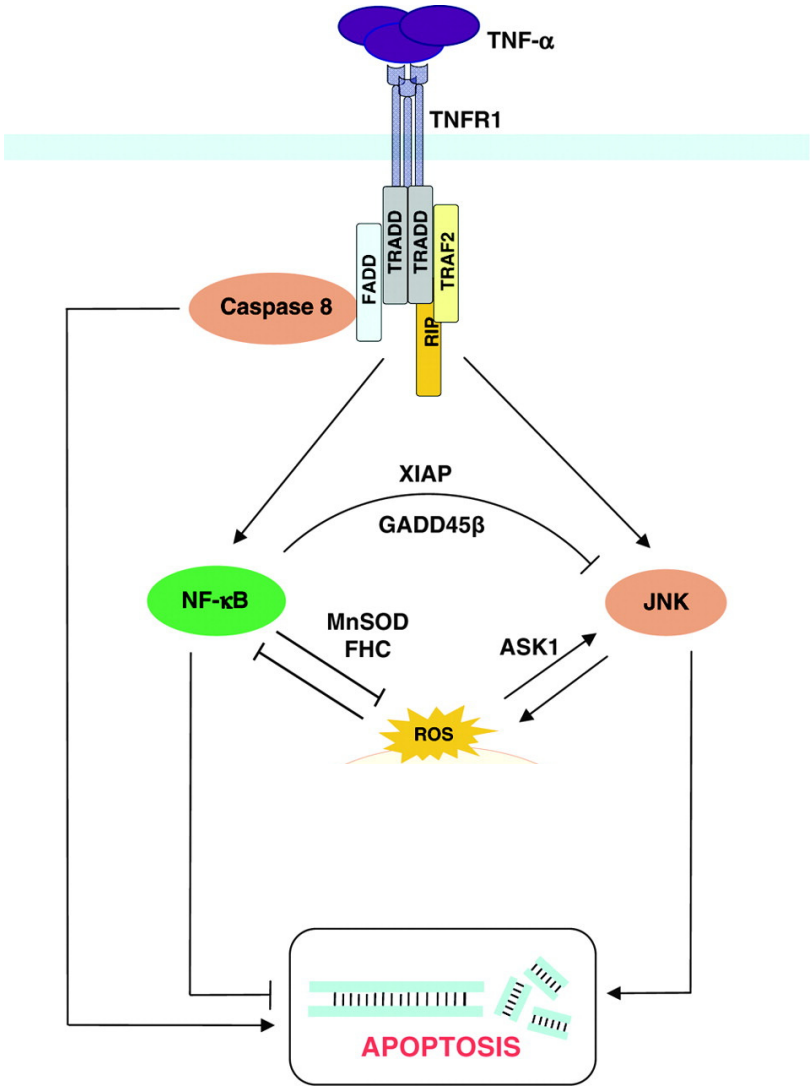

Figure 5: ROS mediates the balance between the pro-apoptotic and anti-apoptotic phenotypes induced by TNF-α. Increased levels of ROS can induce prolonged JNK activation that leads to apoptosis and blocks NF-κB activation to promote apoptosis. Adapted from (115).

κB to inhibit apoptosis. *Chlamydia* also inhibits apoptosis by preventing cytochrome c release and thus promotes its own survival (118, 119). *Chlamydia pneumoniae* causes an increase in expression of the anti-apoptotic host gene *mcl-1* in infected cells (120). *Rickettsia rickettsii* is another pathogen that inhibits host cell apoptosis by increasing NF-κB activation to promote its own survival. Inhibition of NF-κB activation in infected cells results in activation of caspases 8, 9 and 3, followed by an increase in apoptosis (121). *Salmonella typhimurium* uses its protein AvrA to inhibit apoptosis in macrophages (122). AvrA is a 33 kDa protein secreted by *Salmonella typhimurium* that has been characterized as an acetyltransferase that can inhibit JNK activation in host cells (123).

Yersinia pestis, *Yersinia enterocolitica*, and *Yersinia pseudotuberculosis* have plasmids that contain genes for a type III secretion system (TTSS) that is necessary for their virulence. TTSS is responsible for secretion of Yop proteins (124). YopJ of *Yersinia pseudotuberculosis* inhibits MAPK and NF-κB pathways, and induces apoptosis of infected macrophages (125–128). In the meantime, the actions of other Yop proteins affect the cell signaling network and the organization of the cytoskeleton host cell to prevent phagocytosis of the bacteria (124). These actions of YopJ and other Yop proteins are thought to help the survival of the bacteria by inhibiting the innate immune response of the host cells (128).

Bordetella pertussis, the bacterium that causes whooping cough, secretes many adhesins to attach to the host ciliated cells and toxins to cause lesions and host cell death after it arrives in the host respiratory tract (129). *Bordetella pertussis* induces apoptosis of J774A.1 cells and murine alveolar macrophages. This mechanism is thought to benefit *Bordetella pertussis* by eliminating macrophages that can kill it in the lungs so that it can

infect the epithelial cells and replicate. The pro-apoptotic phenotype of *Bordetella pertussis* depends on one of the secreted toxins, adenylate cyclase-hemolysin (AC-Hly) (130). AC-Hly consists of an adenylate cyclase domain and a pore-forming repeat in a toxin hemolysin domain. AC-Hly is secreted by a type I secretion mechanism (131). Upon entrance into the cell, the adeylate cyclase domain binds to calmodulin and is activated to catalyze the synthesis of cAMP from ATP (132). Increased amounts of cAMP disrupt cellular functions and induce apoptosis (130).

Streptococcus pneumoniae induces apoptosis of alveolar macrophages which leads to the clearance of the bacteria from the lungs. Inhibition of caspase activation in the *S. pneumoniae* infected host cells decreased the rate of apoptosis and inhibited the killing of *S. pneumoniae* (133). *S.pneumoniae* inhibits the upregulation of expression of the anti-apoptotic protein Mcl-1 and blockage of this inhibition results in decreased apoptosis and killing of *S.pneumoniae*. Infection of Mcl-1 transgenic mice with *S. pneumoniae* led to decreased apoptosis of alveolar macrophages and better survival of the bacteria compared to infection of nontransgenic mice (134).

As shown in the examples above, inhibition of apoptosis by bacterial pathogens promotes their survival and inhibition of the innate immune response. Inhibition of apoptosis is achieved by different strategies, including activation of NF-κB, inhibition of JNK activation and increasing expression of host anti-apoptotic proteins. Promotion of apoptosis is also employed by bacterial pathogens to remove cells that can kill them. Therefore, the outcome of apoptosis can be either beneficial or detrimental for the host.

1.4 APOPTOTIC RESPONSE TO MTB

Apoptosis of infected macrophages is suggested to be a way to eliminate suitable growth environments for Mtb (79, 135). Virulence of the mycobacterial strains has an inverse relationship with their ability to induce apoptosis. Virulent strains of mycobacteria, such as *M.tuberculosis* H37Rv, Erdman and *M.bovis* wild type were shown to induce significantly less apoptosis in macrophages than avirulent strains, including *M.tuberculosis* H37Ra, *M.bovis* BCG and *M. kansasii* (135, 136). The relatively high rate of apoptosis of macrophages by avirulent strains was not due to higher intracellular growth. On the contrary while the virulent strains increased in number, the avirulent strains decreased in number, which suggests that the apoptosis of macrophages may help decrease the number of intracellular mycobacteria (135). Induction of apoptosis by Fas ligand (FasL) aids in the killing of intracellular Mtb by human blood monocyte derived macrophages (137).

Inside the phagosomes of macrophages, the mycobacteria are safe from being presented to T cells through MHCI and CD1. Apoptosis is a way for the host to overcome this problem. Following apoptosis, the apoptotic blebs are taken up by uninfected macrophages and dendritic cells. The apoptotic blebs contain mycobacterial proteins and cell wall lipids (138). The dendritic cells that have taken up the apoptotic blebs then present the enclosed mycobacterial antigens to $CD8^+$ T cells via MHCI and CD1. This pathway of cross-presentation leads to the activation of $CD8^+$ T cells (138–140). $CD8^+$ T cells are important in the immune response against Mtb as mice lacking $CD8^+$ T cells are more susceptible to infection with Mtb. $CD8^+$ T cells are also responsible for macrophage activation via production of IFN-γ and killing of mycobacteria infected cells (138, 141).

Vaccination of mice with apoptotic blebs from mycobacteria-infected macrophages was also shown to protect against tuberculosis (140).

1.4.1 Inhibition of apoptosis by Mtb

Mtb can inhibit apoptosis that is induced by other factors. FasL by itself is enough to induce apoptosis in macrophages. It was shown that when Mtb infected macrophages were treated with FasL the percentage of apoptotic cells had decreased compared to uninfected cells. It was also found that in Mtb infected macrophages, the expression of Fas on the surface is down regulated, which can explain the decrease in apoptosis following FasL treatment (137).

TNF-α can also induce apoptosis. Infection of macrophages with both virulent and avirulent Mtb were shown to induce TNF-α secretion from the cells. However, infection with virulent Mtb also led to production of soluble TNF-α receptor 2 (sTNFR2) (142). This process can decrease the amount of TNF-α interacting with TNFR, which would lead to inhibition of apoptosis of Mtb infected cells.

Infection of cells with mycobacteria results in the up-regulation of anti-apoptotic genes of the Bcl-2 family, such as *mcl-1* (143) and *bfl-1* (144). Reducing Mcl-1 protein expression in the infected cells by using antisense oligonucleotides leads to an increase in apoptosis of the cells infected with virulent Mtb. Reducing Mcl-1 amount also leads to decreased survival of virulent Mtb inside the cells (143). In mice, after infection with Mtb, the expression of the anti-apoptotic gene *bcl-2* increased, whereas the expression of pro-apoptotic gene *bax* decreased (145). BCG infection can inhibit *S*-nitroso-*N*-acetylpenicillamine induced apoptosis in macrophages from wild type mice by more than

50% but cannot inhibit apoptosis induced in macrophages from A1 knock-out mice, which lack the anti-apoptotic gene *bfl-1* (144). These data show that mycobacteria can manipulate regulation of both the host genes and proteins to increase anti-apoptotic gene expression and/or decrease pro-apoptotic gene expression in order to inhibit apoptosis and thus survive inside the host cell. Since it was shown that avirulent mycobacteria induced more apoptosis, these strains would be expected to lead to higher cellular immunity via cross-presentation to $CD8^+$ T cells. Production of new avirulent vaccine strains of mycobacteria that induce high levels of apoptosis can be achieved by identification of mycobacterial anti-apoptotic genes that are responsible for inhibition of apoptosis in host cells. Identification of anti-apoptotic mycobacterial genes can also reveal new targets for the use of antimycobacterial compounds.

1.4.2 Anti-apoptotic genes of Mtb

Previous work by our group and others has identified several anti-apoptotic genes of Mtb. *nuoG* (encodes NuoG subunit of the type I NADH (nicotinamide adenine dinucleotide)-dehydrogenase of Mtb), *secA2* (encodes a protein required for the secretion of superoxide dismutase A [SodA], Alpha-crystallin [Acr] and Rv0390) and *pknE* (protein kinase E, a serine threonine protein kinase) genes are required for inhibition of apoptosis by Mtb (146–148). NuoG inhibits the accumulation of phagosomal ROS, prevents an increase in TNF-α secretion and inhibits host cell apoptosis (149). SecA2 functions in the secretion of proteins SodA, Acr, Rv0390 and KatG. *SecA2* mutant of Mtb is less virulent in SCID mice (150).The anti-apoptotic property of SecA2 seems to come from its involvement in secretion of the protein SodA, since re-establishment of SodA

secretion in *secA2* knock-out Mtb reversed the pro-apoptotic phenotype of the *secA2* knock-out (146). KatG secretion is also defective in *secA2* knock-out Mtb (150), but KatG was not involved in apoptosis inhibition as re-establishment of SodA secretion was enough to reverse the pro-apoptotic phenotype of *secA2* mutant strain (146). SodA enzyme converts superoxide radicals to hydrogen peroxide and oxygen, thereby protecting the bacteria against oxidative damage (151). An Mtb mutant that had reduced SodA levels is pro-apoptotic and less virulent than wild-type Mtb (151). The *pknE* promoter is induced when the cells are exposed to nitric oxide donors and *pknE* is involved in regulating the host cell arginase pathway by increasing arginase 1 and arginase 2 activities for survival of Mtb (152). Increased arginase 1 and arginase 2 activities lead to decreased NO production as they compete with iNOS for L-arginine (153). *pknE* is also involved in inhibiting expression of several TLRs (152).

The common point of these three anti-apoptotic genes is their role in neutralizing or preventing ROS or NO species. This highlights the involvement of ROS and NO in promoting apoptosis. On the other hand, Mtb has proteins working to inhibit apoptosis by neutralizing or preventing ROS or NO species.

1.4.3 Identification of novel anti-apoptotic genes of Mtb

In order to identify Mtb genes that are responsible for the inhibition of apoptosis, a gain-of-function genetic screen was performed using a strain of non-pathogenic *M.smegmatis* (147). The mc^2155 strain that was used has the ability to grow fast and is also easily transformable (154). The human monocytic leukemia cell line THP-1 was used as host cells for this screen. Early studies showed that infection of THP-1 cells with

M.smegmatis led to a much higher level of apoptosis (~ 40%) compared to uninfected (less than 5%) or BCG infected cells (less than 10%) just 16 hr after infection (147). For the gain of function screen, 312 Mtb genomic fragments were used to transform *M.smegmatis*. The 312 *M.smegmatis* clones were then used to infect THP-1 cells. Five clones with reduced apoptosis were identified. The cosmids that enabled *M.smegmatis* to inhibit apoptosis were extracted from the clones and were used to transfect *M.smegmatis* again. This was done to confirm that the decreased apoptosis was due to the presence of the cosmids in *M.smegmatis*. The decrease in apoptosis was reproducible for two of the five clones (147).

Although the 2 cosmids were able to reduce the pro-apoptotic phenotype of *M.smegmatis*, *M.smegmatis* clones with the cosmids still induced high levels of apoptosis (between 15 and 25%) (147). This was probably due to the ability of *M.smegmatis* to strongly induce apoptosis faster than other mycobacteria. To better assess the effects of the cosmids in inhibition of apoptosis induction, *M.kansasii*, a facultative pathogenic species was used. *M.kansasii* induces high levels of apoptosis but is slower in killing the host cells (significant levels of apoptosis induced after 3 days). The 2 cosmids that showed consistent decrease of apoptosis in *M.smegmatis* as well as the empty cosmid vector were transformed into *M.kansasii*. The clones with these cosmids induced significantly lower amounts of apoptosis compared to the empty cosmid containing *M.kansasii* (147).

To find smaller regions inside one of the cosmids (named J21) that are responsible for the inhibition of apoptosis, four sections within J21 were knocked out in Mtb using phage transduction (Velmurugan K, unpublished) (Figure 6). In addition to the

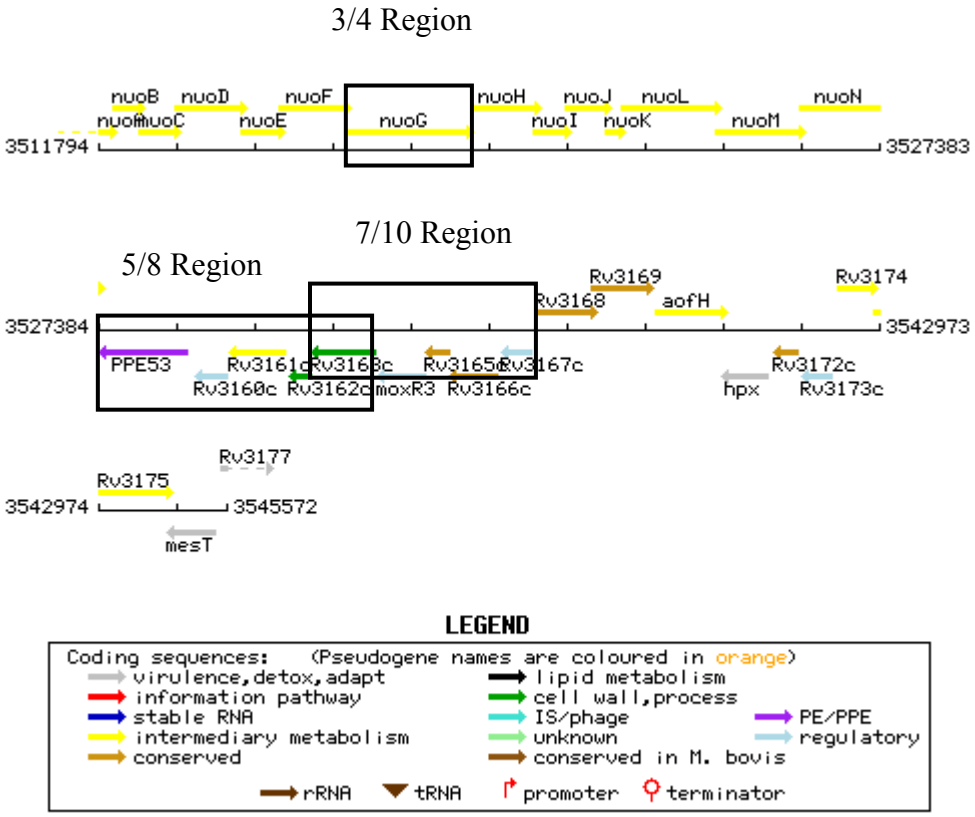

Figure 6: The J21 cosmid. The J21 cosmid that has been identified as a region that contains anti-apoptotic genes has the Mtb genomic sequence from 3511000bp to 3546000bp (44). J21 region was shown to contain anti-apoptotic genes (147).

discovery of anti-apoptotic gene *nuoG*, the 7/10 region was found to contain anti-apoptotic genes (Velmurugan K, unpublished) (Figure 7). As expected from an apoptosis inducing knock-out strain, Δ7/10 was shown to be less virulent than wild type Mtb in a survival experiment using SCID mice (Velmurugan K, unpublished) (Figure 8). The 7/10 region contains five complete genes: *MoxR3*, *Rv3167c*, *Rv3165c, Rv3166c* and *Rv3163c.* *Rv3163c* is a secreted protein that previous data suggests is not involved in apoptosis (29; Velmurugan K, unpublished). Individual knock outs of *MoxR3*, *Rv3167c*, *Rv3165c, and* *Rv3166c* were made via phage transduction and were used in THP-1 infections. Initial data showed increased apoptosis upon infection with Δ*Rv3165c* and Δ*Rv3167c* (Miller J, unpublished) (Figure 9). Therefore, the preliminary data suggested that *Rv3165c* and *Rv3167c* were the anti-apoptotic genes in the 7/10 region. The research that is presented here was performed to confirm that Δ*Rv3165c* and Δ*Rv3167c* were pro-apoptotic, to find the pathways involved in apoptosis of Δ*Rv3165c* and Δ*Rv3167c* infected cells and to characterize Rv3165c and Rv3167c.

1.5 SUMMARY AND SIGNIFICANCE

Mtb continues to kill millions of people every year (3). One of the reasons of failure in the eradication of Mtb is the low success rate of the current BCG vaccine (22, 23). Another reason is the lack of drugs that can kill Mtb in weeks compared to the current drugs that take months to be effective (37). That is why it is necessary to develop new and effective prevention and treatment methods against TB. To achieve this goal it is necessary to understand the mechanisms by which Mtb survives in the host. One of these mechanisms might be the prevention of apoptosis of infected host cells. A better

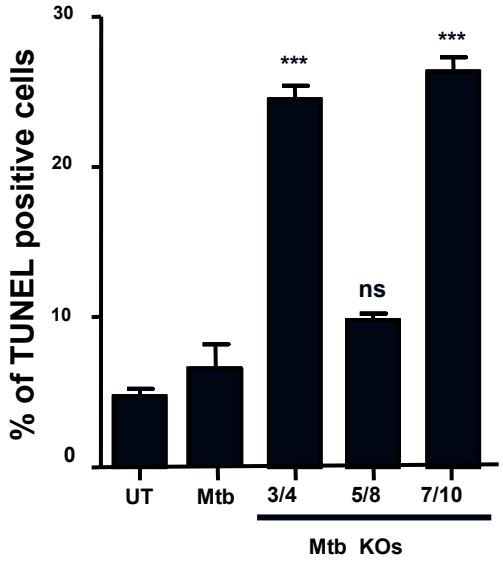

Figure 7: 3/4 and 7/10 regions of the J21 cosmid contain anti-apoptotic genes. Mtb and knock-outs lacking the 3/4 or 5/8 or 7/10 regions were used to infect THP-1 macrophages. Mtb knock-outs lacking the 3/4 or 7/10 regions were found to induce significantly more apoptosis compared to Mtb. Data are the mean ± SEM of a representative experiment performed in duplicate. UT, untreated; ns, not significant; ***, $0.0001 < p < 0.001$ (Experiment performed by Kamalakannan Velmurugan).

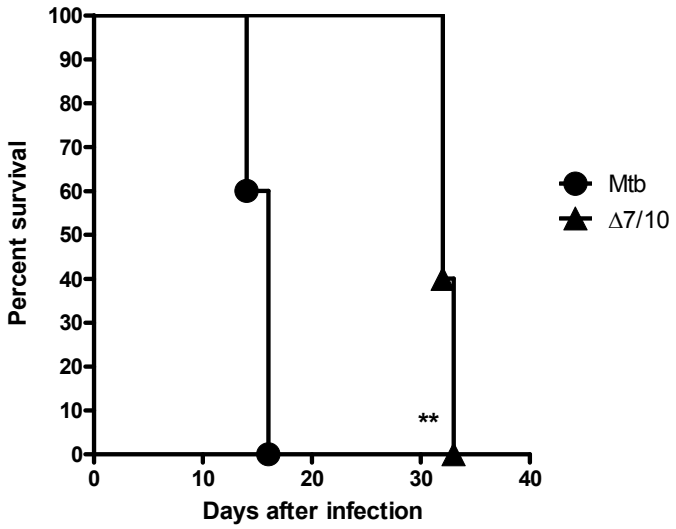

Figure 8: Deletion of the 7/10 region in Mtb reduces its virulence in SCID mice. Five SCID mice were infected by injection of 10^6 Mtb or Δ7/10 in the tail and monitored. Mtb infected mice died on the 14^{th} and 16^{th} days, while Δ7/10 infected mice died on 32^{nd} and 33^{rd} days. Log-rank test found the curves to be significantly different. **, $0.001 < p < 0.01$ (Experiment performed by Kamalakannan Velmurugan).

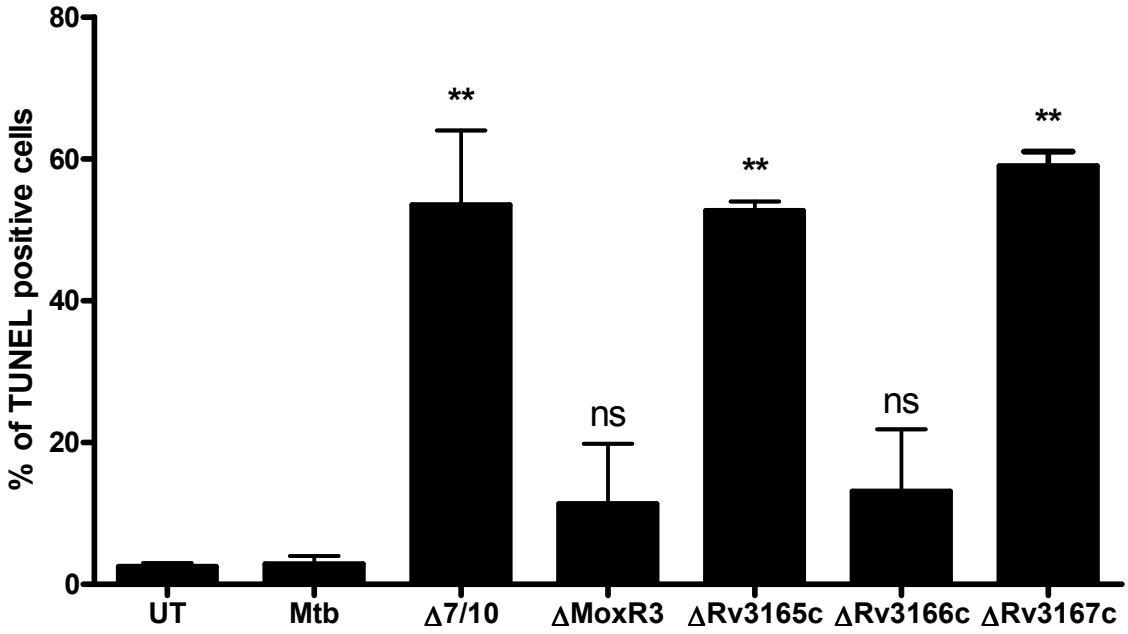

Figure 9: Preliminary experiments indicate *Rv3165c* and *Rv3167c* genes as the anti-apoptotic genes in the 7/10 region. THP-1 macrophages were infected with Mtb and the knock-outs for 5 days. The cells were collected and stained with TUNEL to determine the % of apoptotic cells. Data are the mean ± SEM of a representative experiment performed in duplicate. **, $0.001 < p < 0.01$ (Experiment performed by Jessica Miller).

understanding of this mechanism will help in the development of vaccine strains that do not prevent host cell apoptosis and hence induce a better immune response. Also, identification of Mtb components that inhibit apoptosis can reveal new targets for drugs. Drugs that target anti-apoptotic components of Mtb would help the immune system to kill the intracellular Mtb that is hard to target with other drugs. Previously a genomic DNA region of Mtb was identified to contain anti-apoptotic genes (147). The goals of my research were to identify some of the genes in this region, characterize the genes and identify the mechanisms by which the products of these genes inhibit host cell apoptosis.

CHAPTER 2 MATERIALS AND METHODS

2.1 MATERIALS

SCID mice (BALB/c background) were from Jackson Laboratories (Bar Harbor, ME). The anti-myc antibody (9E 10) developed by [Bishop, J.M.] was obtained from the Developmental Studies Hybridoma Bank developed under the auspices of the NICHD and maintained by The University of Iowa, Department of Biology (Iowa City, IA). Cleaved caspase-8, cleaved caspase-9, cleaved caspase-3 antibodies were purchased from Cell Signaling Technology® (Danvers, MA). Anti-actin antibody was purchased was from Santa Cruz Biotechnology, Inc. (Santa Cruz, CA). Anti-GroEL, anti-LAM, anti-DnaK, and anti-FAP antibodies were purchased from Colorado State University through the TB Vaccine Testing and Research Materials Contract as part of NIH, NIAID Contract No. HHSN266200400091C (Fort Collins, CO). Horse radish peroxidase-conjugated goat anti-mouse IgG, horse radish peroxidase-conjugated goat anti-rabbit IgG, horse radish peroxidase-conjugated donkey anti-goat IgG, alkaline phosphatase conjugated streptavidin (Streptavidin-AP) were purchased from Jackson ImmunoResearch Laboratories Inc. (West Grove, PA). Cytometric Bead Array kit for human inflammatory cytokines was purchased from BD Biosciences (San Jose, CA). N-acetyl cysteine, and Hygromycin B were purchased from EMD Chemicals (Philadelphia, PA). FLICA™ kits were purchased from ImmunoChemistry Technologies $_{LLC}$ (Bloomington, MN). In Situ Cell Death Detection Kit, Fluorescein for TUNEL and LightCycler® 480 SYBR Green I Master for qPCR, PhosSTOP phosphatase inhibitor cocktail tablets and cOmplete, Mini, EDTA-free protease inhibitor cocktail tablets were purchased from Roche (Indianapolis, IN). Ribo-zero™ and ScriptSeq™ mRNA-Seq Library Preperation kits for RNA

sequencing were purchased from Epicentre (Madison, WI). Human CCL3/MIP-1 alpha DuoSet and Human CCL20/MIP-3 alpha DuoSet ELISA kits were purchased from R&D Systems® (Minneapolis, MN). Lysis buffer for protein microarray was supplied by Kinexus (Vancouver, Canada). Electroporation cuvettes were purchased from VWR (Bridgeport, NJ). Fetal calf serum was purchased from Thermo Scientific (Logan, UT). Human serum was purchased from Gemini Bio-Products (West Sacramento, CA). Gentamicin, and TRIzol® Reagent were purchased from Invitrogen™ (Grand Island, NY). Three well slides were purchased from Electron Microscopy Sciences (Hatfield, PA). BrightStar® Psoralen-Biotin Kit and BrightStar® BioDetect™ Nonisotopic Detection Kit for Southern blots, and TURBO DNA-*free*™ were purchased from Ambion (Grand Island, NY). AlkPhos Direct™ hybridization buffer was purchased from Amersham (Piscataway, NJ). Centriplus® YM-3 centrifugal filters were purchased from Millipore™ (Billerica, MA). Thermo Scientific SuperSignal West Femto Substrate, Thermo Scientific SuperSignal West Pico Chemiluminescent Substrate, Thermo Scientific Pierce BCA™ Protein Assay Kit, Costar 96-Well EIA/RIA plates for ELISA, Triton® X-100, Phorbol 12-myristate 13-acetate (PMA), kanamycin, streptomycin, Tween®-80, and Thermo Scientific Phusion® RT-PCR Kit for reverse transcription were purchased from Fisher (Pittsburgh, PA). Proteinase K was purchased from Fermentas (Glen Burnie, MD). Staurosporine, xanthine oxidase, xanthine, glutathione, DPI, lysozyme, protease inhibitor cocktail were purchased from Sigma (St. Louis, MO).

2.2 BACTERIA AND CULTURE CONDITIONS

M. tuberculosis H37Rv (ATCC 25618) was obtained from the American Type Culture Collection (Manassas, VA). Middlebrook 7H9 medium supplemented with 0.5% glycerol, 0.05% Tween-80, and 10% ADS (Albumin, 5% w/v, dextrose, 2% w/v, NaCl, 0.85% w/v) or ADC (Albumin, 5% w/v, dextrose, 2% w/v, catalase, 0.003% w/v, NaCl, 0.85% w/v) was used to grow Mtb strains (155). Mycobacteria containing plasmids with antibiotic resistance genes were grown in the presence of 50μg/ml hygromycin or 40μg/ml kanamycin or 20μg/ml streptomycin.

2.3 *IN VITRO* HYDROGEN PEROXIDE PRODUCTION

Bacteria were collected by centrifugation and resuspended in PBS to adjust their concentration to 10^6 bacteria/ml. To produce hydrogen peroxide *in vitro*, 250μM xanthine and 0.1U/ml xanthine oxidase were added to the bacteria and the bacteria were shaken for 90 min at 37 ^{o}C.

2.4 CREATION OF COMPLEMENTS OF KNOCKOUTS

For complementation of the Δ*Rv3165c* knockout, the sequence from 200bp upstream of *Rv3165c* to 110bp downstream of *Rv3165c* was cloned into the integrating vector pDB60 that contains a streptomycin resistance gene. The insertion of the correct sequence was confirmed by plasmid sequencing. The plasmid was electroporated into Δ*Rv3165c* and colonies were grown and selected as mentioned below. For complementation of Δ*Rv3167c* knockout, the sequence from 60bp upstream of *Rv3167c* to the 3' end of *Rv3167c* was cloned into the extrachromosomal expression vector

pmv261. The plasmid was electroporated into Δ*Rv3167c* and colonies were grown and selected as mentioned below.

2.5 CREATION OF RV3165C-MYC AND RV3167C-MYC EXPRESSING BCG

To make Rv3167c-myc, the sequence from 60bp upstream of *Rv3167c* to the 3' end of *Rv3167c* with the myc tag sequence was cloned into the extrachromosomal expression vector pmv261. The plasmid was electroporated into BCG and colonies were grown and selected as mentioned below. To make Rv3165c-myc, the sequence from 50bp upstream of *Rv3165c* to the 3' end of *Rv3165c* with the myc tag sequence was cloned into the extrachromosomal expression vector, pmv261. The plasmid was electroporated into BCG and colonies were grown and selected as mentioned below.

2.6 ELECTROPORATION OF PLASMIDS

To electroporate plasmids, 5ml of late log phase culture was centrifuged at 2000g for 10 min and the cells were washed three times with an equal volume of wash solution (10% glycerol with 0.05% Tween-80). The final pellet was resuspended in $1/10^{th}$ the original volume of wash solution. Bacteria (400µl) were added to a 2mm electroporation cuvette containing 2-5µl of plasmid. Bacteria were electroporated at 2.5kV; 25uFD; 1000Ω in a BioRad GenePulser Xcell™ electroporator. 7H9 (1ml) medium was added to the bacteria, which were allowed to recover for 3hr for *M. smegmatis* or 24hr for slow growers (Mtb, BCG, *M. kansasii*). The cells were then plated on 7H10 agar plates containing the appropriate selective medium and incubated for 3-4 days (*M.smegmatis*) or 3 weeks (Mtb, BCG) at 37 ^{o}C. Resulting colonies were grown in 7H9 medium with

appropriate antibiotic and the cultures were screened by PCR, Southern or western blot to check for uptake of the plasmid.

2.7 CELL CULTURE MAINTENANCE

Each vial of human acute monocytic leukemia cell line THP-1 (ATCC™ TIB-202™) was thawed at 37 ^{o}C in a water bath and the cells were washed with RPMI-1640 medium and resuspended in 20ml RPMI-1640 supplemented with heat inactivated 10% fetal calf serum. Cells were grown in a 37 ^{o}C incubator in the presence of 5% CO_2. THP-1 cells were passaged before their concentration reached 0.8 x 10^6 cells/ml.

2.8 INFECTIONS

For infections, 0.6-0.9 million THP-1 cells per ml were plated into 24 well plates in the presence of 20ng/ml phorbol 12-myristate 13-acetate and incubated for 20hr. Before infection, cells were washed three times with magnesium/calcium-free phosphate buffered saline (PBS) and 0.5ml of infection medium (RPMI-1640, 10% heat inactivated FCS, 5% human serum) was added to each well. Bacteria to be used in the infections were washed once with PBS containing 0.05% Tween®-80 (PBST). A sample of bacteria was mixed in equal ratio with 10% formalin in a cuvette and the OD was measured. Cells were infected at a multiplicity of infection (MOI) of 3:1 by adding three times the amount of bacteria per cell and incubating the plates for 4hr at 37 ^{o}C in the presence of 5% CO_2. Infection media was removed after 4hr and the wells were washed two times with PBS and then 1ml chase medium (RPMI-1640, 10% heat inactivated FCS, 100µg/ml gentamicin) was added to each well. Cells were then incubated for the indicated times. At

the end of infections, the chase media in the wells were placed in 15ml tubes and PBS with 5mM ethylenediaminetetraacetic acid (EDTA) was added to the wells to lift the cells. The lifted cells were added to the 15ml tubes and centrifuged. The cell pellets were resuspended in 4% paraformaldehyde overnight at 4^{o}C to fix cells and kill intracellular Mtb. For infections on slides, 120,000 cells were plated into each well of 3-well slides and incubated as mentioned before. When glutathione, N-acetyl cysteine, diphenylene iodonium were used they were included both in the infection and the chase media.

2.9 DETECTION OF APOPTOSIS

To detect apoptosis in THP-1 cells, the In Situ Cell Death Detection Kit, Fluorescein was used. This kit labels the free 3'-OH termini of DNA with fluorescein-dUTP using the enzyme terminal deoxynucleotidyl transferase (TdT). The reaction is called TdT-mediated dUTP-X nick end labeling (TUNEL). Before TUNEL, cells were washed two times with PBS and permeabilized with permeabilization solution that contained 0.1% Triton® X-100 and 0.1% sodium citrate on ice for 3 min. Cells in each sample were incubated with 50µl TUNEL solution that is a mix of the enzyme, nucleotides and the buffer. After 1hr at 37 ^{o}C the cells were washed two times and resuspended in PBS. Flow Cytometric analysis of cells was done using either a Becton Dickinson FACSCalibur™, FacsCanto™ II, FacsAria™ or Accuri® C6. For measuring apoptosis of cells on slides, after the last wash of the cells, wells were left to dry, ProLong® Gold antifade reagent with DAPI was added to the wells and coverslips were placed. Slides were left overnight at room temperature and images of cells were taken

using a Zeiss LSM 710 laser scanning microscope and processed using AxioVision LE software.

2.10 DETERMINATION OF NECROTIC CELL DEATH

To quantify the levels of necrosis in infected cells, ToxiLight® BioAssay Kit (Lonza, Rockland, ME) was used. Briefly, 20 µl of cell supernatant from each well was added to the wells of a white bioluminescence compatible 96 plate in triplicate and mixed with 100 µl of Adenylate Kinase detection reagent (reconstituted in assay buffer). After 5 min of incubation the luminescence was measured by a BioTek® Synergy microplate reader.

2.11 DETERMINATION OF THE NUMBER OF LIVE BACTERIA AFTER INFECTION

To determine the effect of apoptosis on the intracellular growth of Mtb, Δ*Rv3165c,* and Δ*Rv3167c*, for each time point 3 wells of differentiated THP-1 macrophages were infected with those strains. Following infection, THP-1 cells were lysed at 0 hr, 1 day and 2 day time points for 3:1 MOI infections and 0 hr, 1 day, 2 day, 3 day, 4 day and 6 day time points for 0.5:1 MOI infections using 0.1% Triton X-100 in PBS. No gentamicin was used in the chase media in order to keep any extracellular mycobacteria that might be released after host cell death alive. The lysates were diluted in PBST 10^4, 10^5, 10^6 for time points up to 3 day and 10^5, 10^6 and 10^7 times after 3 day. 10µl from each dilution was spotted three times on square 7H10 plates. That resulted in 9 spots for each well of infection. After 14 days the numbers of colonies in the spots were

counted and all of the 27 counts for the 3 wells were averaged (The numbers were less in case of contaminations or mixing of spots).

2.12 MYCOBACTERIA GENOMIC DNA ISOLATION

Bacteria (10ml) were centrifuged at 2000 g for 10 min and resuspended in 1ml lysis buffer (25mM Tris-HCl, 10mM EDTA, 50mM glucose) and centrifuged again. The pellet was resuspended in 450µl lysis buffer. Lysozyme (50µl, 10mg/ml) was added, mixed gently and the sample was incubated at 37 ^{o}C overnight. Sodium dodecyl sulfate (100µl) and proteinase K (50µl, 10mg/ml) were added to the sample, mixed and incubated at 55^{o}C for 30 min. NaCl (200µl, 5M) was added to the sample followed by 160µl 65 ^{o}C preheated CTAB (Cetrimide saline solution: 0.1g/ml cetrimide, 0.04g/ml NaCl). The sample was incubated at 65^{o}C for 10 min. An equal volume (~ 1ml) chloroform-isoamyl alcohol (24:1) was added to the sample, mixed gently and the sample was centrifuged at 12,000 g for 5 min. The aqueous phase was placed in a new tube and mixed with 0.7X volume isopropanol and mixed gently. The sample was incubated at room temperature for 5-10 min and centrifuged at 16,000 g for 10 min. The pellet was washed with 1ml 70% ethanol, centrifuged at 16.000g for 5 min and air dried. The pellet was resuspended in 50µl water.

2.13 SOUTHERN BLOTTING

The probe DNA for southern blots of *Rv3165c* was made by PCR using the primers that were used to amplify the 5' end of *Rv3165c* for knockout production. The probe DNA for southern blots of *Rv3167c* was made by PCR using the primers that were

used to amplify the 3' end of *Rv3167c* for knockout production. The probes were labeled with biotin using BrightStar® Psoralen-Biotin Kit. Genomic DNA isolated from the clones was digested with XhoI for *Rv3165c* southern blots and with EcoRI for *Rv3167c* southern blots. The DNA fragments were separated by agarose gel electrophoresis, transferred to charged nylon membrane, and denatured with 0.4N NaOH. The probe was denatured at 90 ^{o}C for 10 min in the presence of 10mM EDTA and hybridized to the membrane at 55 ^{o}C for 16 hr in hybridization buffer (AlkPhos Direct™ hybridization buffer with 0.5M NaCl). The membrane was washed and the probe was detected using a BrightStar® BioDetect™ Nonisotopic Detection Kit.

2.14 CASPASE ACTIVITY DETECTION

Caspase activity was detected by Fluorescent-Labeled Inhibitor of Caspases (FLICA™). A working solution of the FLICA™ reagent was added to the cells and incubated for 1hr at 37 ^{o}C. Cells were washed two times and resuspended with PBS. Analysis was accomplished using flow cytometry.

2.15 WHOLE CELL LYSATE PREPARATION

Cells were lysed using lysis buffer (for mycobacteria: 50mM Tris-HCl [pH 7.5], 5mM EDTA, 0.6% SDS, 10mM Na_3PO4, prokaryotic protease inhibitor cocktail; for THP-1 cells 50mM Tris-HCl, 150mM NaCl, 1% Triton® X-100, eukaryotic protease inhibitor cocktail). To lyse mycobacteria, glass beads were added to the tubes and the cells were lysed for 10 min using a Biospec Mini-Beadbeater-8. Samples were centrifuged at 10,000g for 5 min at 4 ^{o}C and the supernatants were filtered through

Costar® Spin-X® centrifuge tube filters to remove whole bacteria. Thermo Scientific Pierce BCA™ Protein Assay Kit was used to determine protein concentrations (156).

2.16 POLYACRYLAMIDE GEL ELECTROPHORESIS AND WESTERN BLOTTING

Sample protein (≤ 50 µg) was mixed with sample buffer (250mM Tris-HCl, pH 6.8, 8% SDS, 40% glycerol, 10% β-mercaptoethanol and 0.01% bromophenol blue) at a 4:1 ratio and proteins were denatured at 95 ^{o}C for 5 min and placed on ice (155). Samples were pipetted into the wells of 4-20% polyacrylamide gradient gels and separated at 125V using Tris-HEPES-SDS running buffer (Thermo Scientific). Proteins were transferred to a 0.45µm PVDF membrane using Genie® Blotter (Idea Scientific). Membranes were blocked using 5% non-fat dry milk in PBS for 1hr at room temperature and incubated with primary antibodies diluted in the recommended buffer. After secondary antibody incubation, the chemiluminescent signal was produced using SuperSignal West Pico Chemiluminescent Substrate or SuperSignal West Femto Substrate.

2.17 SUBCELLULAR FRACTIONATION

For each fractionation, 50ml cells were centrifuged at 3000g for 15 min. The pellets were washed with PBS, centrifuged again and resuspended in breaking buffer (PBS, 1% protease inhibitor cocktail, 20 µg/ml soybean trypsin inhibitor, 25µg/ml DNase, 50µg/ml RNase). Cells were lysed using a French® Press. Unbroken cells were pelleted at 3000g for 20 min. The supernatants were centrifuged at 100,000g for 2hr to

pellet the cell wall and the cell membrane (cell envelope). The supernatants that contained cellular cytoplasm were transferred to fresh tubes and the pellets were washed with PBS. The pellets were resuspended in the breaking buffer without DNase and RNase.

2.18 CULTURE FILTRATE PREPARATION

To prepare culture filtrates (CF), bacteria were grown in 7H9 medium and passaged three times in Sauton's liquid medium (155), centrifuged and the supernatant was filtered (0.22µm). CFs were concentrated at least 20 times using Centriplus® YM-3 centrifugal filters. Protease inhibitor cocktail (1% final concentration) and soybean trypsin inhibitor (20 µg/ml final concentration) were added to the CFs.

2.19 RNA ISOLATION

Cells were lysed using TRIZOL® Reagent and pipetting. To lyse mycobacteria, 200µl zirconia beads were added to the tubes and the cells were lysed using Biospec Mini-Beadbeater-8. After 5 min at room temperature, chloroform (0.2 volume) was added to the samples and the samples were shaken vigorously for 20 sec and incubated at room temperature for 3 min. Samples were centrifuged for 15 min at 12,000 g at 4 ^{o}C and the aqueous phase was transferred to a new tube. The chloroform extraction was repeated and the final aqueous phase was mixed with an equal volume of isopropanol. After the samples were gently mixed, they were incubated at room temperature for 10 min and spun for 10 min at 12,000 g at 4 ^{o}C. The pellets were washed with 70% ethanol, air dried

and resuspended in RNase free water. TURBO DNA-*free*™ was added to RNA samples to degrade DNA.

2.20 REVERSE TRANSCRIPTION AND REAL-TIME QUANTITATIVE POLYMERASE CHAIN REACTION (RT-QPCR)

cDNA was produced from RNA using the Thermo Scientific Phusion® RT-PCR Kit. For each reaction, cDNA was produced from 500ng RNA using random hexamers. Triplicates were processed for qPCR using a LightCycler® 480 SYBR Green I Master kit and the Bio-Rad CFX96™ real-time PCR machine. qPCR reactions included 0.5µM of each primer and 0.5µl cDNA.

2.21 SAMPLE PREPARATION FOR RNA SEQUENCING

Ribosomal RNA (rRNA) was removed from 5µg RNA samples using Ribo-zero™ kits. To remove bacterial rRNA from infected THP-1 RNA samples Gram(+) Bacterial Ribosomal Removal Solution was included in the reactions. ScriptSeq™ mRNA-Seq Library Preperation kit was used to prepare a RNA sequencing library from these rRNA depleted RNA samples.

2.22 ENZYME LINKED IMMUNOSORBENT ASSAY (ELISA)

CCL3 and CCL20 concentrations in the cell culture supernatants were measured using DuoSet ELISA kits. Briefly, 96-well plates were coated with 2µg/ml (CCL3) or 0.4µg/ml (CCL20) capture antibody. After 16 hr incubation, wells were washed three times with 400µl PBST and blocked with 300µl reagent diluent (1% BSA in PBS) for 1hr

at room temperature. Wells were washed and 100µl of triplicates of sample or standards were added to the wells. After 2hrs at room temperature, wells were washed and 100µl detection antibody (36µg/ml) in reagent diluent was added to the wells for 2hrs at room temperature. Wells were washed and 100µl 1X Streptavidin-AP was added to the wells for 20 min at room temperature. Wells were washed and 100µl substrate solution (1mg/ml *p*-nitrophenyl phosphate disodium salt dissolved in 1.02M diethanolamine, pH 9.8) was added to the wells. The absorbance of samples at 405 nm was measured after 5-10 min.

2.23 MEASUREMENT OF HUMAN INFLAMMATORY CYTOKINE LEVELS IN SUPERNATANTS USING A CYTOMETRIC BEAD ARRAY KIT

BD Cytometric Bead Array (CBA) Human Inflammatory Cytokines Kits were used for measuring the levels of IL-8, IL-1β, IL-6, IL-10, TNF-α and IL-12p70 cytokines in the supernatants 48 hr after infection. 50µl mixed capture beads were mixed with 50µl PE detection reagent and with either 50µl standards or samples. After 3 hr at room temperature, 1ml wash buffer was added and samples were centrifuged. The pellets were resuspended in 300µl wash buffer and samples were analyzed using a flow cytometer.

2.24 INFECTION OF SCID MICE AND DETERMINATION OF THE BACTERIAL LOAD

To infect the mice with mycobacteria, 7 mice were placed in the basket of the Glas-Col® Inhalation Exposure System (Model No A 4212), the lid was closed and clamped. A sterile nebulizer was attached to the machine. $5x10^6$ wild type Mtb in 5ml

PBST was injected into the nebulizer with a syringe. A standard program was employed: 1800 seconds nebulizing time, 1800 seconds cloud decay time, 900 seconds decontamination time. After the UV lights turned off, the mice were removed and placed into their cages. The nebulizer was placed into a solution of vesphene for sterilization. The basket and the inside of the machine were cleaned with vesphene and 70% ethanol. A new sterile nebulizer was attached to the machine to infect the mice with Δ*3167c* and the same protocol was followed.

To determine the bacterial load, three mice per condition were sacrificed the next day. Mice were sedated by placing cotton balls that had 1ml isoflurane into the containers and then killed via cervical dislocation. The thoracic cavity was opened and the lungs were removed. A small piece of the left lung was cut and placed in 10% buffered formalin for histopathology. The rest of the lung was cut into very small pieces with scissors. The pieces were placed in a Stomacher® bag and 4.5ml PBST was added. The bag was sealed and placed in another bag. The bag was then placed in a Stomacher® 80 Biomaster for mashing the lung pieces for 5 min on high setting. The homogenate was filtered through a strainer into a 50ml tube. The bacteria were pelleted by centrifuging for 15 min at 2000g. The pellets were resuspended in 200µl PBST and plated on 7H10 plates. The plates were checked for colonies after 3-4 weeks of incubation at 37 ^{o}C. The numbers of colonies were counted and the numbers were graphed. Mice were observed daily and disease progression was scored as agreed by the University of Maryland Institutional Animal Care and Use Committee (IACUC) until they were in a moribund state and had to be sacrificed.

2.25 STATISTICAL ANALYSIS

Unless otherwise noted, one way analysis of variance (ANOVA) with Tukey post-test was performed using GraphPad Prism® 5 to find the significance of difference between the data values. The graph bars show the mean of the data while the error bars show the standard deviation. Significance is shown as: ns, not significant; *, $0.01 < p < 0.05$; **, $0.001 < p < 0.01$; ***, $0.0001 < p < 0.001$.

CHAPTER 3 RESULTS

3.1 *RV3165C* AND *RV3167C* ARE ANTI-APOPTOTIC GENES

3.1.1 Δ*Rv3165c* and Δ*Rv3167c* induce high levels of apoptosis of THP-1 macrophages

The 7/10 region of the J21 cosmid was shown to contain anti-apoptotic genes of Mtb (Velmurugan, K. unpublished) (Figure 7). Dr. Jessica Miller created single gene deletions of the genes in this region in Mtb H37Rv (Δ*MoxR3*, Δ*Rv3165c*, Δ*Rv3166c*, Δ*Rv3167c*) and her preliminary experiments suggested that *Rv3165c* and *Rv3167c* were the anti-apoptotic genes in the 7/10 region. In order to confirm this, Mtb with single gene deletions (Δ*MoxR3*, Δ*Rv3165c*, Δ*Rv3166c*, and Δ*Rv3167c*) were used to infect PMA-differentiated THP-1 macrophages. THP-1 cells were incubated 4 days after infection and the percentage of apoptotic cells was determined with the TUNEL assay. Δ*Rv3165c* and Δ*Rv3167c* induced significantly higher levels of apoptosis (36.36% and 43.73%) compared to Mtb (11.81%), while other deletions (ΔMoxR3 [14.20%] and Δ3166c [16.53%]) did not (Figure 10). Thus, it was confirmed that the Δ*Rv3165c* and Δ*Rv3167* strains that were used in the infection experiments are pro-apoptotic.

3.1.2 Δ*Rv3165c* and Δ*Rv3167c* are confirmed to be knock-outs for *Rv3165c* and *Rv3167c*

To confirm that Δ*Rv3165c* and Δ*Rv3167c* were knockouts, genomic DNA was isolated from the bacterial cultures and used in PCRs that amplify a 150 bp region in the middle of the genes. Separation of PCR products on an agarose gel confirmed the lack of *Rv3165c* and *Rv3167c* in the Δ*Rv3165c* and Δ*Rv3167c* knockout strains respectively

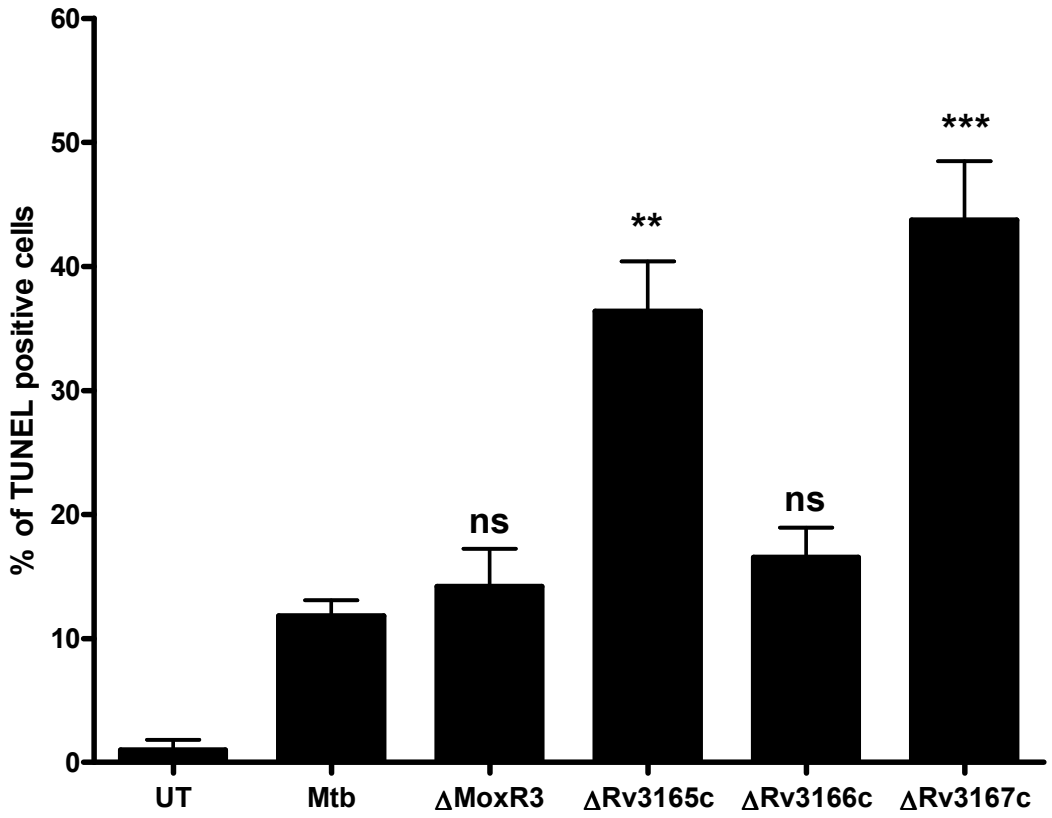

Figure 10: Δ*Rv3165c* and Δ*Rv3167c* induce significantly more apoptosis of THP-1 macrophages. PMA-differentiated THP-1 macrophages were untreated (UT) or infected with Mtb or the knock-out strains for 4 days. The cells were collected and stained with TUNEL to determine the % of apoptotic cells. Data are the mean ± SEM of three independent experiments performed in duplicate (n=6). Statistical significance was determined by one way analysis of variance (ANOVA) with Tukey post-test: ns, not significant; **, $0.001 < p < 0.01$; ***, $0.0001 < p < 0.001$.

(Figure 11). Genomic DNA was also digested with restriction enzymes to give different sizes of DNA fragments around the genes. Southern blots were performed to show the size difference of the bands that hybridized to the probes. Wild type Mtb should give a band of 2003bp with the probe after XhoI digestion of its genomic DNA, while Δ*Rv3165c* should give a 6422bp band (Figure 12A). Wild type Mtb should give a band of 6045bp with the probe after EcoRI digestion of its genomic DNA, while Δ*Rv3167c* should give a 2620bp band (Figure 12C). Southern blots confirmed the insertion of the hygromycin fragment inside the genes in the knock-out bacteria (Figure 12B, 12D). These experiments confirmed the lack of *Rv3165c* in Δ*Rv3165c* strain and lack of *Rv3167c* in Δ*Rv3167c* strain.

3.1.3 Δ*Rv3165c* and Δ*Rv3167c* complementation reverses their pro-apoptotic phenotypes

To show that the pro-apoptotic phenotype of Δ*Rv3165c* and Δ*Rv3167c* resulted from the lack of the genes and no other additional genetic mutation or epigenetic factor, the knockouts were complemented by reintroducing the knocked-out gene. Following the complementations the bacteria were used to infect PMA-differentiated THP-1 cells for 2 days. Both knockouts were complemented as the 65.18% apoptosis rate induced by Δ*Rv3165c* went down to 19.85% which is not significantly different than the 10.49% induced by Mtb (Figure 13A). Similarly, the 83.41% apoptosis rate induced by Δ*Rv3167c* went down to 8.75% which is not significantly different from the 15.75% induced by Mtb (Figure 13B). The difference in the apoptosis of THP-1 macrophages infected by Δ*Rv3165c* and Δ*Rv3167c* in the screening of 7/10 region (Figure 10) versus the later

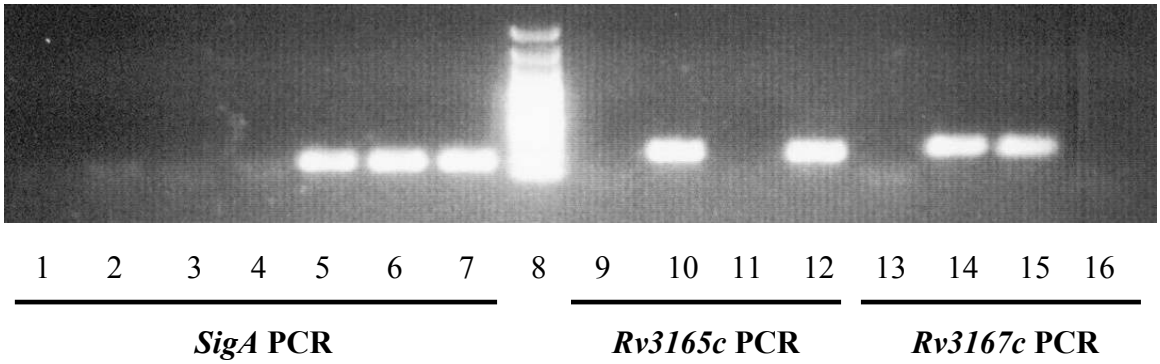

Figure 11: Confirmation of deletion of *Rv3165c* and *Rv3167c* by RT-PCR. cDNA was synthesized from RNA samples isolated from wild-type Mtb and the knock-out strains. Primers amplifying 235 and 281 bp regions in the middle of *Rv3165c* and *Rv3167c* respectively were used in PCR reactions.

1: No cDNA control
2: Mtb RNA
3: Δ*Rv3165c* RNA
4: Δ*Rv3167c* RNA
5: Mtb cDNA
6: Δ*Rv3165c* cDNA
7: Δ*Rv3167c* cDNA
8: 100 bp DNA ladder
9: No cDNA control
10: Mtb cDNA
11: Δ*Rv3165c* cDNA
12: Δ*Rv3167c* cDNA
13: No cDNA control
14: Mtb cDNA
15: Δ*Rv3165c* cDNA
16: Δ*Rv3167c* cDNA

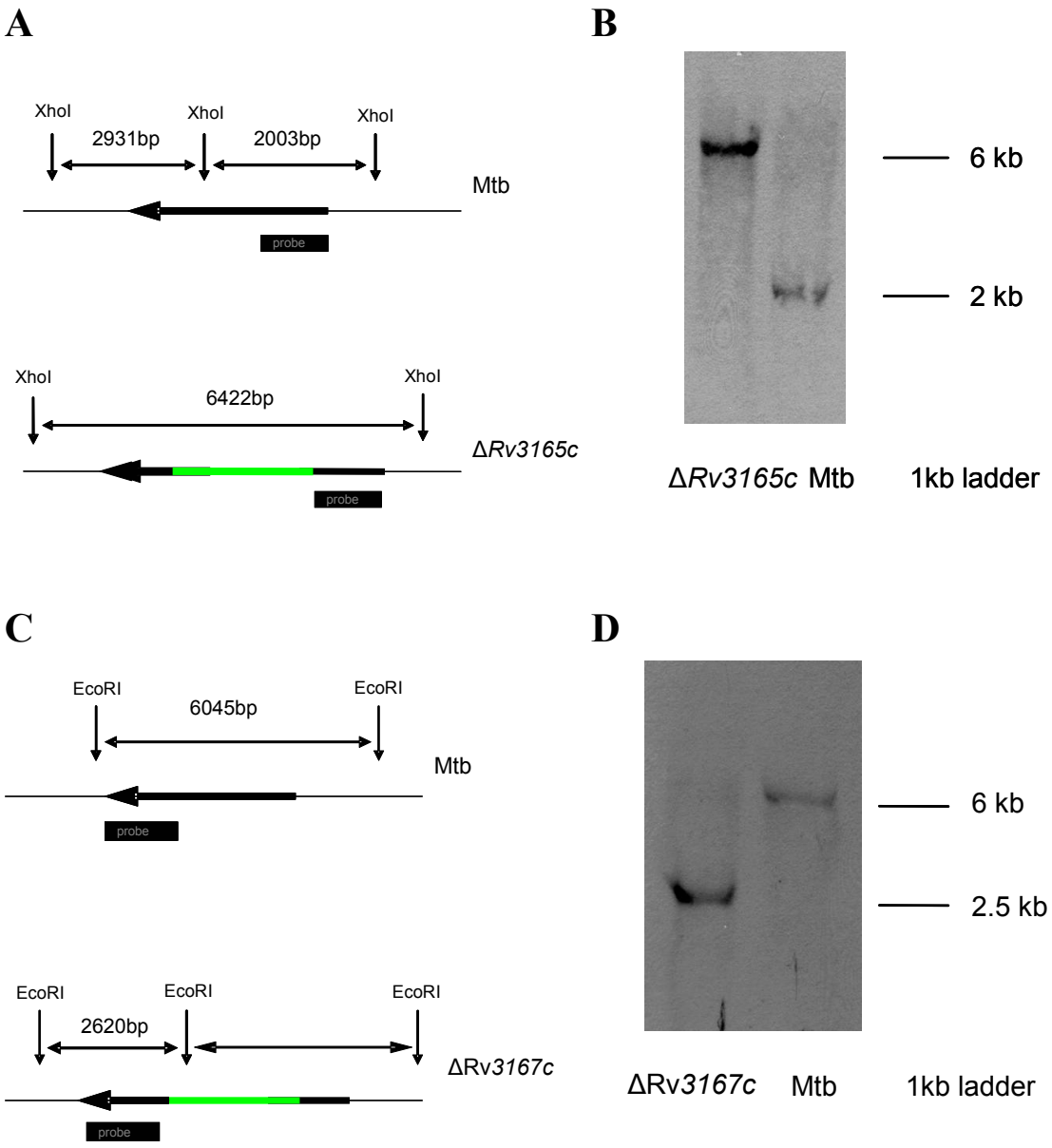

Figure 12: Confirmation of the insertion of the hygromycin resistance gene into the *Rv3165c* and *Rv3167c* genes. The theoretical sizes of fragments that would be detected with the probes after digestion of Mtb and Δ*Rv3165c* genomic DNA with XhoI (A) or digestion of Mtb and Δ*Rv3167c* genomic DNA with EcoRI (C). Arrows represent the genes, green regions inserted in the genes represent hygromycin genes. Southern experiments confirmed the sizes of the DNA fragments in Mtb and the knock-outs (B, D).

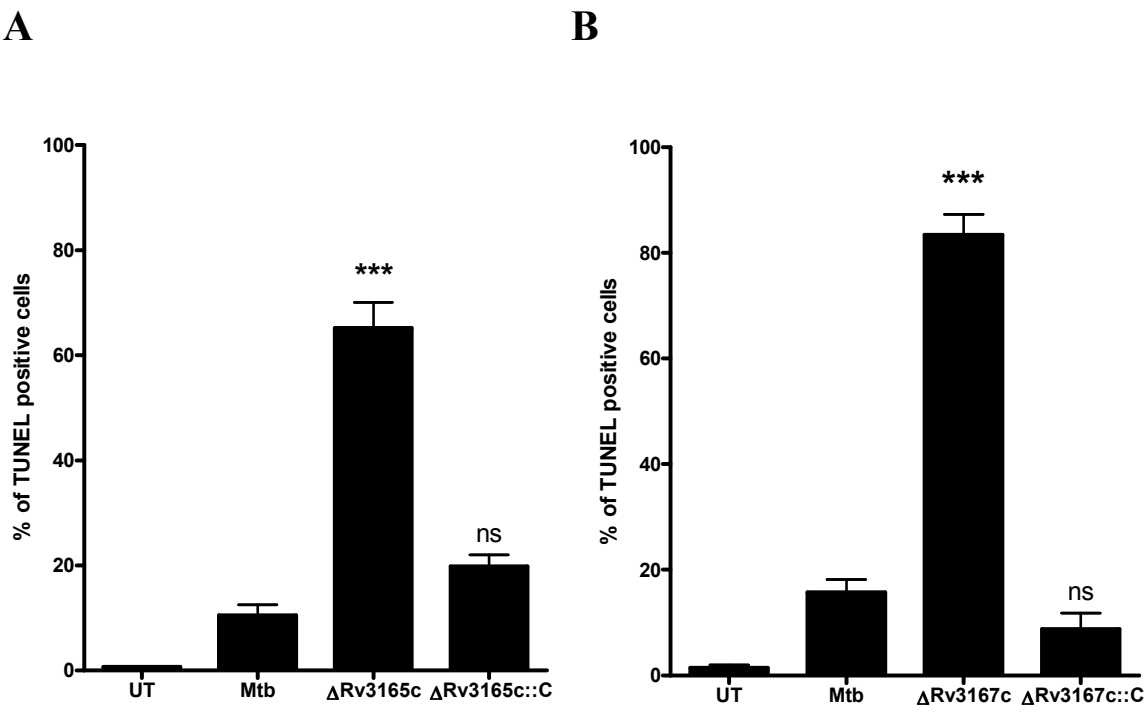

Figure 13: Complementation of Δ*Rv3165c* and Δ*Rv3167c* reverses their pro-apoptotic phenotypes. THP-1 cells were infected with Mtb, Δ*Rv3165c* and its complement or with Δ*Rv3167c* and its complement for 2 days. The cells were collected and stained with TUNEL to determine the % of apoptotic cells. Data are the mean ± SEM of three independent experiments performed in duplicate (n=6). Statistical significance was determined by one way analysis of variance (ANOVA) with Tukey post-test: ns, not significant; ***, $0.0001 < p < 0.001$.

experiments (Figure 13) is attributed to the use of different stocks of THP-1 cells and/or batches of heat inactivated fetal calf serum. Although in the later experiments infected cells go through higher rates of apoptosis in a shorter amount of time, this phenotype has stayed consistent for all of the experiments.

To confirm that Δ*Rv3165c*::C and Δ*Rv3167c*::C were complements, genomic DNA was isolated from the bacterial cultures and digested with restriction enzymes to give different size fragments of DNA around the genes. Southern blots were performed to show the size differences of the bands hybridized to the probes. Southerns confirmed the presence of an extra band from the complementation plasmid in the complements (Figure 14, 15). Thus, it was confirmed that Δ*Rv3165c*::C and Δ*Rv3167c*::C were complements and that through complementation the pro-apoptotic phenotypes of Δ*Rv3165c* and Δ*Rv3167c* were reversed. It was also confirmed that the pro-apoptotic phenotypes of Δ*Rv3165c* and Δ*Rv3167c* were due to lack of *Rv3165c* and *Rv3167c* respectively.

3.1.4 Apoptosis of infected cells inhibits the intracellular growth of Δ*Rv3167c*

Apoptosis of infected macrophages reduces the number of phagocytosed mycobacteria (135, 157). To determine the effect of apoptosis on the intracellular growth of Δ*Rv3165c* and Δ*Rv3167c*, THP-1 macrophages were infected with Mtb, Δ*Rv3165c* and Δ*Rv3167c* at an MOI of 3:1. Infected THP-1 cells were lysed right after infection, and 1 day and 2 days post infection, and the numbers of live intracellular bacteria were determined. No significant differences were observed between Mtb and the knockout strains for the three time points (Figure 16A). In order to find if there were live extracellular mycobacteria in the chase media and if their number would make a

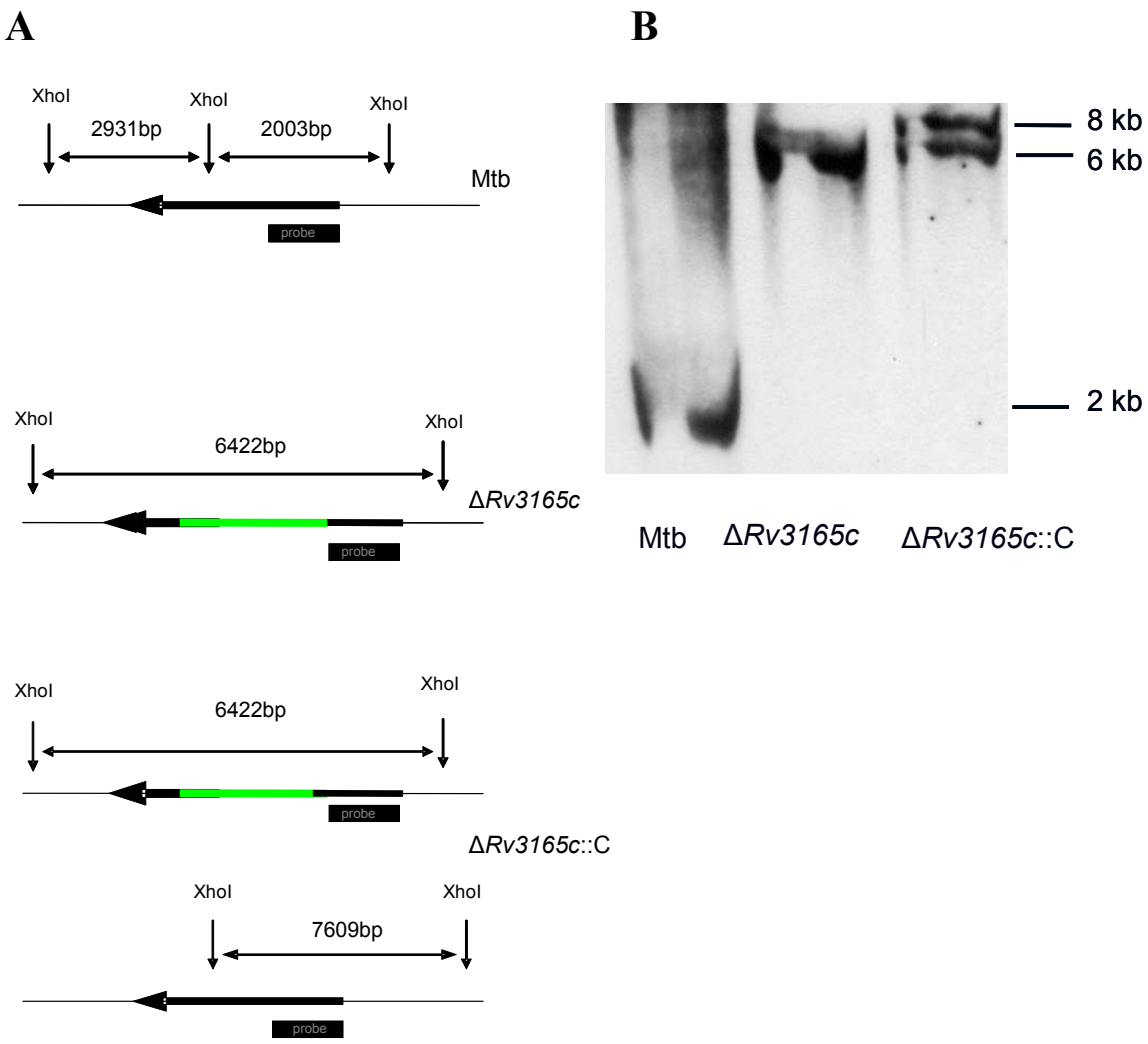

Figure 14: Confirmation of complementation of Δ*Rv3165c* by southern blot. The theoretical sizes of fragments that would be detected with the probes after digestion of Mtb, Δ*Rv3165c* and Δ*Rv3165c*::C genomic DNAs with XhoI (A). Southern experiment showed the presence of the expected extra band in the complement of Δ*Rv3165c* (B). The integrating plasmid used for Δ*Rv3165c* complementation produced a 7609 bp band.

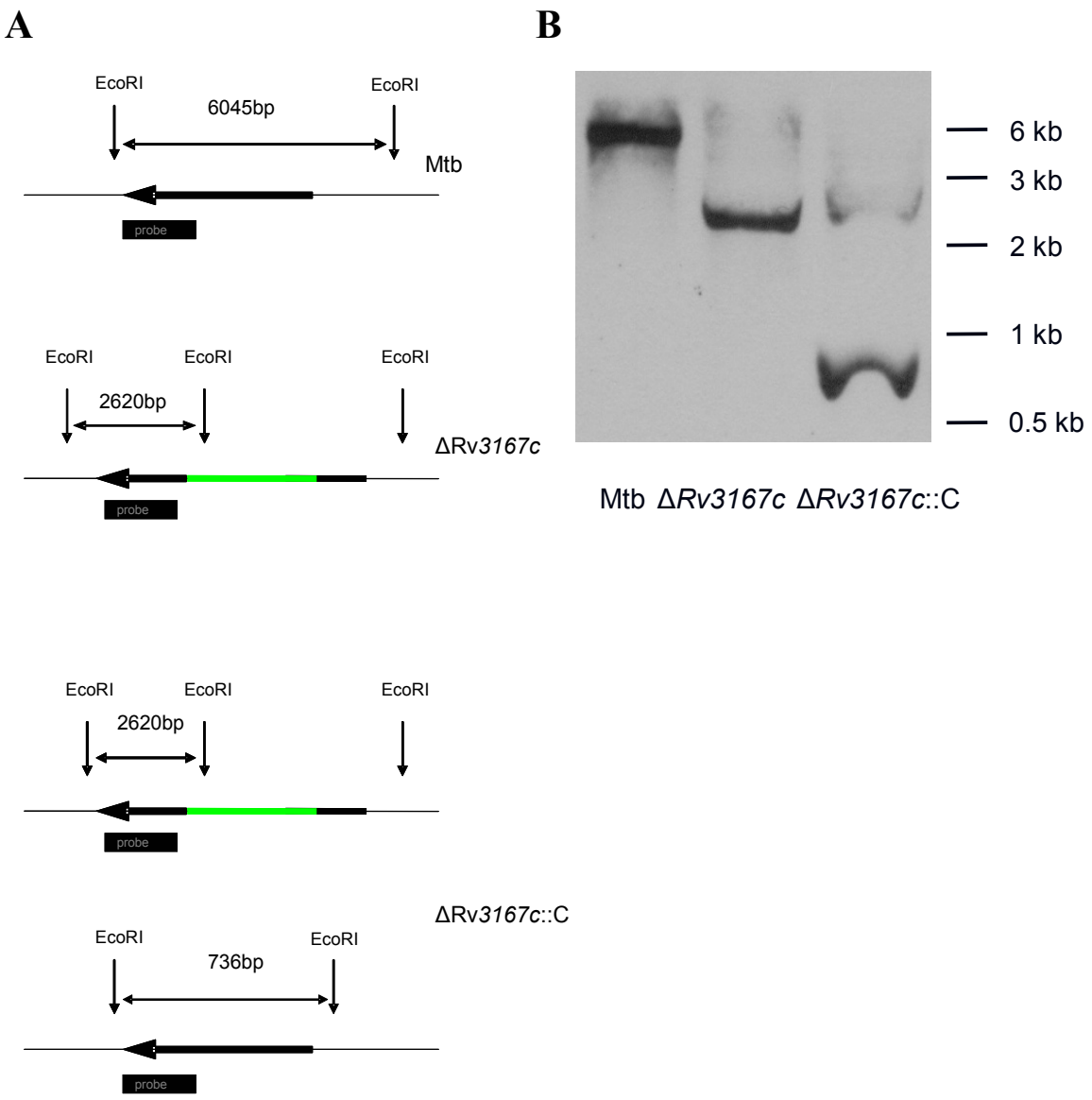

Figure 15: Confirmation of complementation of Δ*Rv3167c* by southern blot. The theoretical sizes of fragments that would be detected with the probes after digestion of Mtb, Δ*Rv3167c* and Δ*Rv3167c*::C genomic DNAs with EcoRI (A). Southern experiment showed the presence of the expected extra band in the complement of Δ*Rv3167c* (B). The episomal plasmid used for Δ*Rv3167c* complementation produced a 736 bp band.

A

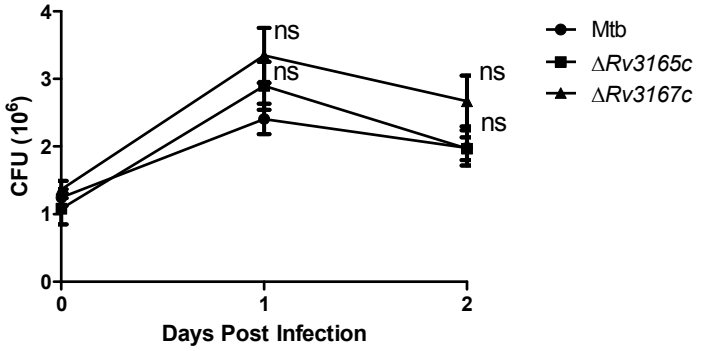

B

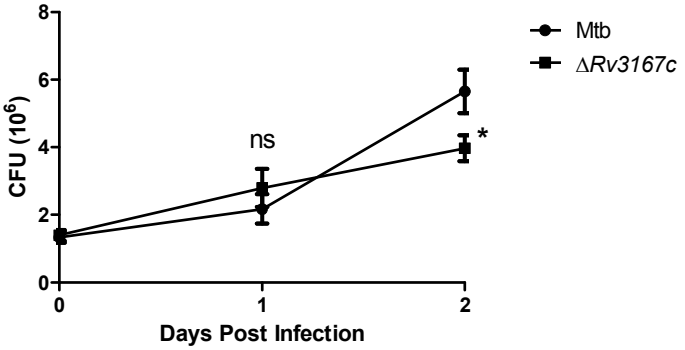

Figure 16: Apoptosis inhibits growth of Δ*Rv3167c* inside macrophages. THP-1 macrophages were infected with Mtb or Δ*Rv3165c* or Δ*Rv3167c* at an MOI of 3:1 with (A) or without (B) gentamicin in the chase media (3 wells per condition). Cells were lysed right after 4 hr of infection (0 day), 1 and 2 day after infection. Dilutions were made and spotted on 7H10 plates. Numbers of colonies were counted 14 days after incubation at 37^{o}C. Data are the mean ± SEM of two independent experiments performed in triplicates (n=6). Statistical significance was determined by one way analysis of variance (ANOVA) with Tukey post-test. *, $0.05 < p < 0.01$. See materials and methods for a detailed protocol.

difference in the total number of live mycobacteria, gentamicin was omitted in the chase media. When gentamicin was omitted from the chase media and the experiment was repeated for Δ*Rv3167c* the number of Δ*Rv3167c* was 30% less than the number of Mtb 2 day post infection indicating that the difference is due to the extracellular mycobacteria (Figure 16B). From there on no gentamicin was used in the chase media for those infections. The presence of gentamicin-sensitive mycobacteria suggests that some of the intracellular mycobacteria that were released via apoptosis got out of the apoptotic bodies and/or some of the intracellular mycobacteria got out of the cells via other ways (158, 159). When the infections were done with an MOI of 0.5:1 no significant difference was observed between Mtb and Δ*Rv3167c* for the three time points (Figure 17A). However when the numbers of bacteria were determined 6 day post infection the number of Δ*Rv3167c* was 56% less than the number of Mtb, showing that apoptosis of Δ*Rv3167c* infected cells inhibited the growth of Δ*Rv3167c* while Mtb continued to grow (Figure 17B). A preliminary experiment performed with Δ*Rv3167c*::C in addition to Mtb and Δ*Rv3167c* did not reveal any significant difference between the numbers of bacteria up to 3 day post infection but the experiment has to be repeated with further time points to be comparable to the previous experiments (Figure 17C). In order to find the rate of necrosis of THP-1 macrophages infected with Mtb and Δ*Rv3167c* and confirm that it is apoptosis that inhibits the growth of Δ*Rv3167c* in infected cells, the release of intracellular adenylate kinase (AK) into cell culture supernatant was measured by means of the ToxiLight® bioluminescence Assay 2 day post infection (Figure 18). At an MOI of 3:1, cells infected with Δ*Rv3167c* were significantly less necrotic (12%) compared to cells infected with Mtb (25.6%). At an MOI of 0.5:1, cells infected with Δ*Rv3167c* were not

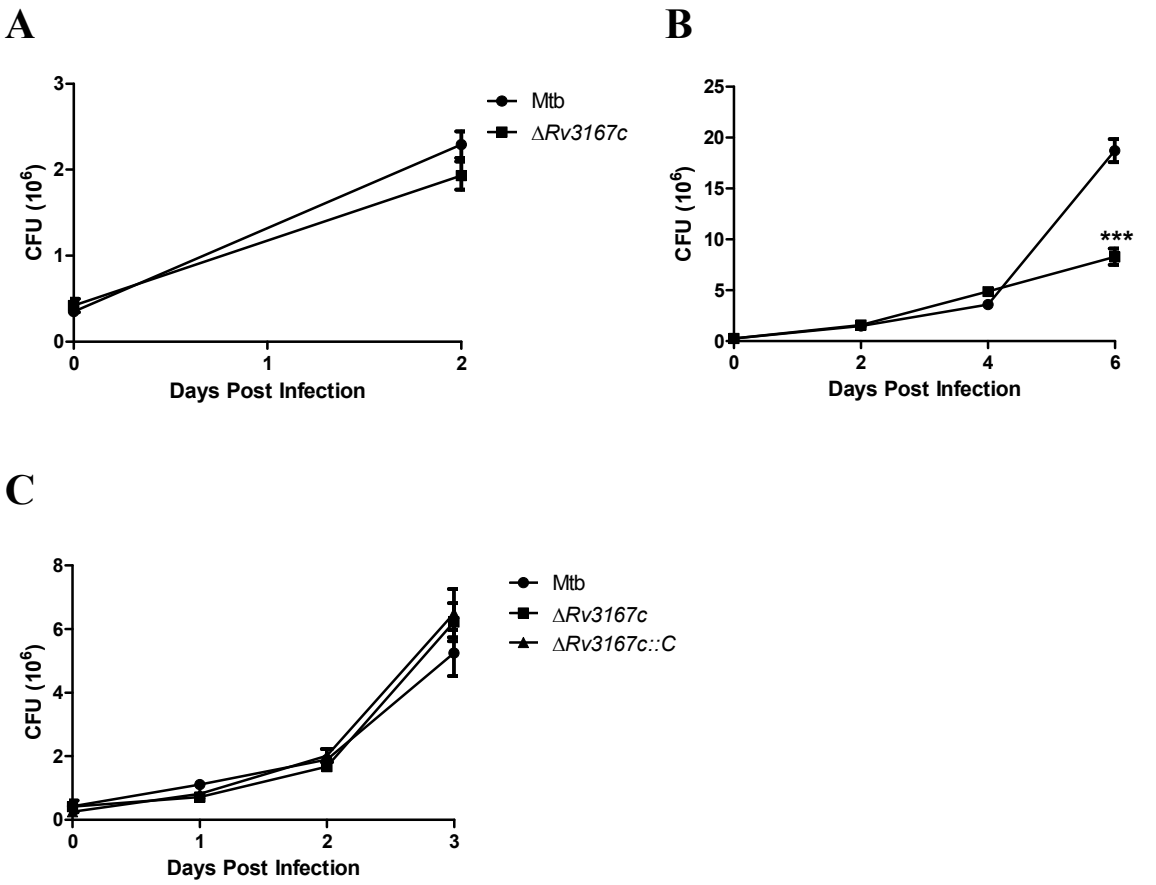

Figure 17: Apoptosis inhibits growth of Δ*Rv3167c* inside macrophages. THP-1 macrophages were infected with Mtb or Δ*Rv3167c* or Δ*Rv3167c*::C at an MOI of 0.5:1 (3 wells per condition). Cells were lysed right after 4hr of infection (0 day) and 2 day after infection (A) or 0 day, 2 day, 4 day and 6 day after infection (B) or 0 day, 1 day, 2 day and 3 day after infection (C). Dilutions were made and spotted on 7H10 plates. Numbers of colonies were counted 14 days after incubation at 37°C. Data are the mean ± SEM of two independent experiments performed in triplicate (n=6) (A and B) or the mean ± SEM of one experiment performed in triplicate (n=3) (C). Statistical significance was determined by one way analysis of variance (ANOVA) with Tukey post-test. ***, $0.0001 < p < 0.001$. See materials and methods for a detailed protocol.

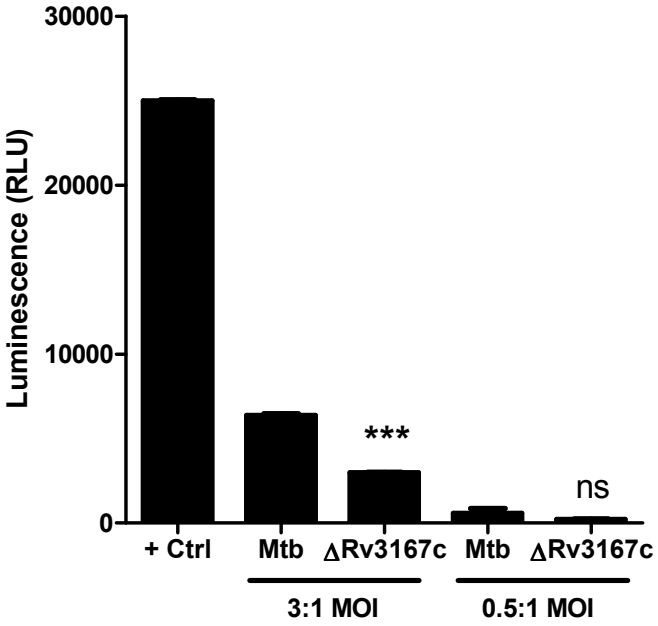

Figure 18: A low percentage of Δ*Rv3167c* infected THP-1 cells go through necrosis. AK release assay was performed 2 day post infection of THP-1 macrophages at MOIs of 3:1 and 0.5:1. Staurosporine was added to the cells as positive control. Data are means of triplicates of one representative experiment (n=3). Error bars represent SEM. Statistical significance was determined by one way analysis of variance (ANOVA) with Tukey post-test. ns, not significant; ***, $0.0001 < p < 0.001$.

more necrotic (0.8%) compared to cells infected with Mtb (2.3%). The significantly higher rate of necrosis for Mtb at MOI of 3:1 but not at 0.5:1 suggests that Mtb induces necrosis at higher MOIs. These results also suggest that the increased numbers of Mtb seen 2 day post infection following 3:1 MOI infection is due to Mtb replicating inside THP-1 cells, causing necrosis and getting out of the cell. The experiments with gentamicin strengthen this idea since the presence of gentamicin kills extracellular bacteria and neither an increase in numbers of Mtb nor a difference compared to Δ*Rv3167c* were seen (Figure 16A).

3.2 ANALYSIS OF EFFECTS OF Δ*RV3165C* OR Δ*RV3167C* INFECTION ON THE HOST CELLS

3.2.1 Δ*Rv3165c* and Δ*Rv3167c* induce high levels of caspase-3 and/or 7 and 8 activities in THP-1 cells

Apoptosis of macrophages infected with mycobacteria is mediated by the effector caspases 3 and 7 (79, 160, 161). In order to find if caspases are involved in the pro-apoptotic phenotype of Δ*Rv3165c* and Δ*Rv3167c* in 24hr infected cells, cells were stained with FLICA™ reagent. FLICA™ reagent consists of a fluorescent dye attached to a caspase inhibitor, which is a peptide sequence that binds to caspases. When the FLICA™ reagent enters the cell it binds to active caspase and is retained in the cell during the washes. The number of cells that contain activated caspase is then determined by flow cytometry. When caspase-3 and 7 FLICA™ reagent was used it was found that a higher percentage of THP-1 cells infected with Δ*Rv3165c* or Δ*Rv3167c* had caspase-3 and/or 7

activity (17.21% and 17.89% respectively) compared with Mtb infected cells (8.30%) (Figure 19A). Similarly, when caspase-8 FLICA™ reagent was used it was found that a higher percentage of THP-1 cells infected with Δ*Rv3165c* or Δ*Rv3167c* had caspase-8 activity (27.29% and 28.45% respectively) compared to Mtb infected cells (11.80%) (Figure 19B). However staining of the 24hr infected THP-1 cells with caspase-9 FLICA™ reagent showed that a similar percentage of THP-1 cells infected with Mtb, Δ*Rv3165c* or Δ*Rv3167c* had caspase-9 activity (7.84%, 11.1%, 13%) respectively (Figure 19C). These experiments showed that caspases-3 and/or 7 and 8 were activated in Δ*Rv3165c* and Δ*Rv3167c* infected THP-1 cells and that apoptosis of Δ*Rv3165c* and Δ*Rv3167c* infected cells was likely a result of the extrinsic pathway of caspase activation.

3.2.2 Inhibiting ROS production or scavenging ROS leads to loss of the pro-apoptotic phenotype of Δ*Rv3165c* and Δ*Rv3167c*

Increased levels of ROS can promote apoptosis by inducing prolonged JNK activation and blocking NF-κB activation (115). Previous work in our lab showed that the pro-apoptotic phenotype of Δ*nuoG* was abolished in the presence of ROS inhibitor or scavengers and that the phagosomes of cells infected with Δ*nuoG* had higher levels of ROS (149). Therefore, in order to investigate the involvement of host cell produced ROS in the apoptosis of Δ*Rv3165c* and Δ*Rv3167c* infected cells, ROS production was blocked by NADPH oxidase inhibitor diphenylene iodonium (DPI). Alternatively ROS scavengers were added to the infection and chase media to block the effects of ROS. Blocking ROS production by DPI led to loss of the pro-apoptotic phenotypes of Δ*Rv3165c* and Δ*Rv3167c*. 88.51% and 91.81% apoptosis seen in the Δ*Rv3165c* and

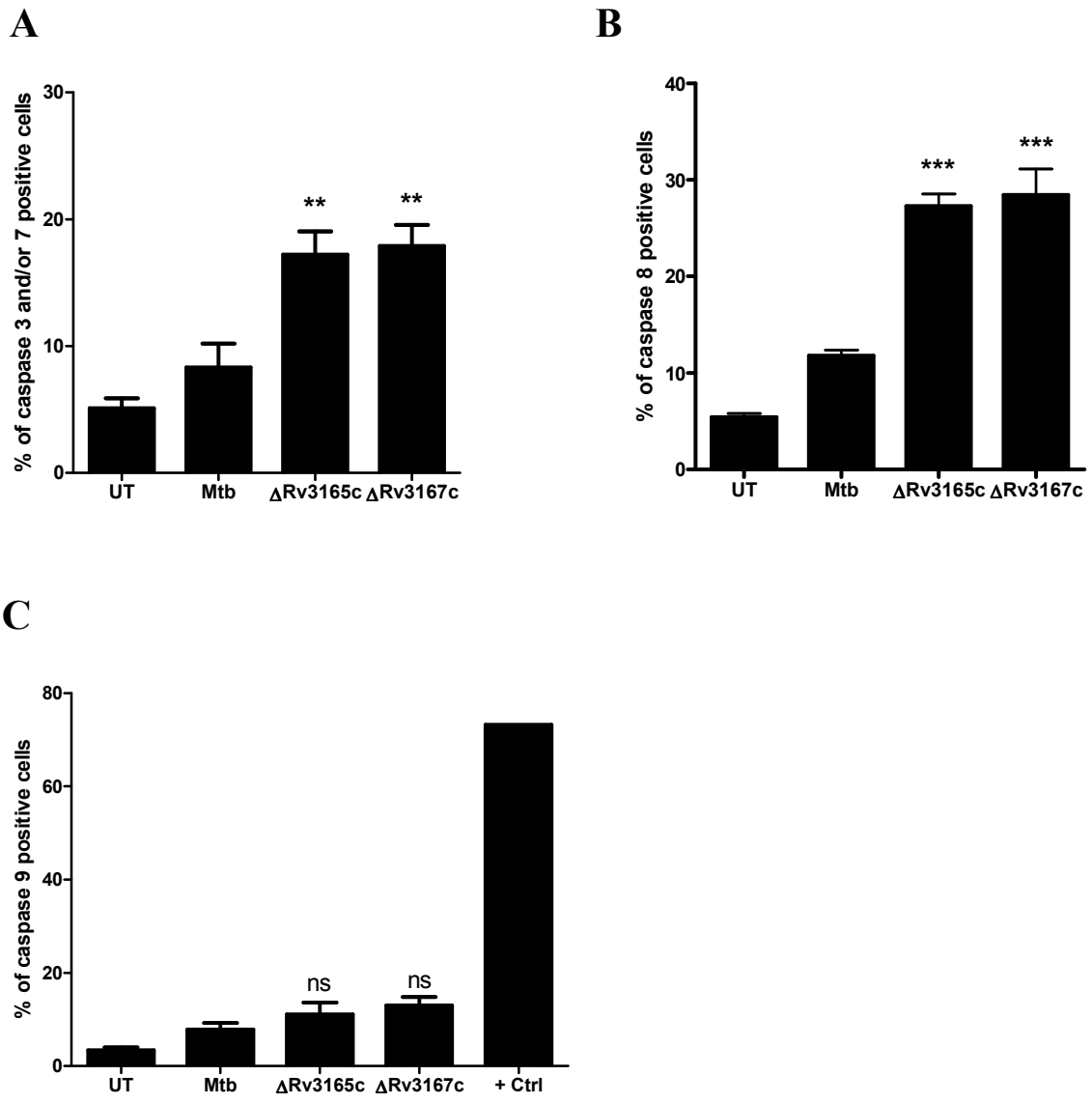

Figure 19: Δ*Rv3165c* and Δ*Rv3167c* induce significantly higher levels of caspase-3 and/or 7 and 8 but not caspase-9 activity in THP-1 cells. Caspase activities were detected by staining cells 24hr after infection with the FLICA™ reagent. For + control staurosporine (1μM) was added to uninfected cells. Data are the mean ± SEM of two independent experiments performed in duplicate (n=4). Statistical significance was determined by one way analysis of variance (ANOVA) with Tukey post-test. ns, not significant; **, $0.001 < p < 0.01$; ***, $0.0001 < p < 0.001$.

Δ*Rv3167c* infected cells was reduced to 15.98% and 17.76% respectively compared to 13.63% apoptosis in Mtb infected cells (Figure 20A). Addition of glutathione to the media led to a decrease of apoptosis from 24.13% and 18.48% for Δ*Rv3165c* and Δ*Rv3167c* infected cells to 1.05% and 0.51% respectively. Addition of NAC decreased the apoptosis levels to 1.03% and 1.84% (Figure 20B). Removal of ROS by these two methods and the loss of the pro-apoptotic phenotype of the knock-outs showed the involvement of ROS in the apoptosis of infected cells.

3.2.3 Secreted cytokine profile of cells infected with Mtb versus Δ*Rv3167c* or Δ*Rv3167c*::C

To identify any possible differences in the levels of IL-8, IL-1β, IL-6, IL-10, TNF-α and IL-12p70 after infection in the supernatants of THP-1 macrophages, the BD Cytometric Bead Array (CBA) Human Inflammatory Cytokines Kit was used. This kit was chosen as it could detect Th1 cytokines IL-12 and TNF-α, pro-inflammatry cytokines IL-1β and IL-6, and IL-10, which down regulates Th1 responses. No significant difference was found in the levels of these cytokines in the supernatants of THP-1 macrophages infected for 2 days with Mtb, Δ*Rv3167c* or Δ*Rv3167c*::C (Figure 21). Δ*Rv3167c* and its complement were chosen in this experiment due to sample limitations of the kit. However, in some of the following experiments *Rv3165c* was omitted due to the complexity and hardship of working with two strains compared to one. The lack of difference in the levels of cytokines tested indicates that the pro-apoptotic phenotype of Δ*Rv3167c* is not due to an increase or decrease in the secretion of these cytokines by the host cells.

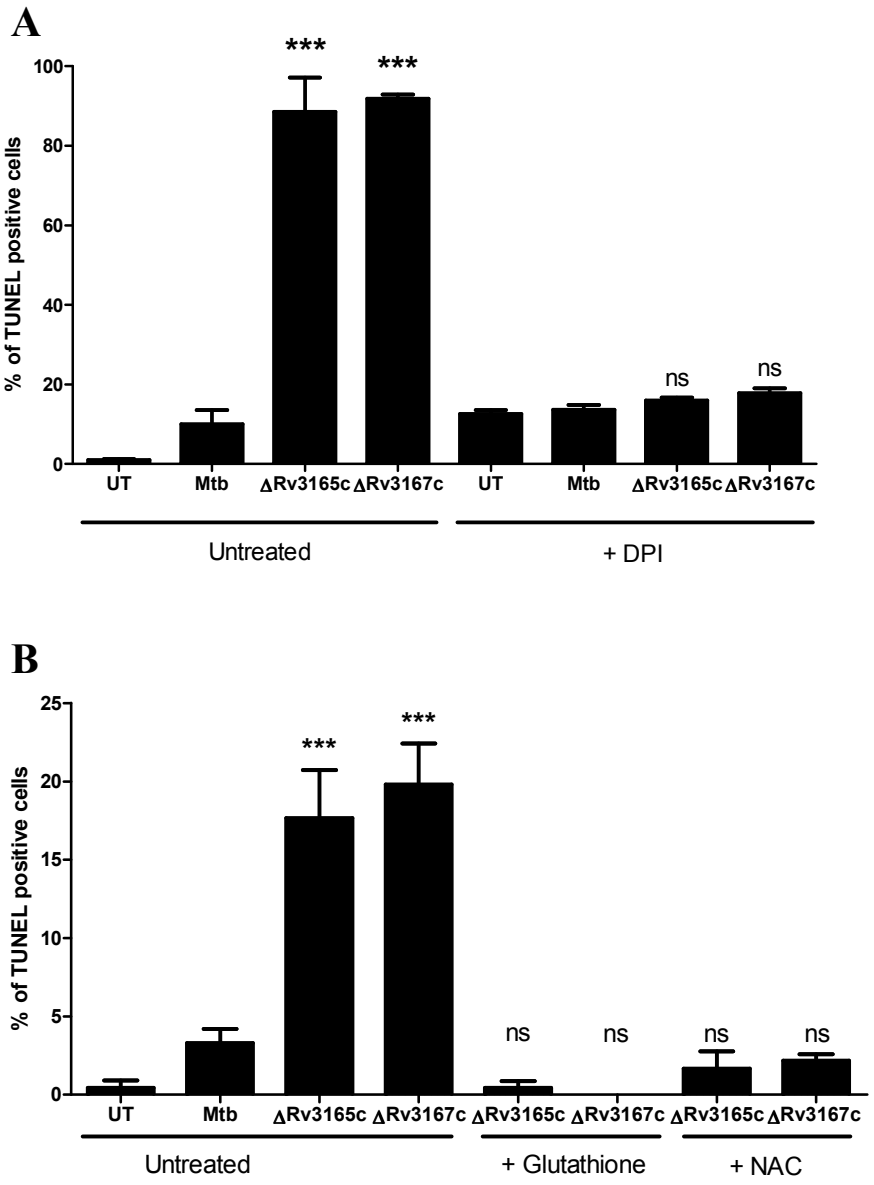

Figure 20: Inhibiting ROS production of scavenging ROS abolishes apoptosis induction by Δ*Rv3165c* and Δ*Rv3167c*. Infected THP-1 cells were incubated with DPI (A) or Glutathione or NAC (B) and were collected 2 days (A) or 36hrs (B) after infection and stained with TUNEL to determine the % of apoptotic cells Data are the mean ± SEM of two independent experiments performed in duplicate (n=4) (A) or the mean ± SEM of a representative experiment with four replicates per group (n=4) (B). Statistical significance was determined by one way analysis of variance (ANOVA) with Tukey post-test. ns, not significant; ***, $0.0001 < p < 0.001$.

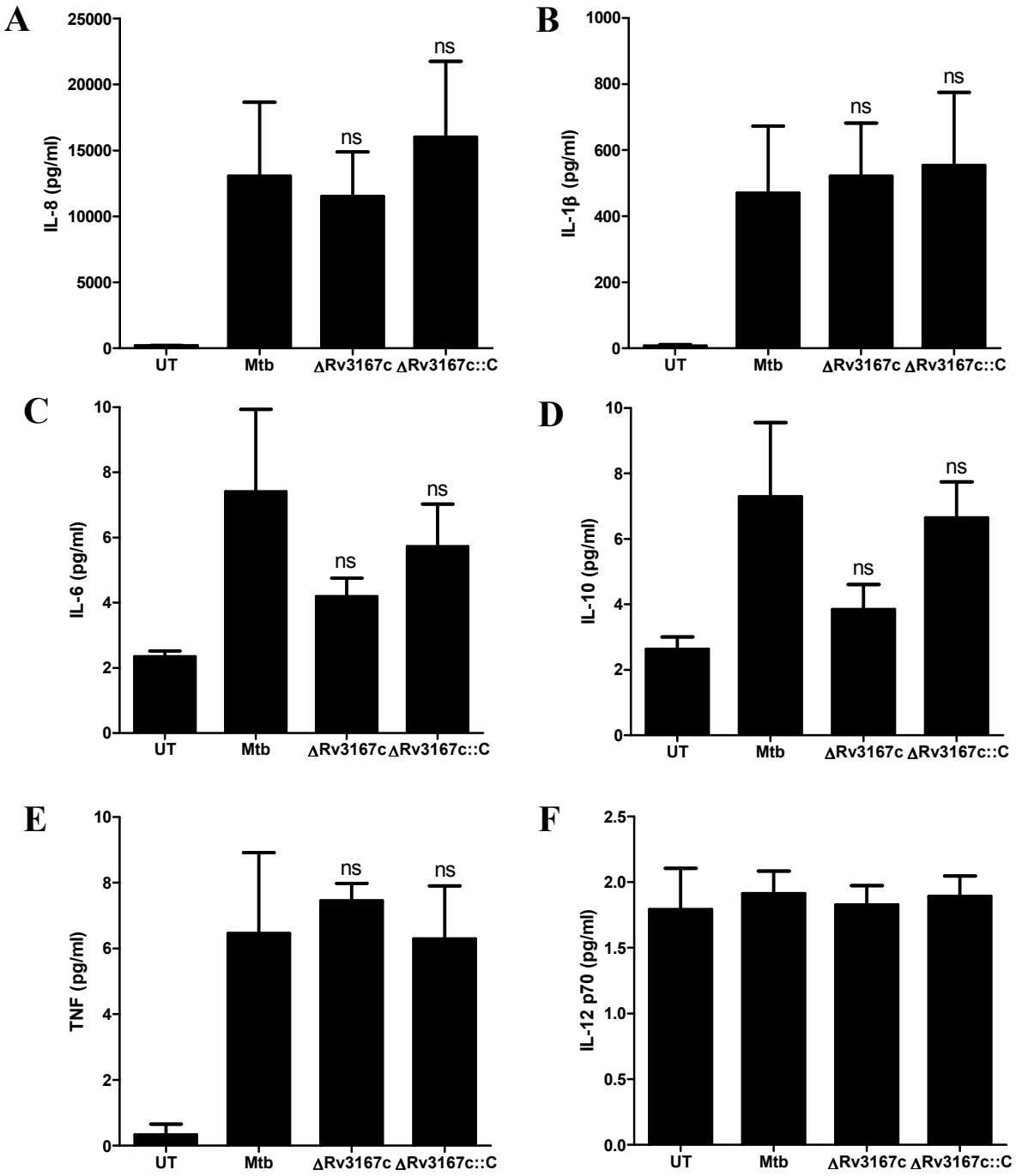

Figure 21: Detection of the amounts of cytokines in the supernatants of uninfected or Mtb or Δ*Rv3167c* or Δ*Rv3167c*::C infected THP-1 macrophages. A BD CBA kit was used to measure the amounts of IL-8 (A), IL-1β (B), IL-6 (C), IL-10 (D), TNF-α (E) and IL-12 p70 in the supernatants of uninfected THP-1 macrophages or THP-1 macrophages infected with Mtb or Δ*Rv3167c* or Δ*Rv3167c*::C. Data are the mean ± SEM of two independent experiments performed in duplicate (n=4). Statistical significance was determined by one way analysis of variance (ANOVA) with Tukey post-test versus Mtb. ns, not significant.

3.2.4 Deletion of *Rv3167c* changes the expression of host genes *in vivo*

In order to better understand how Δ*Rv3167c* induces apoptosis of THP-1 macrophages, the host gene expression profile was determined by RNA sequencing. RNA was isolated from uninfected THP-1 macrophages and from those that were infected with Mtb or Δ*Rv3167c* for 16hr. rRNA was removed from the total RNA samples and a RNA sequencing library was prepared. Sequencing of this library showed that there were 2332 differentially regulated genes in THP-1 macrophages infected with Mtb vs. Δ*Rv3167c*. 1223 genes were upregulated in Mtb infected THP-1 macrophages compared to 1109 genes in Δ*Rv3167c* infected THP-1 macrophages. There were few bacterial transcripts that were detected in these samples and comparison of bacterial gene expression could not be made. Real time qPCR (RT-qPCR) was used for selected transcripts to validate the results of RNA sequencing. *CCL20* was chosen as it is upregulated in Mtb infected monocytes. In addition, *CCL20* downregulates ROS production and inhibits apoptosis of monocytes infected with mycobacteria (162). *CCL3* was chosen as it is induced in macrophages after infection with Mtb and inhibits intracellular growth of Mtb (163). In addition since both molecules are secreted, ELISA could be employed to find their concentrations in the supernatants of infected cells. According to RNA sequencing, Mtb infected cells had 10 fold more *CCL3* FPKMs (fragment per kilobase of transcript per million mapped reads) than untreated cells and Δ*Rv3167c* infected cells had 62 fold more (Figure 22A). RT-qPCR result was similar to RNA sequencing result for *CCL3* expression (*CCL3* was 48.85 fold upregulated in Mtb infected cells and 316.11 fold upregulated in Δ*Rv3167c* infected cells) (Figure 22B). According to RNA sequencing, Mtb infected cells had 351 fold more *CCL20* FPKMs

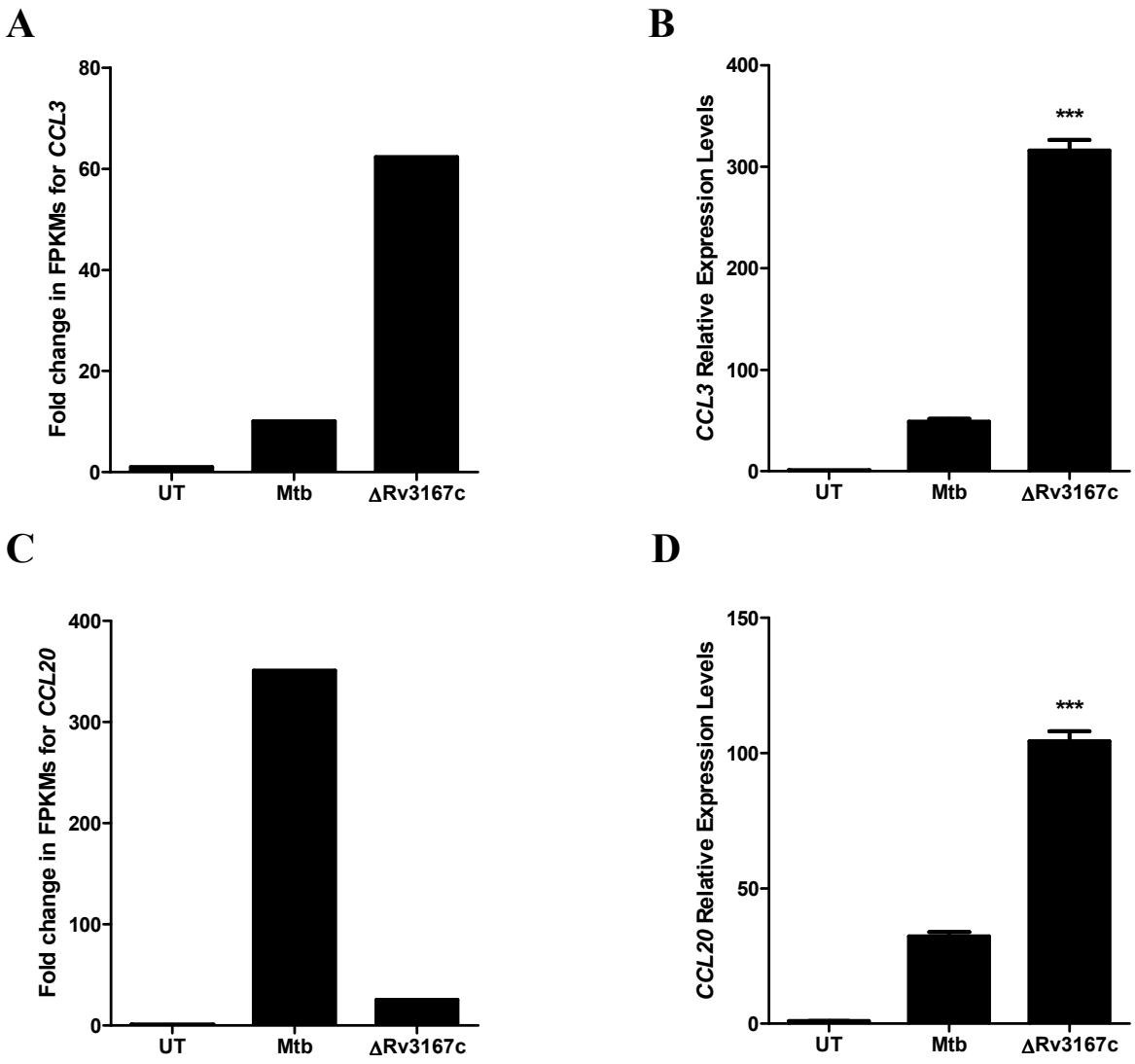

Figure 22: Regulation of *CCL3* and *CCL20* expression in Mtb and Δ*Rv3167c* infected THP-1 macrophages. *CCL3* and *CCL20* expression levels were determined in Mtb and Δ*Rv3167c* infected THP-1 macrophages 16 hr after infection by RNA sequencing (A and C) or by real-time qPCR (B and D). Plotted values are fold change in FPKMs for *CCL3* (A) or *CCL20* (C) relative to untreated cells. For B and D data are the mean ± SEM of one experiment performed in triplicate (n=3) and the results are depicted as fold change relative to Mtb infected cells and normalized for expression of the housekeeping gene GAPDH. Statistical significance was determined by one way analysis of variance (ANOVA) with Tukey post-test. ***, $0.0001 < p < 0.001$.

then untreated cells and Δ*Rv3167c* infected cells had 26 fold more (Figure 22C). RT-qPCR showed a different trend compared to RNA sequencing result for *CCL20* expression (*CCL20* was 32.32 fold upregulated in Mtb infected cells and 104.4 fold upregulated in Δ*Rv3167c* infected cells) (Figure 22D). These results confirmed the upregulation of *CCL3* following infection with Mtb.

In order to find which of the results was correct for *CCL20* and confirm *CCL3* results at the protein level, ELISA was used to assay for CCL3 and CCL20. ELISA for CCL3 showed that there was significantly more CCL3 in the supernatants of Δ*Rv3167c* infected THP-1 macrophages (227 pg/ml) than Mtb infected ones (184 pg/ml) 24 hrs after infection. ELISA also showed that 48 hr after infection, there was significantly more CCL3 in the supernatants of Δ*Rv3167c* infected THP-1 macrophages (267 pg/ml) than Mtb infected ones (69 pg/ml) (Figure 23A). The decrease in CCL3 levels in untreated and Mtb infected cells between 24 and 48 hr is thought to be due to degradation. Cancer cell lines are implicated in degradation of CCL3 (164) and THP-1 cell line can also be degrading CCL3 in the supernatant. The lack of a decrease for Δ*Rv3167c* might be due to high levels of CCL3 translation in the cells that hides a decrease in CCL3 levels in the supernatant. While ELISA confirmed CCL3 expression differences that were seen both in RNA sequencing and qPCR, CCL20 protein levels were slightly lower in the supernatants of Δ*Rv3167c* infected THP-1 macrophages (540 pg/ml) than in the supernatants of Mtb infected ones (737 pg/ml) 24 hrs after infection and also similar in the supernatants of Δ*Rv3167c* infected THP-1 macrophages (676 pg/ml) compared to the supernatants of Mtb infected ones (760 pg/ml) 48 hrs after infection (Figure 23B). Therefore ELISA of CCL20 did not validate the RNA sequencing or qPCR result. These

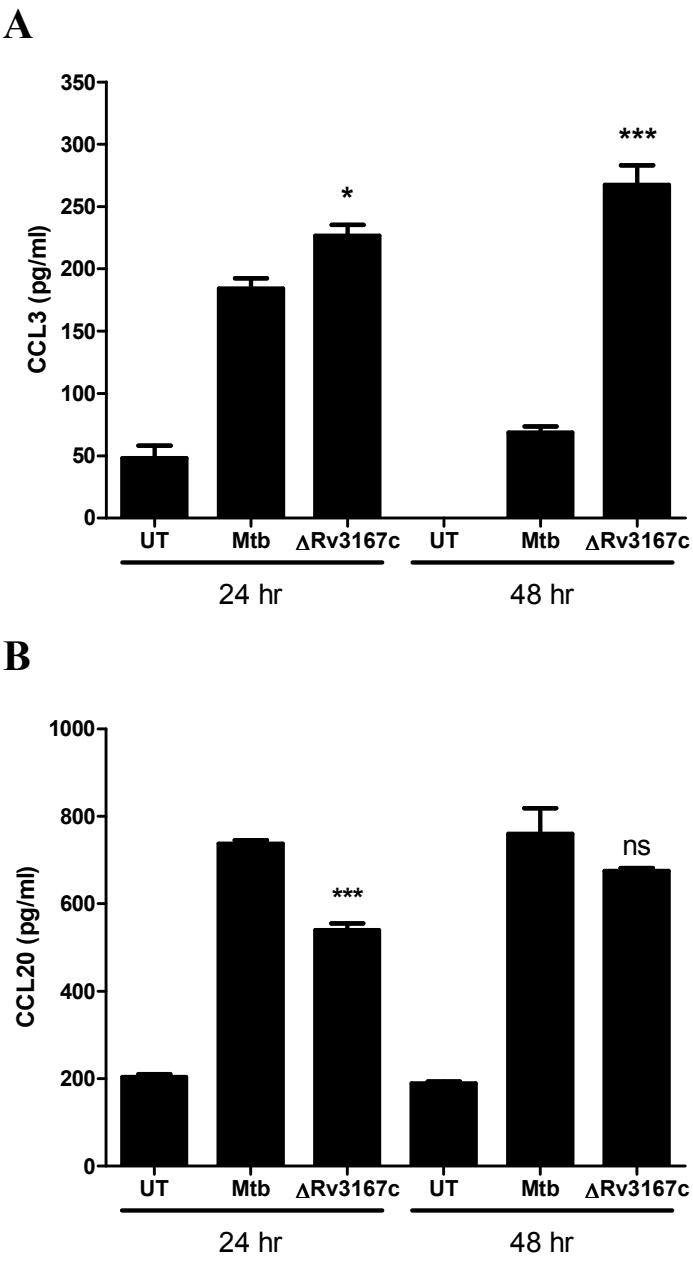

Figure 23: ELISA confirms upregulation of *CCL3* expression in Δ*Rv3167c* infected THP-1 macrophages. CCL3 and CCL20 protein concentrations in the cell culture supernatants were measured using DuoSet ELISA kits. Data are the mean ± SEM of two experiments performed in triplicate (n=6). Statistical significance was determined by one way analysis of variance (ANOVA) with Tukey post-test versus Mtb. ns, not significant; *, $0.05< p <0.01$; ***, $0.0001< p < 0.001$.

results show that a biological replicate of the RNA sequencing experiment is necessary and that the results need to be confirmed by qPCR. Also it is important to show that the differences in gene expression lead to differences in protein expression since it is mostly the difference in protein levels (or activation or deactivation of proteins) that can make a difference in the phenotype.

3.2.5 Deletion of *Rv3167c* changes the expression of host pro-apoptotic and anti-apoptotic proteins *in vivo*

In order to find if the differences in the gene expression levels led to differences in protein expression and phosphorylation, the expression and phosphorylation state of some of the host proteins was determined. Whole cell lysates of THP-1 macrophages infected with Mtb or Δ*Rv3167c* were prepared 8 and 24hrs after infection. 100µg of samples were sent to Kinexus Bioinformatics Corporation, which used the protein samples in antibody microarray experiments. For the antibody microarray, proteins in the whole cell lysates were attached to fluorescent dye. Control and treated proteins were loaded on the same microarray side by side. After incubation, slides are washed and scanned. Analysis of the results showed that 33 proteins were differentially regulated in cells infected with Mtb vs. Δ*Rv3167c* for 8hr (Figure 24A). Twenty four proteins were differentially regulated in cells infected with Mtb vs. Δ*Rv3167c* for 24hr (Figure 24B). After 8hrs of infection several pro-apoptotic proteins like ABL1, AIFM1, BID, ASK1, and BAK were upregulated in Δ*Rv3167c* infected THP-1 macrophages. Anti-apoptotic proteins like RAF1, MAPKK5, RB1, PPP5C, AKT3, SMAD1 were down regulated in Δ*Rv3167c* infected THP-1 macrophages compared to Mtb. After 24 hr of infection

A

Target Protein Name	Phospho Site (Human)	Full Target Protein Name	Z score (VB1)	Z score (VB2)	Z-score Difference (VB2-VB1)	Z-ratio (VB2, VB1)
Hsp27	S82	Heat shock 27 kDa protein beta 1 (HspB1)	-4.36	-1.87	2.48	7.84
Abl	Pan-specific	Abelson proto-oncogene-encoded protein-tyrosine kinase	-0.87	0.19	1.06	3.35
4E-BP1	S65	Eukaryotic translation initiation factor 4E binding protein 1 (PHAS1)	-0.85	0.16	1.01	3.20
4E-BP1	T45	Eukaryotic translation initiation factor 4E binding protein 1 (PHAS1)	0.20	1.15	0.95	3.00
Adducin a + Adducin g	S726 + S693	Adducin alpha (ADD1) + Adducin gamma (ADD3)	-0.03	0.70	0.73	2.30
Acetylated Lysine	Pan-specific	Acetylated Lysine	-0.88	-0.19	0.69	2.18
PDK1	Pan-specific	3-phosphoinositide-dependent protein-serine kinase 1	0.13	0.82	0.68	2.16
AIF	Pan-specific	Apoptosis inducing factor (programed cell death protein 8 (PDCD8))	0.43	1.10	0.68	2.14
14-3-3 z	Pan-specific	14-3-3 protein zeta (cross-reacts with other isoforms)	-0.08	0.59	0.67	2.13
CASP9	Pan-specific	Caspase 9 (ICE-like apoptotic protease 6 (ICE-LAP6), Mch6, APAF3)	-1.22	-0.54	0.67	2.13
Cdc25C	S216	Cell division cycle 25C phosphatase	-1.34	-0.66	0.67	2.12
ATF2	Pan-specific	Activating transcription factor 2 (CRE-BP1)	-1.13	-0.51	0.62	1.97
PARP1	Pan-specific	Poly [ADP-ribose] polymerase 1 (ADPRT)	-2.43	-1.81	0.62	1.95
Hsp40	Pan-specific	DnaJ homolog, subfamily B member 1	-0.11	0.44	0.55	1.73
AcCoA carboxylase	S80	Acetyl coenzyme A carboxylase	0.97	1.49	0.52	1.63
Bid	Pan-specific	BH3 interacting domain death agonist	0.04	0.55	0.51	1.60
ErbB2 (HER2)	Pan-specific	ErbB2 (Neu) receptor-tyrosine kinase	-0.49	0.01	0.50	1.59
ASK1 (MAP3K5)	S1046	Apoptosis signal regulating protein-serine kinase	-0.02	0.49	0.50	1.59
Bak	Pan-specific	Bcl2 homologous antagonist/killer (BCK2L7)	0.36	0.85	0.49	1.55
ALS2CR7 (PFTAIRE2)	Pan-specific	Amyotrophic lateral sclerosis 2 chromosomal region candidate gene protein-serine kinase 7	-0.16	0.32	0.49	1.54
Synapsin 1	S605	Synapsin 1 isoform Ia	-0.93	-1.41	-0.48	-1.50
RafB (Braf)	Pan-specific	RafB proto-oncogene-encoded protein-serine kinase	0.24	-0.24	-0.48	-1.52
ZIPK	Pan-specific	ZIP kinase (death associated protein-serine kinase 3 (DAPK3))	-0.34	-0.83	-0.49	-1.55
Fes	Pan-specific	Fes/Fps protein-tyrosine kinase	0.65	0.15	-0.49	-1.56
Rb	S780	Retinoblastoma-associated protein 1	-0.05	-0.54	-0.50	-1.57
Smad1/5/8	5/S463+S465/S	Mothers against decapentaplegic homologs 1/5/8	-1.29	-1.82	-0.53	-1.69
PKBg (Akt3)	Pan-specific	Protein-serine kinase B gamma	0.58	0.01	-0.57	-1.79
MEK3 (MAP2K3)	S218	MAPK/ERK protein-serine kinase 3 (MKK3)	-0.14	-0.71	-0.58	-1.83
PP5C	Pan-specific	Protein-serine phosphatase 5 - catalytic subunit (PPT)	-0.18	-0.80	-0.62	-1.96
Rb	Pan-specific	Retinoblastoma-associated protein 1	-0.31	-1.00	-0.69	-2.19
MEK5 (MAP2K5)	Pan-specific	MAPK/ERK protein-serine kinase 5 (MKK5)	0.86	0.10	-0.77	-2.42
Rab5	Pan-specific	Ras-related protein Rab-5A	-0.66	-1.50	-0.84	-2.64
Raf1	Pan-specific	Raf1 proto-oncogene-encoded protein-serine kinase	0.60	-0.32	-0.92	-2.90

B

Target Protein Name	Phospho Site (Human)	Full Target Protein Name	Z score (VB5)	Z score (VB6)	Z-score Difference (VB6-VB5)	Z-ratio (VB6, VB5)
ANKRD3	Pan-specific	Ankyrin repeat domain protein-serine kinase 3 (RIPK4, DIK)	-0.04	1.30	1.34	3.48
ERP72	Pan-specific	ER protein 72 kDa (protein disulfide isomerase-associated 4)	-1.04	0.11	1.15	2.98
AK2	Pan-specific	Adenylate kinase 2	-0.04	0.94	0.98	2.54
Ksr1	Pan-specific	Protein-serine kinase suppressor of Ras 1	-0.87	0.03	0.90	2.33
IKKb	Pan-specific	Inhibitor of NF-kappa-B protein-serine kinase beta	-0.71	0.17	0.88	2.29
Erk2	Pan-specific	Extracellular regulated protein-serine kinase 2 (p42 MAP kinase)	-0.61	0.24	0.85	2.21
ASK1 (MAP3K5)	S1046	Apoptosis signal regulating protein-serine kinase	0.03	0.80	0.77	2.00
Erk5	Pan-specific	Extracellular regulated protein-serine kinase 5 (Big MAP kinase 1 (BMK1))	-0.90	-0.15	0.75	1.96
ASK1 (MAP3K5)	Pan-specific	Apoptosis signal regulating protein-serine kinase	0.64	1.38	0.75	1.93
ILK1	Pan-specific	Integrin-linked protein-serine kinase 1	-1.30	-0.56	0.74	1.93
Cdc25C	S216	Cell division cycle 25C phosphatase	-1.33	-0.64	0.70	1.81
AIF	Pan-specific	Apoptosis inducing factor (programed cell death protein 8 (PDCD8))	0.50	1.17	0.67	1.74
Aurora C (AIK3)	Pan-specific	Aurora Kinase C (serine/threonine-protein kinase 13)	-0.83	-0.22	0.62	1.60
eIF4E	Pan-specific	Eukaryotic translation initiation factor 4 (mRNA cap binding protein)	-0.79	-0.18	0.61	1.58
S6Kb1	Pan-specific	Ribosomal protein-serine S6 kinase beta 1	1.76	1.17	-0.59	-1.52
Hsp27	S82	Heat shock 27 kDa protein beta 1 (HspB1)	-1.93	-2.52	-0.59	-1.54
SODD	Pan-specific	Silencer of death domains (Bcl2 associated athanogene 4 (BAG4))	0.60	0.00	-0.60	-1.56
PP1/Cb	Pan-specific	Protein-serine phosphatase 1 - catalytic subunit - beta isoform	-0.06	-0.69	-0.64	-1.65
PAK1	T212	p21-activated kinase 1 (alpha) (serine/threonine-protein kinase PAK 1)	1.15	0.51	-0.64	-1.67
MEK1 (MAP2K1)	Pan-specific	MAPK/ERK protein-serine kinase 1 (MKK1)	-0.11	-0.75	-0.65	-1.68
PP2A/Aa/b	Pan-specific	Protein-serine phosphatase 2A - A regulatory subunit - alpha and beta isoforms	0.12	-0.54	-0.66	-1.72
Rab5	Pan-specific	Ras-related protein Rab-5A	-1.18	-1.86	-0.68	-1.77
Tyk2	Pan-specific	Protein-tyrosine kinase 2 (Jak-related)	0.46	-0.23	-0.69	-1.79
MLK3	Pan-specific	Mixed-lineage protein-serine kinase 3	0.63	-0.08	-0.71	-1.85

Figure 24: THP-1 macrophage proteins whose expression or phosphorylation have changed 8 hrs or 24 hrs after infection with Δ*Rv3167c* compared to Mtb. 100µg of whole cell lysates of THP-1 macrophages infected with Mtb or Δ*Rv3167c* were prepared 8 (A) and 24hr (B) after infection and used in antibody microarray experiments. Z scores are calculated by subtracting the overall average intensity of all spots within a sample from the raw intensity for each spot, and by dividing it by the standard deviations (SD) of all of the measured intensities within each sample. Z ratios are further calculated by taking the difference between the averages of the observed protein Z scores and dividing by the SD of all of the differences for that particular comparison. A Z ratio of ±1.2-1.5 is inferred as significant. Pink color indicates upregulation in Δ*Rv3167c* infected cells, blue color indicates downregulation in Δ*Rv3167c* infected cells.

expression of pro-apoptotic proteins like RIPK4, AK2, ASK1 and AIFM1 was up regulated in Δ*Rv3167c* infected THP-1 macrophages. At the same time expression of anti-apoptotic proteins like SODD, MKK1 and MLK3 was downregulated in Δ*Rv3167c* infected THP-1 macrophages.

Activation of ABL1 (Abelson tyrosine-protein kinase 1) leads to JNK and p38 MAPK activation followed by induction of apoptosis (165). ASK1 (Apoptosis signal regulating protein-serine kinase, MAP3K5) activation also induces apoptosis through JNK and p38 MAPK (166). ATF2 (Activating transcription factor 2) is a transcriptional activator that gets activated by p38 MAPK and induces apoptosis (167, 168). Increased expression or phosphorylation of these proteins suggests that the apoptosis of Δ*Rv3167c* infected THP-1 macrophages might be regulated via JNK and/or p38 MAPK. According to preliminary experiments, inhibiting p38 MAPK activity reduced the apoptosis levels of Δ*Rv3167c* infected human MDM's to the level of wild-type Mtb infected cells (Srinivasan L, unpublished data).

Some of the proteins that were found to be regulated are involved in caspase-9 activation. Cleaved BID (BH3-interacting domain death agonist) leads to release of cytochrome c from mitochondria and caspase-9 activation (169). BAK (Bcl-2 homologous antagonist/killer) works against the anti-apoptotic function of BCL2 and promotes cytochrome c release and caspase-9 activation (170). Knocking down AKT3 leads to increased caspase-9 activity and apoptosis (171). In addition, caspase-9 was found to be upregulated in the antibody microarray. However, as shown in figure 19 Δ*Rv3167c* infected cells did not have significantly higher levels of active caspase-9.

Therefore, we believe that either these results are false positives or caspase-9 levels go down after 8 hr.

3.3 EFFECT OF DELETION OF *RV3165C* AND *RV3167C* ON MYCOBACTERIAL GENE EXPRESSION

3.3.1 *Rv3165c* and *Rv3167c* are required for the increase of *katG* expression inside host cells

The involvement ROS in the pro-apoptotic phenotype of the knock-out strains suggested that the bacteria might lack mechanisms that are able to counter the effects of ROS. Mtb only has one catalase gene (*katG*) that can neutralize the ROS hydrogen peroxide, which led to the idea that *katG* might be regulated by *Rv3165c* and/or *Rv3167c*.

Rv3167c is a probable transcriptional regulatory protein that might belong to the TetR family of transcription factors (TFRs) (44) and this predicted function raised the possibility that Rv3167c might regulate the expression of other genes. According to InterProScan, a software that can identify protein domains, Rv3167c contains an N-terminal TetR-type DNA-binding (DNB) helix-turn-helix domain and a C-terminal TetR-like transcriptional regulator domain that includes ligand-binding and dimerization (LBD) domain (Figure 25) (172). Most of the TFRs repress transcription of genes when they bind to DNA through their DNB domain. Upon binding of a ligand to their C-terminal (LBD) domain, TFRs detach from DNA (173). There is evidence that some TFRs acting as activators. SczA of *Streptococcus pneumoniae* is a member of TFRs and it is involved in the upregulation of genes associated with Zn^{2+} stress (174). MdoR of *Mycobacterium* sp. Strain JC1, was shown to be a TetR-like transcriptional activator,

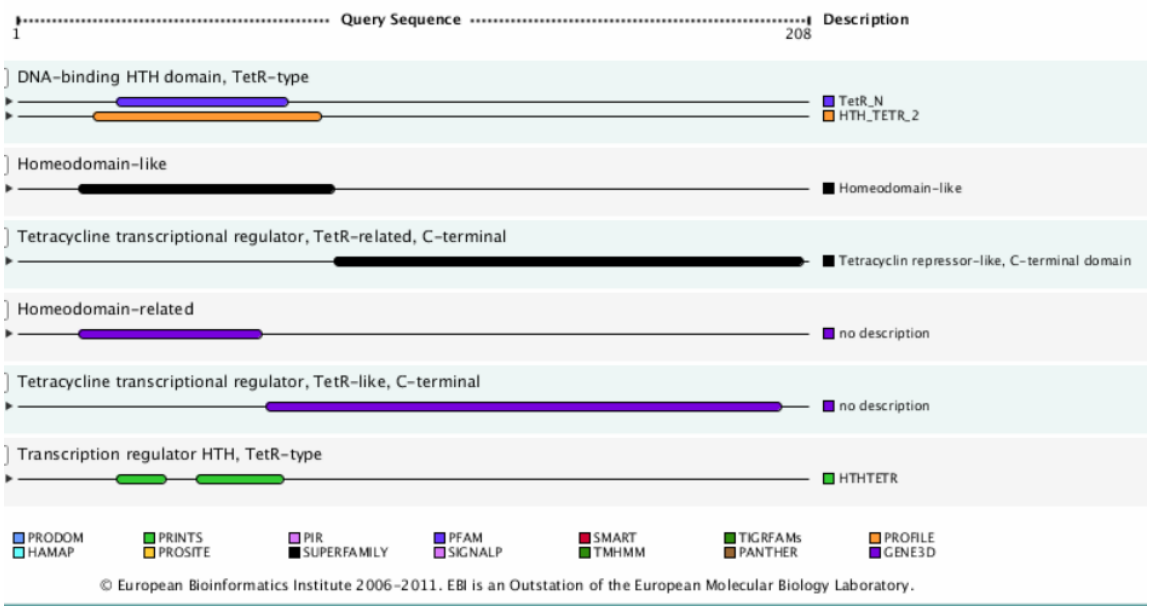

Figure 25: InterProScan result for prediction of protein domains of Rv3167c.

which is implicated in the upregulation of genes necessary for the oxidation of methanol (175).

RNA was isolated from Mtb, Δ*Rv3165c* and Δ*Rv3167c* grown *in vitro* to log phase. Following reverse transcription, real time qPCR was performed to measure *katG* expression. *katG* expression levels were similar in Δ*Rv3165c* (1.31 fold over Mtb) and Δ*Rv3167c* (1.18 fold over Mtb) compared to Mtb and the difference was not statistically significant (Figure 26A).

To check for the effect of ROS on *katG* expression *in vitro*, xanthine and xanthine oxidase were added to Mtb, Δ*Rv3165c* and Δ*Rv3167c in vitro* cultures to induce hydrogen peroxide formation after they were resuspended in PBS. After 90 min of incubation, RNA was isolated from the bacteria. Following reverse transcription, real time qPCR was performed to measure *katG* expression. *katG* expression was found to increase in not only Mtb (23.59 fold over Mtb *in vitro*) but also in Δ*Rv3165c* and Δ*Rv3167c* (33.88 and 33.96 fold over Mtb *in vitro*) (Figure 26B). To determine if Δ*Rv3165c* and Δ*Rv3167c* can upregulate *katG* expression in macrophages as well, THP-1 cells were infected with Mtb, Δ*Rv3165c* and Δ*Rv3167c* for 16hr and RNA was isolated from infected cells. Following reverse transcription, real time qPCR was performed to measure *katG* expression. Although in macrophages Mtb upregulated *katG* expression 12.25 fold over Mtb *in vitro*, Δ*Rv3165c* and Δ*Rv3167c* upregulated *katG* 5.62 and 8.44 fold less than Mtb in macrophages respectively (2.18 and 1.45 fold upregulation over Mtb *in vitro*) (Figure 26C). These results suggest that Mtb requires *Rv3165c* and *Rv3167c* to upregulate *katG* expression during infection of macrophages. As *katG* encodes for catalase, upregulation of *katG* is thought to be required to neutralize ROS during an

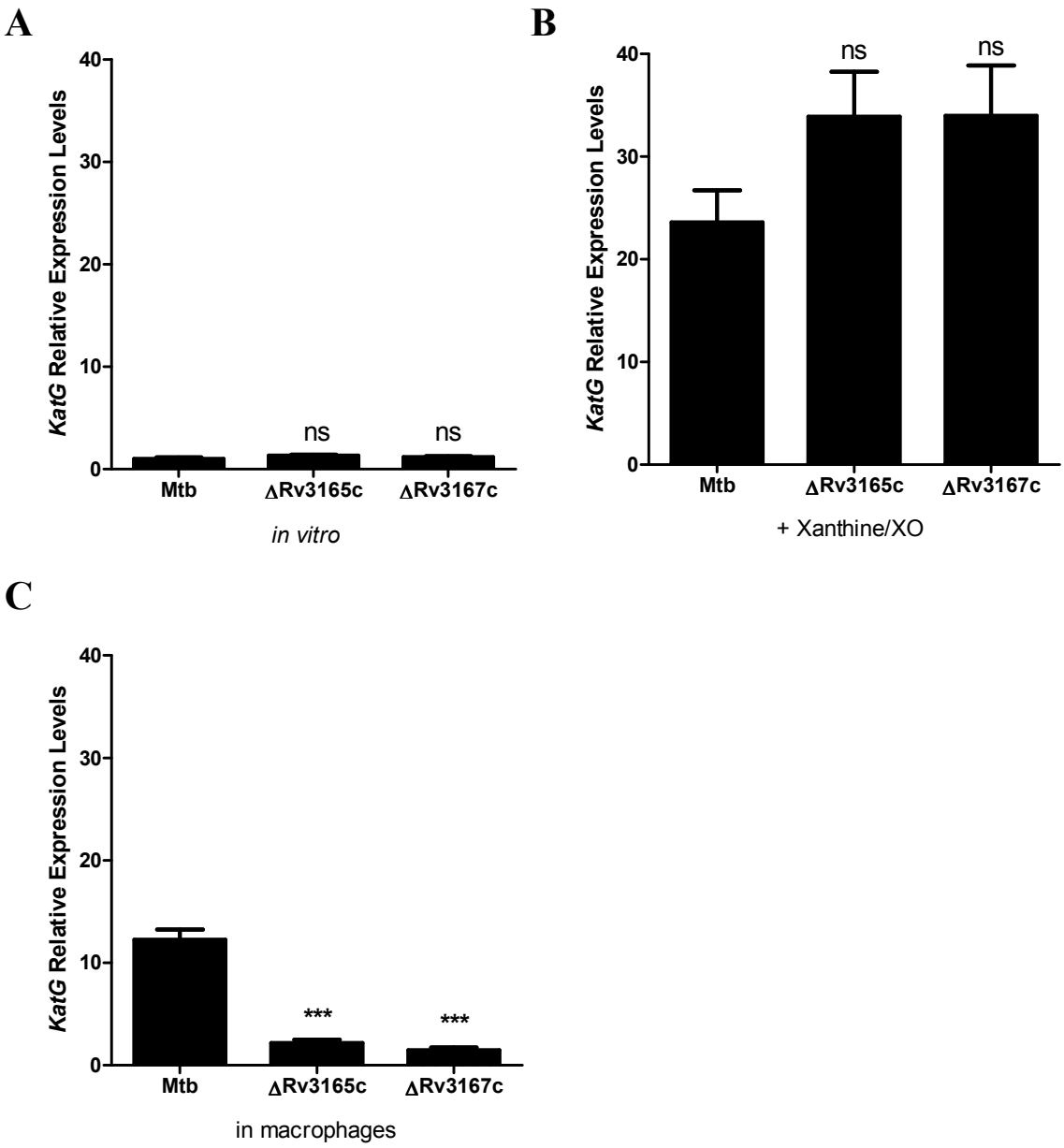

Figure 26: Δ*Rv3165c* and Δ*Rv3167c* do not upregulate *katG* expression in macrophages. RNA was isolated from untreated *in vitro* cultures (A) or xanthine and xanthine oxidase treated *in vitro* cultures (B) or THP-1 cells infected with mycobacteria for 16 hr (C). cDNA was synthesized from RNA and used in real time qPCR experiments. Data are of one representative experiment with three replicates per group (n=3). Error bars represent SEM. Results are depicted as fold change relative to Mtb under the same conditions and normalized for expression of the housekeeping gene *SigA*. Statistical significance was determined by one way analysis of variance (ANOVA) with Tukey post-test. ns, not significant; ***, $0.0001 < p < 0.001$.

infection and lack of upregulation of katG in ΔRv3165c and ΔRv3167c can explain involvement of ROS in the pro-apoptotic phenotypes of those mutants.

3.3.2 *Rv3165c* is required for *Rv3167c* expression inside host cells

As *Rv3167c* is predicted to be a probable transcriptional regulatory protein and *Rv3165c* and *Rv3167c* are close to each other in the Mtb genome, RT-qPCR was performed to determine if *Rv3165c* and *Rv3167c* regulate each others' mRNA expression. To determine if *Rv3165c* and *Rv3167c* exert their anti-apoptotic activity through *nuoG*, its expression was measured as well. The expression of *nuoB* was determined as a control since it is a part of the operon that includes *nuoG* (147). The lack of *Rv3165c* or *Rv3167c* did not affect the expression levels of any of the genes investigated *in vitro* (Figure 27A). *NuoB* and *nuoG* expression levels were not affected by the lack of *Rv3167c* in macrophages either (Figure 27B).

Real time qPCR was used to measure the expression of *Rv3167c* in Δ*Rv3165c*, and *Rv3165c* in Δ*Rv3167c*. *Rv3165c* expression in Δ*Rv3167c* was 1.17 fold increased compared to Mtb in macrophages but that was not a significant difference (Figure 28A). While Mtb upregulated *Rv3167c* expression significantly in macrophages (11.48 fold) compared to Mtb grown in 7H9, Δ*Rv3165c* did not upregulate *Rv3167c* expression significantly in macrophages (1.43 fold over Mtb) (Figure 28B). Therefore, it was concluded that *Rv3165c* was required for induced *Rv3167c* expression in macrophages.

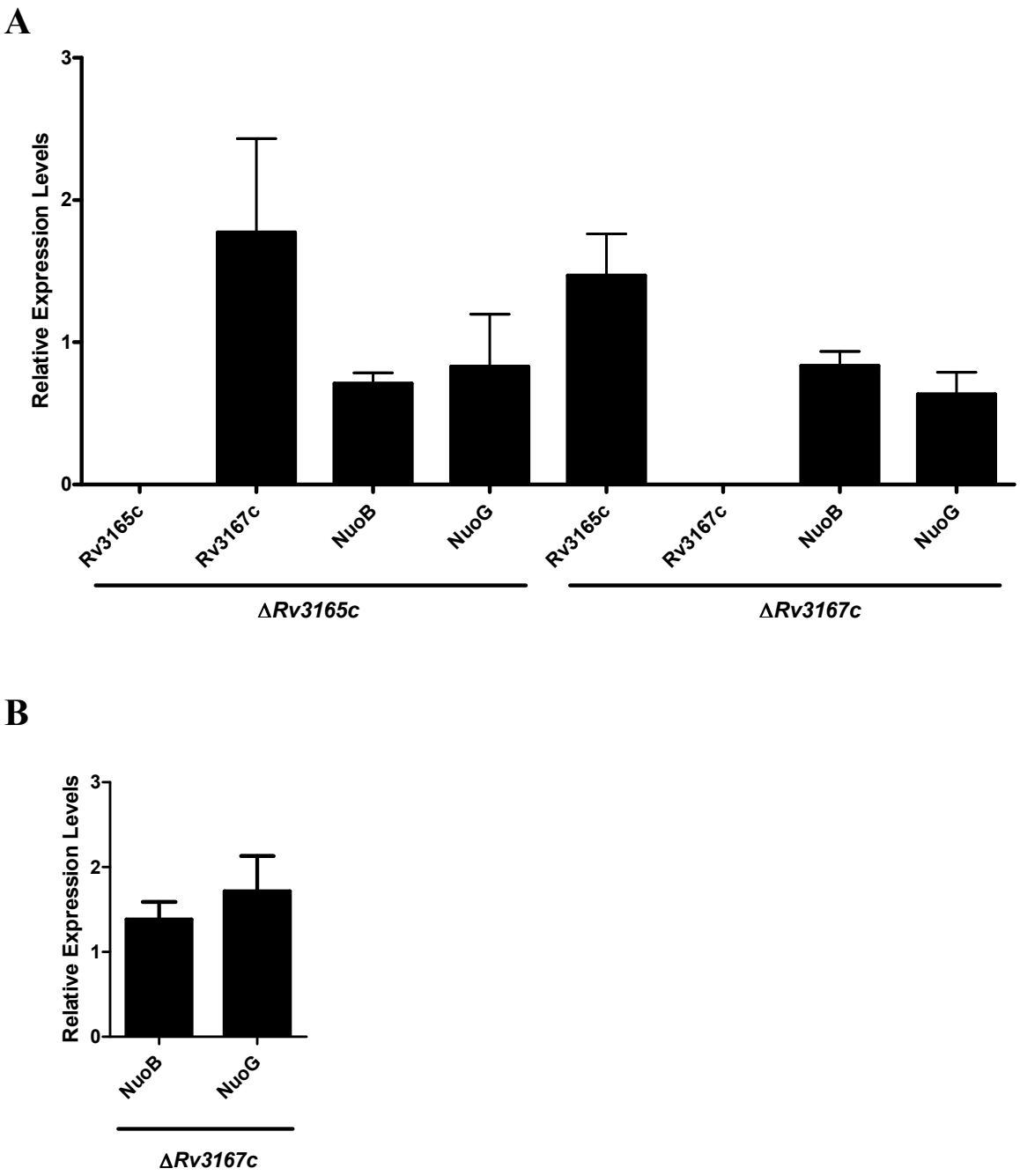

Figure 27: Regulation of *Rv3165c*, *Rv3167c*, *katG*, *nuoB*, *nuoG in vitro* and in macrophages. RNA was isolated from *in vitro* Mtb, Δ*Rv3165c* and Δ*Rv3167c* cultures and from THP-1 cells infected with Mtb or Δ*Rv3167c* for 16 hr. cDNA was synthesized from the RNA and used in real time qPCR experiments. Data are the mean ± SEM of three (n=9) (A) or two (B) independent experiments performed in triplicate (n=6). Statistical significance was determined by one way analysis of variance (ANOVA) with Tukey post-test. Results are depicted as fold change relative to Mtb *in vitro* (A) or relative to Mtb in macrophages (B) and normalized for expression of the housekeeping gene *SigA*.

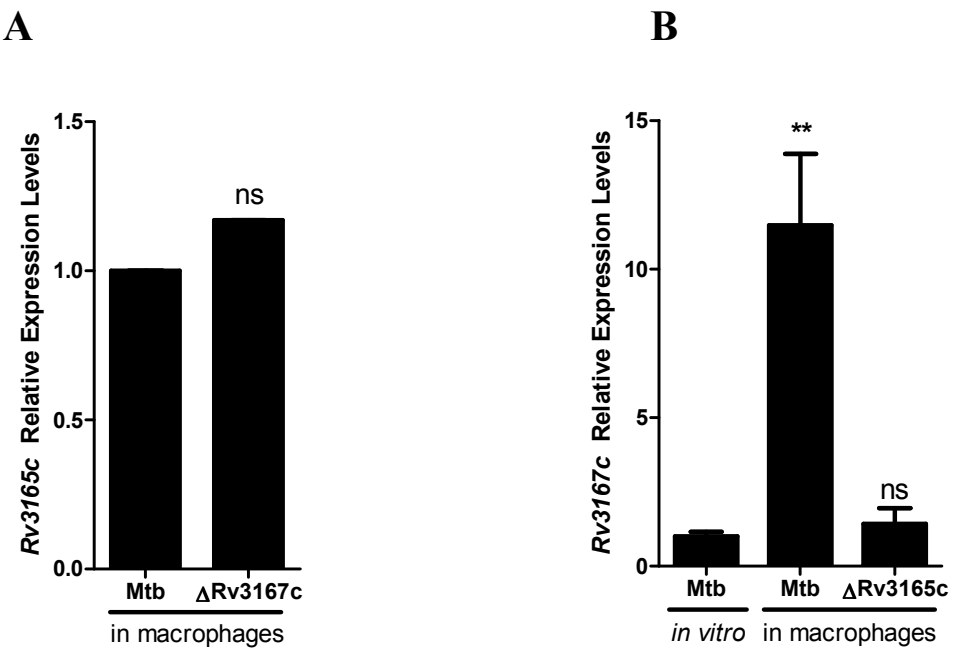

Figure 28: Δ*Rv3165c* do not upregulate *Rv3167c* expression in macrophages. RNA was isolated from *in vitro* Mtb, Δ*Rv3165c* and Δ*Rv3167c* cultures and from THP-1 cells infected with these strains for 16 hr. cDNA was synthesized from the RNA and used in real time qPCR experiments. Data are of a representative experiment (out of 3) with three replicates per group (n=3). Error bars represent SEM. Results are depicted as fold change relative to Mtb in macrophages (A) or Mtb *in vitro* and normalized for expression of the housekeeping gene *SigA*. Statistical significance was determined by one way analysis of variance (ANOVA) with Tukey post-test. ns, not significant; **, $0.001 < p < 0.01$.

3.4 ANALYSIS OF CELLULAR LOCALIZATIONS OF RV3165C AND RV3167C

To obtain information about the cellular localizations and better understand the functions of Rv3165c and Rv3167c, myc-tagged Rv3165c and Rv3167c were expressed in BCG. Subcellular fractions were prepared and the distributions of the myc-tagged proteins in those fractions were analyzed. Additionally possible presence of the myc-tagged proteins in the culture filtrates was investigated.

3.4.1 Rv3165c is in the cell envelope, whereas Rv3167c is in the cytoplasm

TMHMM Server v. 2.0 (software for prediction of transmembrane helices in proteins) predicts that Rv3165c is a transmembrane protein (Figure 29A) whereas Rv3167c is secreted (176). Rv3165c is a hypothetical unknown protein whereas Rv3167c is a probable transcriptional regulatory protein. For Rv3167c to be involved in transcriptional regulation it must be in the cytoplasm. To confirm predicted cellular localizations, myc-tagged versions of Rv3165c and Rv3167c were produced in BCG using the extrachromosomal expression vector pMV261. Subcellular fractions of BCG cultures expressing either Rv3165c-myc or Rv3167c-myc were prepared. Equal percentages of cell envelope and cell cytoplasm fractions were separated by PAGE and proteins were detected by western blotting. Anti-myc antibody was used to detect myc-tagged proteins. Rv3165c was localized mostly to the cell envelope whereas Rv3167c was solely located in the cytoplasm (Figure 29B). This result confirmed the predicted locations of the proteins. LAM and DNAK were used as cell fraction markers. Mtb LAM is present soely in the cell envelope fraction and DNAK (probable chaperone protein) is present solely in the cytosolic fraction.

A

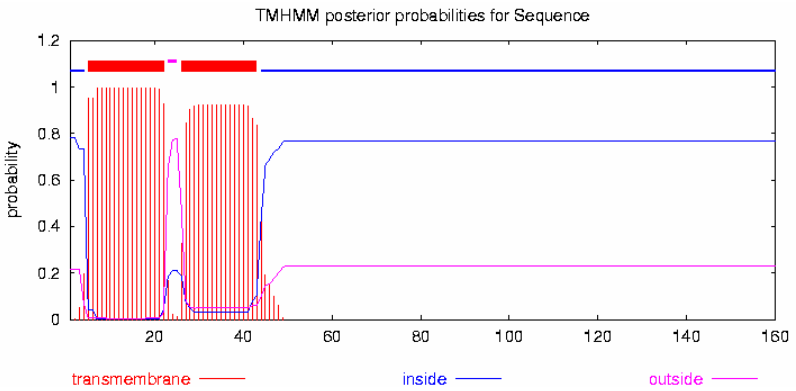

Inside 1-4 aa

TM helix 5-22 aa

Outside 23-25 aa

TM helix 26-43 aa

Inside 44-160 aa

B

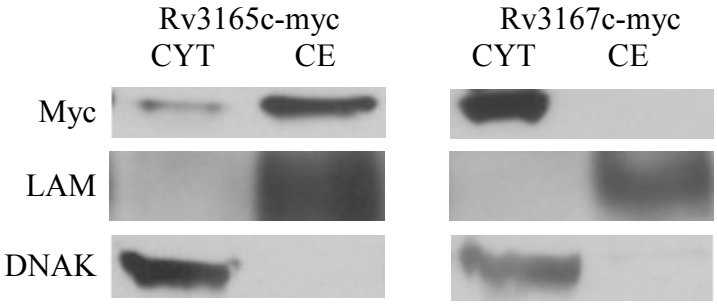

CYT: Cytosolic fraction
CE: Cell envelope fraction

C

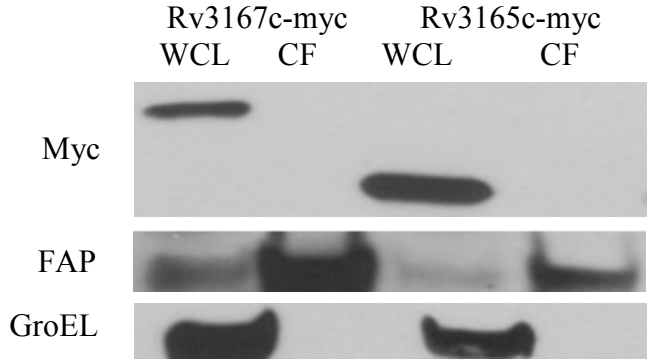

WCL: Whole cell lysate
CF: Culture filtrare

Figure 29: Rv3165c is in the cell envelope and Rv3167c is in the cytoplasm.
Prediction of transmembrane helices of Rv3165c by TMHMM (A). BCG clones expressing myc tagged Rv3165c or Rv3167c were grown to late log phase, lysed using a French® Press and the cell envelope fraction was separated from the cytosolic fraction. Fractions were separated by PAGE for western blotting. Anti-myc antibody was used for detection of myc tagged proteins. Anti-LAM and anti-DNAK antibodies were used for detection of LAM and DNAK in the fractions (B). BCG clones expressing myc tagged Rv3165c or Rv3167c were grown in Sauton's medium to late log phase, the cells were collected and the culture filtrate was concentrated. Equal percentages of the whole cell lysate and the culture filtrate fractions were loaded in the gel. Anti-FAP and anti-GroEL antibodies were used for detection of FAP and GroEL in the fractions (C).

3.4.2 Rv3165c and Rv3167c are not secreted

To check if either of the two proteins was secreted, culture filtrates (CF) of BCG expressing the myc-tagged proteins were prepared and concentrated. CF samples and whole cell lysates (WCL) were separated by PAGE and proteins were detected by western blotting. Anti-myc antibody was used to detect myc-tagged proteins. Both of the proteins were only detected in the WCL, showing that they were not secreted (Figure 29C). Anti-FAP antibody was used to show the presence of FAP (fibronectin attachment protein) mostly in the CF fraction (some FAP is present in the cell membrane, which is why it is detected in the WCL fraction). Anti-GroEL antibody was used to show the presence of GroEL (probable chaperone protein) solely in the WCL fraction and that there was no cellular death and lysis that would have released proteins to the CF.

3.5 VIRULENCE OF Δ*RV3167C* KNOCK-OUT STRAIN

In order to determine whether knocking out Rv3167c in Mtb changed its virulence especially because of its increased pro-apoptotic phenotype, eight SCID mice per condition were infected with Mtb and Δ*Rv3167c* via aerosol route. 24hr later three mice per condition were sacrificed and the bacteria from their lungs were plated. The levels of bacteria in the lungs were similar (264 ± 33 colony forming units of Mtb vs. 297 ± 23 colony forming units of Δ*Rv3167c*) (Figure 30A). The remaining infected mice were observed and scored until they were in a moribund state and had to be sacrificed (Figure 30B).

All of the Δ*Rv3167c* infected mice died on the 28th day of infection while Mtb infected mice died between 33rd and 39th days of infection. A log-rank test found the

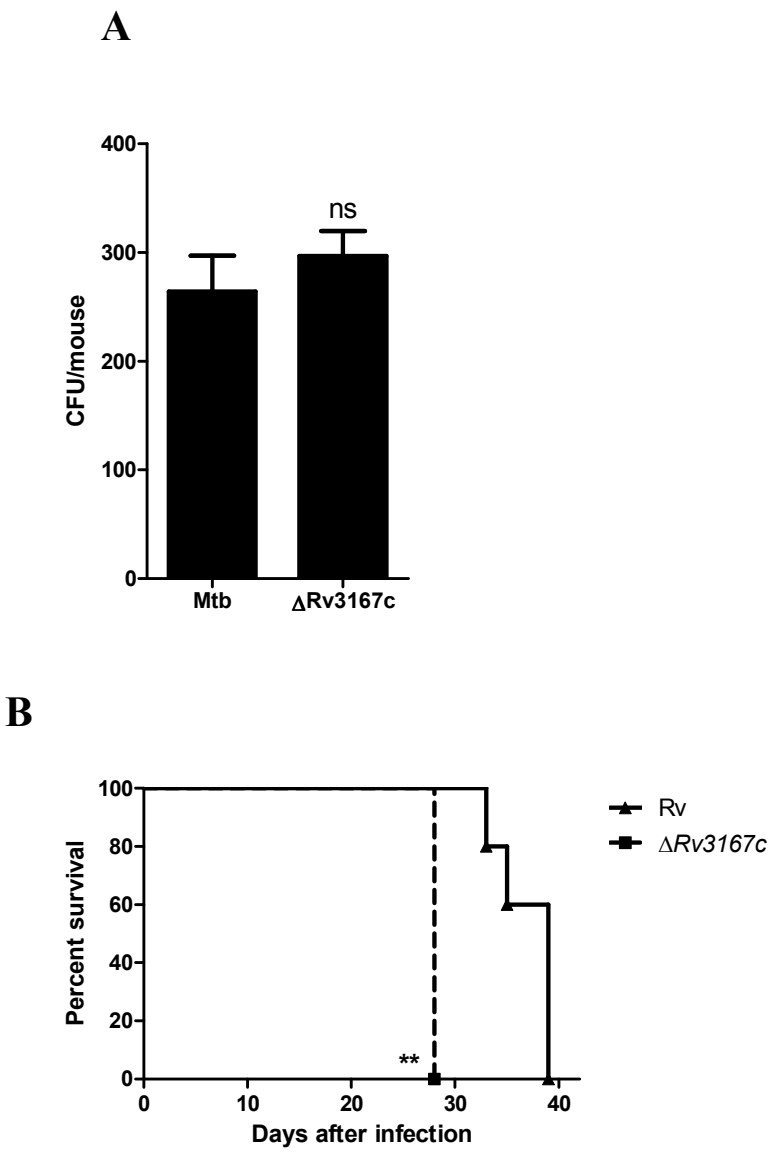

Figure 30: Δ*Rv3167c* is not less virulent than Mtb in mice. 8 SCID mice were aerosol infected with a low dose of Mtb or Δ*Rv3167c*. A) Colony forming units (CFU) in the lungs were shown to be not significantly different between Mtb and Δ*Rv3167c* (3 mice per condition were sacrificed. Statistical significance was determined by one way analysis of variance (ANOVA) with Tukey post-test). B) The remaining 5 mice per condition were monitored. All of the Δ*Rv3167c* infected mice died on the 28th day of infection while Mtb infected mice died between 33rd and 39th days of infection. Statistical significance was determined by a log-rank test. **, $0.001 < p < 0.01$.

survival curves to be significantly different indicating possibly that Δ*Rc3167c* is more virulent than Mtb. This experiment has to be repeated to confirm this phenotype of Δ*Rv3167c* in SCID mice.

According to a study designed and supervised by our collaborator Dr.Petros C. Karakousis at Johns Hopkins University School of Medicine, Δ*Rv3167c* is not less virulent than Mtb in guinea pigs. Guinea pigs were infected with Mtb, Δ*Rv3167c*, Δ*Rv3167c*::C or Δ*NuoG* strains by aerosol infection at a low-dose and the numbers of mycobacteria in the lungs were determined 1, 28 and 56 day post-infection (Figure 31A). Although the number of ΔRv3167c was significantly higher than the number of wild-type Mtb by day 28, they were similar by day 56. The body weights of the guinea pigs were measured before they were sacrificed and found to be similar for all of the strains at the three time points (Figure 31B). The experiment in mice together with the experiment in guinea pigs suggest that Δ*Rv3167c* is not less virulent than wild-type Mtb.

3.6 SUMMARY

Mtb inhibits apoptosis of infected host cells and this is thought to enable Mtb to survive and prevent a successful immune response from the host. I was able to identify *Rv3165c* and *Rv3167c* as two novel anti-apoptotic genes of Mtb. THP-1 macrophages infected with Mtb knock-out strains lacking *Rv3165c* or *Rv3167c* (Δ*Rv3165c*, Δ*Rv3167c*) had high levels of apoptosis. Apoptosis depended on caspase-8 and 3 and/or 7, but not on caspase-9 in THP-1 macrophages, suggesting the involvement of extrinsic but not intrinsic caspase activation. Inhibiting ROS production or scavenging ROS inhibited the apoptosis of Δ*Rv3165c* or Δ*Rv3167c* infected macrophages. ROS is thought to promote

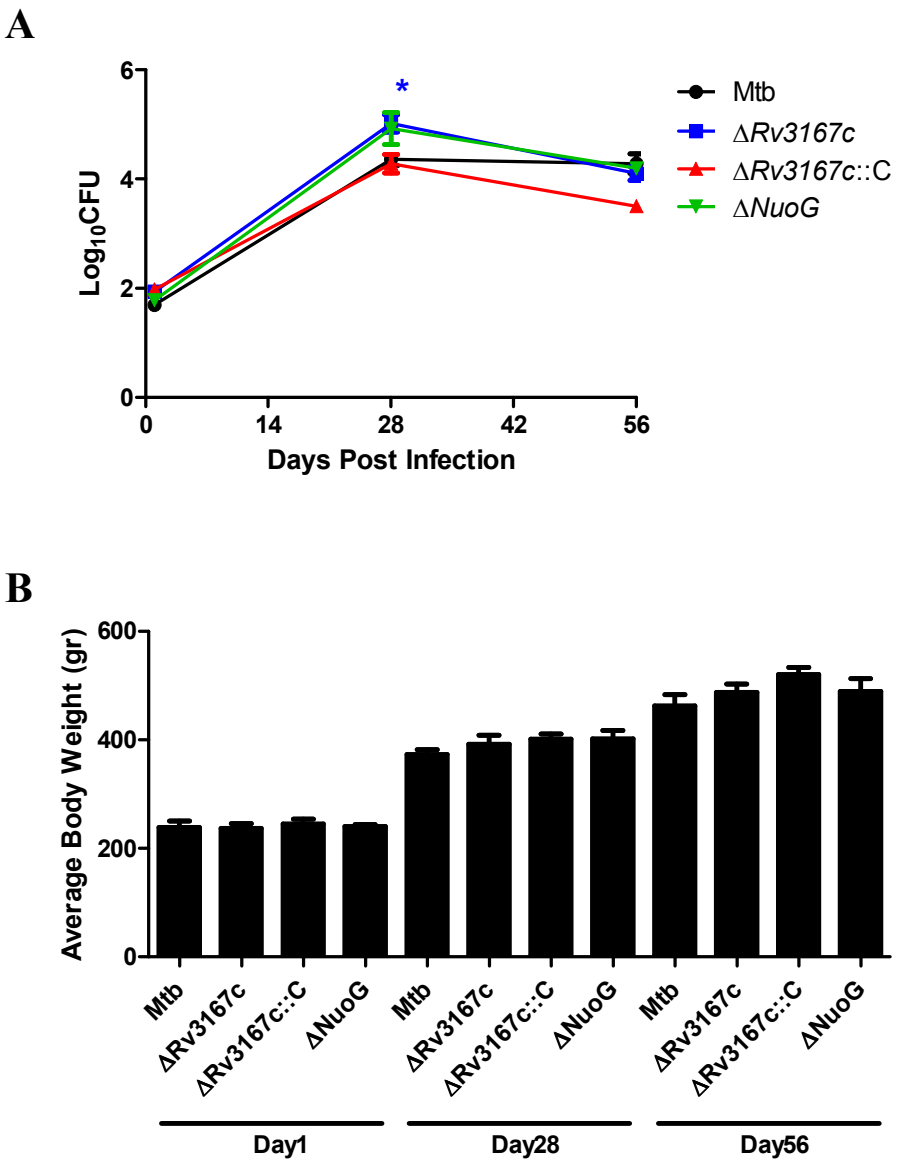

Figure 31: Δ*Rv3167c* is not less virulent than Mtb in guinea pigs. Guinea pigs were infected with Mtb, Δ*Rv3167c*, Δ*Rv3167c*::C or Δ*NuoG* (12 guinea pigs per group; n=12) by aerosol infection at a low-dose (less than 100 bacteria per guinea pig) and four guinea pigs were sacrificed per strain per time point for determination of number of mycobacteria in the lungs (A). The body weights of the guinea pigs were measured before they were sacrificed (B). Statistical significance was determined by one way analysis of variance (ANOVA) with Tukey post-test. *, $0.05 < p < 0.01$. (Experiment designed and supervised by our collaborator Dr.Petros C. Karakousis at Johns Hopkins University School of Medicine.)

the pro-apoptotic cell signaling pathways, but not start them (103). However, the signal that activates the extrinsic caspase activation in Δ*Rv3165c* or Δ*Rv3167c* infected macrophages is not known at this point.

Preliminary RNA sequencing and antibody microarray experiments identified host cell components that may be differentially regulated in Δ*Rv3167c* infected cells compared to Mtb infected cells. Confirmation of these targets will help identify the host cell pathways that Mtb manipulates to inhibit host cell apoptosis and qPCR and other methods will be used to confirm Mtb genes that are involved in apoptosis inhibition.

Δ*Rv3165c* and Δ*Rv3167c* failed to upregulate the expression of the only catalase of Mtb, *katG*. Therefore, this suggests that Mtb may need to upregulate *katG* expression in order to neutralize host cell produced ROS to inhibit apoptosis. However, there is also evidence contradicting these results, which is mentioned in the discussion. Rv3165c was found to reside mainly in the cell envelope while Rv3167c, which is predicted to be a probable transcriptional regulator, was found to be exclusively in the cytosol of mycobacteria. *Rv3165c* was found to be required for upregulation of *Rv3167c* expression.

An experiment using SCID mice as well as another one using guinea pigs suggest that Δ*Rv3167c* is not less virulent than wild-type Mtb as predicted. It was expected that this pro-apoptotic mutant would be less virulent as it was shown for the other pro-apoptotic mutants of Mtb. Further experimentation is necessary to confirm this phenotype of Δ*Rv3167c*.

CHAPTER 4 DISCUSSION

The presented data established the requirement of *Rv3165c* and *Rv3167c* for apoptosis inhibition by Mtb in THP-1 macrophages. In addition to THP-1 macrophages, experiments using human blood monocyte derived macrophages and guinea pig alveolar macrophages confirmed the pro-apoptotic phenotype of Δ*Rv3165c* and Δ*Rv3167c* (Hurley, B. unpublished). The complementation of Δ*Rv3167c* was done with the myc-tagged *Rv3167c* and it is thought that the tag does not affect the structure and function of Rv3167c since the N-terminus of TetR-like transcriptional regulators is surface-exposed (173). In addition, Δ*Rv3167c* was successfully complemented and this suggests that myc-tagged Rv3167c was functional.

Infection of THP-1 macrophages either at 3:1 or 0.5:1 MOI inhibits growth of Δ*Rv3167c* (Figure 16, 17). The difference was observed in 3:1 MOI infection when gentamicin was omitted in the chase media, indicating that the difference is due to extracellular mycobacteria. From there on no gentamicin was used in the chase media for those infections. The increasing trend of the graph for Mtb after day 1 in the absence of gentamicin compared to the decreasing trend in the presence of gentamicin suggests that there are many extracellular Mtb that got out of the cells alive, presumably via necrosis. When the infections were done at an MOI of 0.5:1 no difference in the numbers of bacteria were observed up to 4 day after infection. This was expected since the apoptotic phenotype is observed around 4-5 day after infection at that MOI. When the infections with different MOIs are compared, 0.5:1 MOI infection has higher inhibitory effect on the growth of Δ*Rv3167c*. This is thought to be due to the presence of uninfected

bystander macrophages which can take up the apoptotic blebs resulting from the apoptosis of infected macrophages and kill the mycobacteria inside better (177). A recent study however suggests that the effect of uninfected macrophages was contact independent and they produced a soluble molecule that acted on the infected macrophages to increase their antibacterial activities (178).

Apoptosis of infected cells is reported to kill the intracellular mycobacteria (79, 135) and our data shows that apoptosis prevented Δ*Rv3167c* from replicating as much as Mtb. This suggests that in our infection system, either apoptosis kills Δ*Rv3167c* less effectively than what has been shown before or apoptosis diminishes the replicating niche for Δ*Rv3167c*, thereby prevent Δ*Rv3167c* from replicating as much as Mtb but it does not necessarily kill it. The number of total mycobacteria (live and dead) can de determined by microscopy after infection to better analyze the effect of apoptosis on Δ*Rv3167c*. Apoptosis rate was higher in Δ*Rv3167c* infected cells, whereas the rate of necrosis was significantly lower compared to Mtb infected cells. This is consistent with the reports suggesting that Mtb uses necrosis to break free from the cell, unharmed and spreads to other uninfected cells (66, 67). Although the necrosis rate is high for Mtb infected cells, the percentage of viable cells that can accommodate Mtb is higher, which can lead to increased numbers of Mtb. The higher numbers of Mtb is also probably due to the ability of Mtb to replicate to bigger numbers inside the cell without causing apoptosis compared to pro-apoptotic mutants.

Apoptosis induced by Δ*Rv3165c* and Δ*Rv3167c* was found to involve caspases. Since only caspase 8 but not caspase 9 activity was increased in the knock-out infected cells, the extrinsic pathway of caspase activation was activated. TNF-α, FasL and TRAIL

(TNF-related apoptosis-inducing ligand) induce apoptosis through caspase-8 activation (87, 179). TNF-α secretion was not affected in the knock-out infected cells but the involvement of FasL or TRAIL in caspase-8 activation is unknown at this point.

The pro-apoptotic phenotype of Δ*nuoG* is abolished in the presence of ROS inhibitor or scavengers and the phagosomes of cells infected with Δ*nuoG* have higher levels of ROS (149). In order to investigate the involvement of ROS in the pro-apoptotic phenotype of Δ*Rv3165c* and Δ*Rv3167c*, ROS production was inhibited or ROS was scavenged. As in the case of Δ*nuoG* both of these methods abolished the pro-apoptotic phenotypes of Δ*Rv3165c* and Δ*Rv3167c*. The amounts of apoptosis induced by Δ*Rv3165c* and Δ*Rv3167c* in the experiments done on the slides were lower since the time point was 36 hr instead of 48 hr and some of the apoptotic cells were not adherent at the end of infection and were washed off. These experiments indirectly showed that there was an increase in ROS production in the Δ*Rv3165c* and Δ*Rv3167c* infected cells. ROS detection reagents will be employed to test for differences in the levels of ROS produced by infected cells. This will directly show if Δ*Rv3165c* and Δ*Rv3167c* infected cells have higher levels of ROS, presumably in the phagosome. The source of ROS can be mitochondrial or phagosomal so experiments will be done with PLB XR-CGD cells, a cell line that lacks the *cybb* gene (no Nox2 expression) to find if the source of ROS is phagosomal or not (180).

The expression of 2332 host genes was found to be significantly affected due to the lack of *Rv3167c* in Mtb via RNA sequencing. RT-qPCR and ELISA were performed to check the expression of two genes, *CCL3* and *CCL20*. Although the *CCL3* result was confirmed, RT-qPCR of *CCL20* gave the opposite result of RNA sequencing and ELISA

of *CCL20* gave a result different than RNA sequencing and RT-qPCR. According to these results, it is imperative to repeat RNA sequencing and confirm its results via another technique like RT-qPCR. A biological replicate of RNA sequencing will reduce the number of false positives from the initial data. However, the gene transcription data have to be carefully interpreted since they do not necessarily reflect how the translation is affected. The antibody microarray gave a smaller number of host targets to look at as it analyzed the expression of only 812 proteins and phosphorylation of 262 amino acids. The regulation of these targets has to be confirmed with western blots since only 30 to 45% of the changes in the protein levels detected by the antibody microarray can be reproduced by western blots according to Kinexus.

Although the expression of *katG* increased *in vitro* in ROS treated knock-outs, the knock-outs were defective in upregulating *katG* expression in macrophages. One explanation for these results is that the ROS produced *in vitro* are much more than the amount in macrophages and thus can upregulate *katG* expression through different mechanisms that do not require the presence of Rv3165c or Rv3167c. If the amount of ROS added *in vitro* is dosed down, a difference in *katG* expression might be observed similar to the difference in macrophages. Another explanation is that Mtb needs Rv3165c and Rv3167c to respond to ROS in macrophages but not *in vitro*. This could be due to the presence of other factors in macrophages, such as pH and ingredients of the phagosome that only allow Rv3165c and Rv3167c to respond to ROS.

Our lab previously tested a *katG* mutant to see its effect on host cell apoptosis. THP-1 macrophages infected with a *katG* mutant had significantly higher levels of apoptosis compared to wild type Mtb (149). However, this mutant (INH34 strain) also

lacked the neighboring genes *Rv1907c*, *furA*, *Rv1910c*, *lppc*, and *fadB5* (181). A mutant strain that lacks only *katG* had a similar apoptotic phenotype as wild-type Mtb (Srinivasan L, unpublished data). These findings indicate that *katG* by itself is not essential for apoptosis inhibition by Mtb. In line with this idea, another graduate student in our lab, Jeff Quigley, showed that in addition to *katG*, other genes around *katG* mentioned above are not upregulated in Mtb in the absence of Rv3167c in macrophages. Therefore it is likely that Rv3167c acts as a regulator of *katG* and the other genes around it to prevent apoptosis. Quigley also showed that three sigma factors *sigB*, *sigE* and *sigH* were upregulated by Rv3167c *in vivo*. Interestingly, *katG* and the genes around it that are regulated by Rv3167c contain putative binding sites for the same sigma factors regulated by Rv3167c according to the software Virtual Footprint (182). According to recent research Δ*sigH* infected macrophages were more apoptotic and had higher caspase-3 and 7 activity compared to Mtb infected cells (183). These data suggest that Rv3167c regulates certain sigma factors (or regulators of sigma factors), which in turn regulate the other genes that are involved in inhibition of apoptosis.

Although Δ*katG* inhibits apoptosis of THP-1 macrophages just like Mtb, Δ*katG* was less virulent compared to Mtb when they were used in infecting immunocompetent C57BL/6 mice (184). Complementation of *katG* restored the virulent phenotype in the same mice. When gp91 knock-out mice (no phagocyte superoxide production) were infected with Mtb and Δ*katG*, both strains showed similar virulence, suggesting that *katG* was involved in neutralizing peroxides produced by phagocyte NADPH oxidase and thus increasing the persistence of Mtb (184, 185). Δ*katG* did not replicate in murine bone marrow derived macrophages (BMDM) as well as Mtb but showed similar replication in

mice during the early stages of infection (184). This difference is probably due to the simplicity of one system versus the complexity of the other one that involve many different cell types. The seemingly conflicting results for *katG* deletion mutants may be due to different cell types used *in vitro* (THP-1 versus murine BMDM). It is possible that Δ*katG* gives a phenotype that is different than Mtb only in murine cells. The apoptotic phenotype of Δ*katG* in the mouse lungs needs to be analyzed to further understand the decreased virulence of Δ*katG*. As mentioned before, although in addition to other proteins KatG secretion is also defective in *secA2* knock-out Mtb (150), re-establishment of SodA secretion was enough to reverse the pro-apoptotic phenotype of *secA2* mutant strain (146). This result also suggests that KatG is not involved in apoptosis inhibition.

The requirement of *Rv3165c* for the upregulation of *Rv3167c* in macrophages indicates a possible mechanism whereby Mtb upregulates *Rv3167c* expression to possibly inhibit apoptosis and that this requires the presence or activity of Rv3165c to do so. Rv3165c might be interacting directly with Rv3167c. As another possibility Rv3165c might be interacting with another protein to increase the amount of *Rv3167c.* A detailed predicted model is discussed below.

A working model for *Rv3165c* and *Rv3167c* emerged after the cellular localizations of these proteins were determined. Previous evidence showed that *Rv3165c* was required for *Rv3167c* expression, that both *Rv3165c* and *Rv3167c* were required for *katG* upregulation in infected macrophages and that ROS inhibition led to decreased apoptosis of Δ*Rv3165c* and Δ*Rv3167c* infected cells. In addition, Rv3167c is predicted to be a transcriptional regulatory protein. These results suggest the following working model, whereby Rv3165c resides in the plasma membrane and Rv3167c is in the

cytoplasm of Mtb. Without a signal that Rv3165c senses, the expression of *Rv3167c* is low (Figure 32A). When Rv3165c senses an extracellular signal that is thought to be either ROS or an oxidized molecule, it relays the signal directly or indirectly to Rv3167c. This relay causes an increase in *Rv3167c* expression (Figure 32B). Rv3167c then acts as a transcriptional regulator and upregulates expression of bacterial genes that inhibit apoptosis and downregulates the expression of bacterial genes that can induce apoptosis. Using either one or both of these strategies Mtb inhibits host cell apoptosis (Figure 32C).

Bacteria employ protein sensors for ROS detection. Some of these sensors contain cysteine (C) in C-X-X-C (X is any amino acid) motifs. As the oxidation sensitive thiol groups of cysteines are oxidized, disulphide bonds are formed between the two cysteines in the motif, causing a conformational change of the protein structure and a change in the activity of the protein. Other bacterial sensors detect oxidative stress through iron *via* the Fenton reaction ($Fe^{2+} + H_2O_2 \rightarrow Fe^{3+} + {}^{\cdot}OH + {}^{-}OH$). Following detection of oxidative stress, these sensors go through modifications like oxidation of histidines, dityrosine formation or carbonylation (186). An example of these sensors is PerR, which is an iron-dependent oxidative stress sensor of *Bacillus subtilis* that binds to iron or manganese in order to repress its target genes. Following a peroxide dependent stress, one of the histidines in the regulatory binding site of PerR becomes oxidized. This causes the release of iron from PerR followed by derepression of its target genes (187). Although Rv3165c does not contain a C-X-X-C motif, one of its extracellular amino acids predicted by TMHMM Server v. 2.0 is a histidine (Figure 29A). Histidine is one of the amino acids that is sensitive to attack and oxidation by ROS and this oxidation can lead

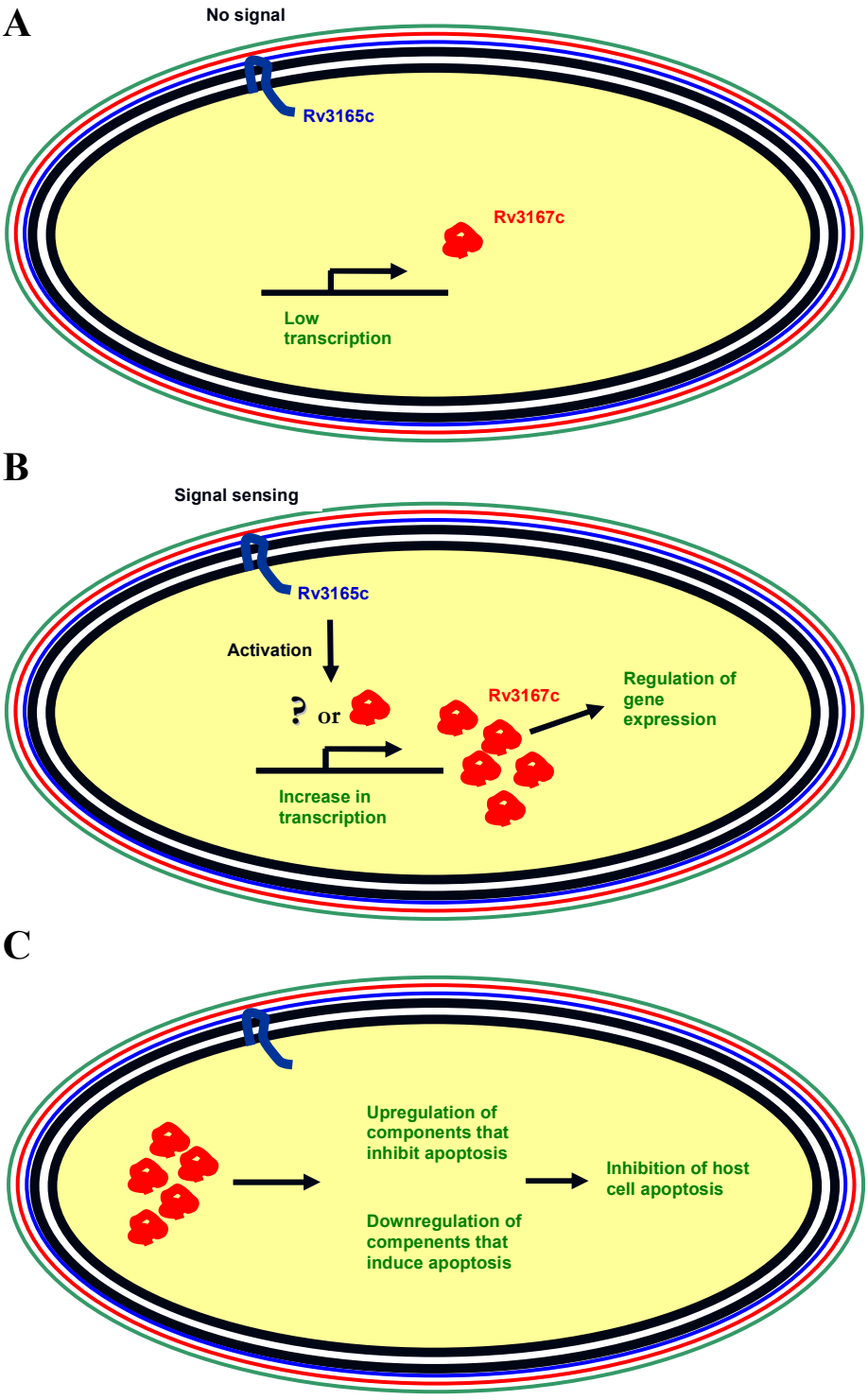

Figure 32: The working model showing the confirmed localizations of Rv3165c and Rv3167c and their predicted functions. Rv3165c is localized to the cell envelope and predicted to sense a signal and relay this signal to Rv3167c. This relay of the signal causes an increase in *Rv3167c* transcription and translation. Increased amounts of Rv3167c causes upregulation of bacterial components that inhibit host cell apoptosis.

to a change in the three dimensional structure of the protein (188, 189). Therefore, it is possible that, like the iron-dependent oxidative sensors, ROS production by the host cell changes the structure of Rv3165c through oxidation of the extracellular histidine and this change in the structure either enables Rv3165c to interact with Rv3167c or with another protein that relays the signal to Rv3167c. Complementation of Δ*Rv3165c* mutant with *Rv3165c* lacking the extracellular histidine will show the importance of that amino acid in signal sensing.

One of the other mechanisms of signal detection by Rv3165c may be via another membrane protein that interacts with Rv3165c and has an extracellular signal sensing domain. This other protein can sense the signal through ligand binding or another mechanism and relay the signal to Rv3165c. Identifying proteins that can interact with Rv3165c through techniques like bacterial two-hybrid system will help validate this signal detection pathway. The points to investigate to prove this model include showing a direct or an indirect interaction between Rv3165c and Rv3167c, showing that Rv3167c regulates expression of other bacterial genes to inhibit host cell apoptosis and that Rv3167c binds to genomic DNA of Mtb to regulate gene expression. TMHMM Server v. 2.0 predicts that for the two-component regulatory system sensors mprB, mtrB, phoR, prrB, senX3, trcS the number of extracellular amino acids varies from 273 to 504 (compared to 3 for Rv3165c) (190–195). The lack of such a big extracellular amino acid stretch of Rv3165c suggests a different mechanism for signal detection by Rv3165c. In addition, according to InterProScan Rv3165c does not have a predicted histidine kinase domain (172) like the sensors of two-component systems (196, 197).

According to InterProScan, Rv3167c lacks any sensor or kinase domain and contains an amino terminal TetR-type DNA-binding helix-turn-helix domain and a carboxy terminal TetR-like transcriptional regulator domain. Lack of a kinase or sensor domain indicates that Rv3167c is not a member of Ser/Thr/Tyr protein kinases or one-component systems that are responsible for many signal transduction pathways (198, 199). All TetR family transcriptional regulators are homodimers and most of them repress transcription of genes (173). As such, demonstration of homodimer formation by Rv3167c will further confirm its classification as a transcriptional regulator. The sequence Rv3167c binds to needs to be identified via methods like chromatin immunoprecipitation in order to characterize it as a repressor or activator of gene transcription. Predicted DNA binding sequences for Rv3167c can be used in electrophoretic mobility shift assays to determine if Rv3167c binds to those sequences. However, the conditions under which Rv3167c binds to DNA may not be replicated *in vitro* and this might lead to false negative results.

The preliminary data from the SCID mice infection experiment suggest that Δ*Rv3167c* is not less virulent than Mtb and the guinea pig infection experiment data suggest that Δ*Rv3167c* and Δ*nuoG* are not less virulent than Mtb. Both of these experiments need to be repeated in order to confirm these results. The number of Δ*Rv3167c* and its apoptotic phenotype in the lungs of the SCID mice have to be determined to make a better correlation between its apoptotic phenotype and virulence. It is possible that Δ*Rv3167c* does not have a pro-apoptotic phenotype in the phagocytic cells of mice and this leads to a similar virulence as wild-type Mtb. Our lab has identified a DNA region of Mtb that was required for inhibition of apoptosis in THP-1

macrophages, whereas lack of this region did not lead to loss of virulence of Mtb in mice (Velmurugan, K. unpublished data). However, the lack of 7/10 region from Mtb led to decreased virulence in SCID mice (Figure 8). On the other hand, that was a single experiment and infection experiments in SCID mice and guinea pigs for Δ*Rv3167c* together present a stronger case. If the decreased virulence of Δ7/10 and similar virulence of Δ*Rv3167c* (and Δ*Rv3165c*) compared to Mtb are confirmed, then this would suggest that the other genes in the 7/10 region may be involved in the virulence of Mtb.

In contrast to the guinea pig infection results, Δ*nuoG* is less virulent in immunocompromised SCID and immunocompetent BALB/c mice (147). But when immunocompetent C57BL/6 mice were infected via aerosol route with Mtb and Δ*nuoG*, Δ*nuoG* did not show any decreased virulence for up to 7 weeks as measured by bacterial counts (Miller J. and Gurses S., unpublished data). Keeping in mind that the guinea pig experiment was also done by aerosol infection whereas the SCID and BALB/c mice infections were done intravenously via a lateral tail vein, the physiologically more relevant experiment would be the one done by aerosol route since that allows Mtb to gain access to the lungs first. In addition, the guinea pig is considered to be a better model than the mouse to study Mtb infection (200, 201). The mouse infections that showed that Δ7/10, Δ*sodA* and Δ*katG* were less virulent than wild-type Mtb were also done by injection of mycobacteria intravenously via a lateral tail vein (151, 184). It is possible that injection of mycobacteria into the animals, especially mice, is not a good model to study virulence of pro-apoptotic mutants and the differences that were observed in the virulence of the pro-apoptotic mutants were due to characteristics of tail vein injections (e.g., high dose of mycobacteria and a different route and spread pattern of mycobacteria

inside the animal). The different set of cells that the pro-apoptotic mutants encounter following a tail injection might be more affective in mounting a response against them than the cells they encounter following an aerosol infection, which might explain why pro-apoptotic Mtb mutants would seem to be less virulent in infections via tail vein injections. Although pro-apoptotic mutants might show differences in various terms in infections of cultured cells or cell lines compared to Mtb, they might not make a difference *in vivo*. To compare the two ways of infection, either Δ*Rv3167c* can be used for infection of mice via tail vein injection or the pro-apoptotic mutants that were shown to be more virulent can be used for infection of mice or guinea pigs via aerosols. If Δ*Rv3167c* is found to be more virulent or the other pro-apoptotic mutants are found to be similarly virulent as Mtb in these experiments, it would suggest that mouse infections via tail vein injection do not give accurate results in terms of the virulence of pro-apoptotic Mtb mutants. This would also suggest that Mtb pro-apoptotic mutants are not good candidates for new vaccines and other phenotypes of Mtb that can elicit a better immune response have to be studied.

Apoptosis of cultured murine and human macrophages following infection decreases the viability of mycobacteria (135, 137, 143). However, a recent study found that during the initial stage of an *in vivo* infection the viability of pro-apoptotic Δ*nuoG* mutant did not decrease after apoptosis of infected cells. The Δ*nuoG* mutant spread to a higher number of lung myeloid cells but was present in a lower number in each cell following infection of immunocompetent C57BL/6J mice (202). Δ*nuoG* infection lead to an earlier activation of $CD4^+$ T cells compared to Mtb. Therefore the seemingly more virulent phenotype of the Δ*Rv3167c* mutant in the SCID mice might be due to the spread

of Δ*Rv3167c* to a higher number of cells through apoptosis and lack of the adaptive immune response. The number of Δ*Rv3167c* bacteria was higher than the number of Mtb in the guinea pig lungs by day 28 but they were not significantly different by day 56. Compared to Mtb, Δ*Rv3167c* infected guinea pig alveolar macrophages go through higher rates of apoptosis (Hurley B., unpublished data). Therefore, it is possible that Δ*Rv3167c* replicated and possibly spread better than Mtb through apoptosis in the early stages of infection followed by a better control of mycobacterial infection by the guinea pigs through adaptive immunity that led to a decrease in the number of bacteria.

In conclusion, I identified two novel anti-apoptotic genes of Mtb that will be added to a short list of anti-apoptotic genes. Several effects of deleting these genes were identified in Mtb as well as in THP-1 macrophages. However, the infection experiments showed that the virulence of one of the mutants, Δ*Rv3167c*, was not less than wild-type Mtb as expected from a pro-apoptotic mutant. Although this lack of difference in the virulence phenotype might be specific for Δ*Rv3167c*, it is also possible that infection experiments done to show the virulence of other pro-apoptotic mutants were flawed. Confirmation of virulence phenotypes of previously found pro-apoptotic mutants via aerosol infection of mice and/or guinea pigs is suggested, as that method of infection is the more physiologically relevant one. On the other hand, if the decreased virulence of pro-apoptotic mutants is not confirmed through aerosol infections, this could mean that apoptosis inhibition by Mtb is irrelevant in terms of its virulence.

BIBLIOGRAPHY

1. Russell, D. G., C. E. Barry, and J. L. Flynn. 2010. Tuberculosis: What we don't know can, and does, hurt us. *Science* 328: 852 -856.

2. Russell, D. G. 2011. Mycobacterium tuberculosis and the intimate discourse of a chronic infection. *Immunological Reviews* 240: 252-268.

3. Global tuberculosis control: WHO report 2011. (WHO/HTM/TB/2011.16).

4. North RJ, Jung Y-J. Immunity to tuberculosis. *Annu. Rev. Immunol.* 2004;22:599-623.

5. Stewart, G. R., B. D. Robertson, and D. B. Young. 2003. Tuberculosis: a problem with persistence. *Nat. Rev. Micro.* 1: 97-105.

6. Wolf, A. J., B. Linas, G. J. Trevejo-Nuñez, E. Kincaid, T. Tamura, K. Takatsu, and J. D. Ernst. 2007. Mycobacterium tuberculosis infects dendritic cells with high frequency and impairs their function in vivo. *J. Immunol.* 179: 2509-2519.

7. Alatas, F., O. Alatas, M. Metintas, A. Ozarslan, S. Erginel, and H. Yildirim. 2004. Vascular endothelial growth factor levels in active pulmonary tuberculosis. *Chest* 125: 2156-2159.

8. Russell, D. G., P.-J. Cardona, M.-J. Kim, S. Allain, and F. Altare. 2009. Foamy macrophages and the progression of the human TB granuloma. *Nat. Immunol.* 10: 943-948.

9. McElvania TeKippe, E., I. C. Allen, P. D. Hulseberg, J. T. Sullivan, J. R. McCann, M. Sandor, M. Braunstein, and J. P.-Y. Ting. Granuloma Formation and Host Defense in Chronic Mycobacterium tuberculosis Infection Requires PYCARD/ASC but Not NLRP3 or Caspase-1. *PLoS One* 5.

10. Flynn, J. L., and J. Chan. 2005. What's good for the host is good for the bug. *Trends Microbiol.* 13: 98-102.

11. Mohan, V. P., C. A. Scanga, K. Yu, H. M. Scott, K. E. Tanaka, E. Tsang, M. C. Tsai, J. L. Flynn, and J. Chan. 2001. Effects of Tumor Necrosis Factor Alpha on Host Immune Response in Chronic Persistent Tuberculosis: Possible Role for Limiting Pathology. *Infect. Immun.* 69: 1847 -1855.

12. Chackerian AA, Alt JM, Perera TV, Dascher CC, Behar SM. Dissemination of Mycobacterium tuberculosis is influenced by host factors and precedes the initiation of T-cell immunity. *Infect. Immun.* 2002 Aug;70(8):4501-4509.

13. Calmette, A. 1927. *La vaccination préventive contre la tuberculose par le "BCG"*. Masson et cie, Paris.

14. Mahairas, G. G., P. J. Sabo, M. J. Hickey, D. C. Singh, and C. K. Stover. 1996. Molecular analysis of genetic differences between Mycobacterium bovis BCG and virulent M. bovis. *J. Bacteriol.* 178: 1274-1282.

15. Philipp, W. J., S. Nair, G. Guglielmi, M. Lagranderie, B. Gicquel, and S. T. Cole. 1996. Physical mapping of Mycobacterium bovis BCG pasteur reveals differences from the genome map of Mycobacterium tuberculosis H37Rv and from M. bovis. *Microbiology (Reading, Engl.)* 142 (Pt 11): 3135-3145.

16. Behr, M. A., M. A. Wilson, W. P. Gill, H. Salamon, G. K. Schoolnik, S. Rane, and P. M. Small. 1999. Comparative genomics of BCG vaccines by whole-genome DNA microarray. *Science* 284: 1520-1523.

17. Gordon, S. V., R. Brosch, A. Billault, T. Garnier, K. Eiglmeier, and S. T. Cole. 1999. Identification of variable regions in the genomes of tubercle bacilli using bacterial artificial chromosome arrays. *Mol. Microbiol.* 32: 643-655.

18. Brosch, R., S. V. Gordon, M. Marmiesse, P. Brodin, C. Buchrieser, K. Eiglmeier, T. Garnier, C. Gutierrez, G. Hewinson, K. Kremer, L. M. Parsons, A. S. Pym, S. Samper, D. van Soolingen, and S. T. Cole. 2002. A new evolutionary scenario for the Mycobacterium tuberculosis complex. *Proc. Natl. Acad. Sci. U.S.A.* 99: 3684-3689.

19. Mostowy, S., D. Cousins, J. Brinkman, A. Aranaz, and M. A. Behr. 2002. Genomic deletions suggest a phylogeny for the Mycobacterium tuberculosis complex. *J. Infect. Dis.* 186: 74-80.

20. Lewis, K. N., R. Liao, K. M. Guinn, M. J. Hickey, S. Smith, M. A. Behr, and D. R. Sherman. 2003. Deletion of RD1 from Mycobacterium tuberculosis mimics bacille Calmette-Guérin attenuation. *J. Infect. Dis.* 187: 117-123.

21. Wiegeshaus, E. H., and D. W. Smith. 1989. Evaluation of the protective potency of new tuberculosis vaccines. *Rev. Infect. Dis.* 11 Suppl 2: S484-490.

22. Fine, P. E. 1995. Variation in protection by BCG: implications of and for heterologous immunity. *Lancet* 346: 1339-1345.

23. Colditz, G. A., T. F. Brewer, C. S. Berkey, M. E. Wilson, E. Burdick, H. V. Fineberg, and F. Mosteller. 1994. Efficacy of BCG vaccine in the prevention of tuberculosis. Meta-analysis of the published literature. *JAMA* 271: 698-702.

24. Jeevan, A., S. E. Ullrich, M. De Gracia, R. Shah, and Y. Sun. 1996. Mechanism of UVB-induced suppression of the immune response to Mycobacterium bovis bacillus Calmette-Guerin: role of cytokines on macrophage function. *Photochem. Photobiol.* 64: 259-266.

25. Wilson, M. E. 2000. Applying experiences from trials of bacille Calmette-Guérin vaccine. *Clin. Infect. Dis.* 30 Suppl 3: S262-265.

26. Jeevan, A., A. K. Sharma, and D. N. McMurray. 2009. Ultraviolet radiation reduces resistance to Mycobacterium tuberculosis infection in BCG-vaccinated guinea pigs. *Tuberculosis (Edinb)* 89: 431-438.

27. Wangoo, A., T. Sparer, I. N. Brown, V. A. Snewin, R. Janssen, J. Thole, H. T. Cook, R. J. Shaw, and D. B. Young. 2001. Contribution of Th1 and Th2 cells to protection and pathology in experimental models of granulomatous lung disease. *J. Immunol.* 166: 3432-3439.

28. Ordway, D. J., L. Costa, M. Martins, H. Silveira, L. Amaral, M. J. Arroz, F. A. Ventura, and H. M. Dockrell. 2004. Increased Interleukin-4 production by CD8 and gammadelta T cells in health-care workers is associated with the subsequent development of active tuberculosis. *J. Infect. Dis.* 190: 756-766.

29. Rook, G. A. W., K. Dheda, and A. Zumla. 2005. Do successful tuberculosis vaccines need to be immunoregulatory rather than merely Th1-boosting? *Vaccine* 23: 2115-2120.

30. Brandt, L., J. Feino Cunha, A. Weinreich Olsen, B. Chilima, P. Hirsch, R. Appelberg, and P. Andersen. 2002. Failure of the Mycobacterium bovis BCG vaccine: some species of environmental mycobacteria block multiplication of BCG and induction of protective immunity to tuberculosis. *Infect. Immun.* 70: 672-678.

31. Palmer, C. E., and M. W. Long. 1966. Effects of infection with atypical mycobacteria on BCG vaccination and tuberculosis. *Am. Rev. Respir. Dis.* 94: 553-568.

32. Orme, I. M., A. R. Roberts, and F. M. Collins. 1986. Lack of evidence for a reduction in the efficacy of subcutaneous BCG vaccination in mice infected with nontuberculous mycobacteria. *Tubercle* 67: 41-46.

33. Ratledge, C., and J. Dale. 1999. *Mycobacteria: molecular biology and virulence*. John Wiley & Sons.

34. Mostowy, S., A. G. Tsolaki, P. M. Small, and M. A. Behr. 2003. The in vitro evolution of BCG vaccines. *Vaccine* 21: 4270-4274.

35. Belley, A., D. Alexander, T. Di Pietrantonio, M. Girard, J. Jones, E. Schurr, J. Liu, D. R. Sherman, and M. A. Behr. 2004. Impact of methoxymycolic acid production by Mycobacterium bovis BCG vaccines. *Infect. Immun.* 72: 2803-2809.

36. Brosch, R., S. V. Gordon, T. Garnier, K. Eiglmeier, W. Frigui, P. Valenti, S. Dos Santos, S. Duthoy, C. Lacroix, C. Garcia-Pelayo, J. K. Inwald, P. Golby, J. N. Garcia, R. G. Hewinson, M. A. Behr, M. A. Quail, C. Churcher, B. G. Barrell, J. Parkhill, and S. T.

Cole. 2007. Genome plasticity of BCG and impact on vaccine efficacy. *Proc. Natl. Acad. Sci. U.S.A.* 104: 5596-5601.

37. Blumberg, H. M., W. J. Burman, R. E. Chaisson, C. L. Daley, S. C. Etkind, L. N. Friedman, P. Fujiwara, M. Grzemska, P. C. Hopewell, M. D. Iseman, R. M. Jasmer, V. Koppaka, R. I. Menzies, R. J. O'Brien, R. R. Reves, L. B. Reichman, P. M. Simone, J. R. Starke, and A. A. Vernon. 2003. American Thoracic Society/Centers for Disease Control and Prevention/Infectious Diseases Society of America: treatment of tuberculosis. *Am. J. Respir. Crit. Care Med.* 167: 603-662.

38. Dover, L. G., and G. D. Coxon. 2011. Current Status and Research Strategies in Tuberculosis Drug Development. *J. Med. Chem.* 54: 6157-6165.

39. Koul, A., E. Arnoult, N. Lounis, J. Guillemont, and K. Andries. 2011. The challenge of new drug discovery for tuberculosis. *Nature* 469: 483-490.

40. Kubica, G. P., and L. G. Wayne. 1984. *The Mycobacteria: a sourcebook*,. Dekker.

41. Gangadharam, P. R. J. 1998. *Basic aspects*. Springer.

42. Brown-Elliott, B. A., and R. J. Wallace. 2002. Clinical and Taxonomic Status of Pathogenic Nonpigmented or Late-Pigmenting Rapidly Growing Mycobacteria. *Clin. Microbiol. Rev.* 15: 716-746.

43. Gill, W. P., N. S. Harik, M. R. Whiddon, R. P. Liao, J. E. Mittler, and D. R. Sherman. 2009. A replication clock for Mycobacterium tuberculosis. *Nat. Med.* 15: 211-214.

44. Cole, S. T., R. Brosch, J. Parkhill, T. Garnier, C. Churcher, D. Harris, S. V. Gordon, K. Eiglmeier, S. Gas, C. E. Barry 3rd, F. Tekaia, K. Badcock, D. Basham, D. Brown, T. Chillingworth, R. Connor, R. Davies, K. Devlin, T. Feltwell, S. Gentles, N. Hamlin, S. Holroyd, T. Hornsby, K. Jagels, A. Krogh, J. McLean, S. Moule, L. Murphy, K. Oliver, J. Osborne, M. A. Quail, M. A. Rajandream, J. Rogers, S. Rutter, K. Seeger, J. Skelton, R. Squares, S. Squares, J. E. Sulston, K. Taylor, S. Whitehead, and B. G. Barrell. 1998. Deciphering the biology of Mycobacterium tuberculosis from the complete genome sequence. *Nature* 393: 537-544.

45. Brennan, P. J., and H. Nikaido. 1995. The envelope of mycobacteria. *Annu. Rev. Biochem.* 64: 29-63.

46. Hoffmann, C., A. Leis, M. Niederweis, J. M. Plitzko, and H. Engelhardt. 2008. Disclosure of the mycobacterial outer membrane: cryo-electron tomography and vitreous sections reveal the lipid bilayer structure. *Proc. Natl. Acad. Sci. U.S.A.* 105: 3963-3967.

47. Ernst, J. D. 1998. Macrophage receptors for Mycobacterium tuberculosis. *Infect. Immun.* 66: 1277-1281.

48. Schlesinger, L. S., C. G. Bellinger-Kawahara, N. R. Payne, and M. A. Horwitz. 1990. Phagocytosis of Mycobacterium tuberculosis is mediated by human monocyte complement receptors and complement component C3. *J. Immunol.* 144: 2771-2780.

49. Schlesinger, L. S. 1993. Macrophage phagocytosis of virulent but not attenuated strains of Mycobacterium tuberculosis is mediated by mannose receptors in addition to complement receptors. *J. Immunol.* 150: 2920-2930.

50. Schlesinger, L. S., S. R. Hull, and T. M. Kaufman. 1994. Binding of the terminal mannosyl units of lipoarabinomannan from a virulent strain of Mycobacterium tuberculosis to human macrophages. *J. Immunol.* 152: 4070-4079.

51. Hoppe, H. J., and K. B. Reid. 1994. Collectins--soluble proteins containing collagenous regions and lectin domains--and their roles in innate immunity. *Protein Sci.* 3: 1143-1158.

52. Downing, J. F., R. Pasula, J. R. Wright, H. L. Twigg 3rd, and W. J. Martin 2nd. 1995. Surfactant protein a promotes attachment of Mycobacterium tuberculosis to alveolar macrophages during infection with human immunodeficiency virus. *Proc. Natl. Acad. Sci. U.S.A.* 92: 4848-4852.

53. Lemos, M. P., J. McKinney, and K. Y. Rhee. 2011. Dispensability of surfactant proteins A and D in immune control of Mycobacterium tuberculosis infection following aerosol challenge of mice. *Infect. Immun.* 79: 1077-1085.

54. Raja, A. 2004. Immunology of tuberculosis. *Indian J. Med. Res.* 120: 213-232.

55. Chaisson, R. E., G. F. Schecter, C. P. Theuer, G. W. Rutherford, D. F. Echenberg, and P. C. Hopewell. 1987. Tuberculosis in patients with the acquired immunodeficiency syndrome. Clinical features, response to therapy, and survival. *Am. Rev. Respir. Dis.* 136: 570-574.

56. Takeuchi, O., K. Hoshino, T. Kawai, H. Sanjo, H. Takada, T. Ogawa, K. Takeda, and S. Akira. 1999. Differential roles of TLR2 and TLR4 in recognition of gram-negative and gram-positive bacterial cell wall components. *Immunity* 11: 443-451.

57. Miao, E. A., E. Andersen-Nissen, S. E. Warren, and A. Aderem. 2007. TLR5 and Ipaf: dual sensors of bacterial flagellin in the innate immune system. *Semin. Immunopathol.* 29: 275-288.

58. López, M., L. M. Sly, Y. Luu, D. Young, H. Cooper, and N. E. Reiner. 2003. The 19-kDa Mycobacterium tuberculosis protein induces macrophage apoptosis through Toll-like receptor-2. *J. Immunol.* 170: 2409-2416.

59. Ferwerda, G., S. E. Girardin, B.-J. Kullberg, L. Le Bourhis, D. J. de Jong, D. M. L. Langenberg, R. van Crevel, G. J. Adema, T. H. M. Ottenhoff, J. W. M. Van der Meer,

and M. G. Netea. 2005. NOD2 and toll-like receptors are nonredundant recognition systems of Mycobacterium tuberculosis. *PLoS Pathog.* 1: 279-285.

60. Fremond, C. M., V. Yeremeev, D. M. Nicolle, M. Jacobs, V. F. Quesniaux, and B. Ryffel. 2004. Fatal Mycobacterium tuberculosis infection despite adaptive immune response in the absence of MyD88. *J. Clin. Invest.* 114: 1790-1799.

61. Gandotra, S., S. Jang, P. J. Murray, P. Salgame, and S. Ehrt. 2007. Nucleotide-binding oligomerization domain protein 2-deficient mice control infection with Mycobacterium tuberculosis. *Infect. Immun.* 75: 5127-5134.

62. Divangahi, M., S. Mostowy, F. Coulombe, R. Kozak, L. Guillot, F. Veyrier, K. S. Kobayashi, R. A. Flavell, P. Gros, and M. A. Behr. 2008. NOD2-Deficient Mice Have Impaired Resistance to Mycobacterium tuberculosis Infection through Defective Innate and Adaptive Immunity. *J. Immunol.* 181: 7157 -7165.

63. Flynn, J. L., M. M. Goldstein, J. Chan, K. J. Triebold, K. Pfeffer, C. J. Lowenstein, R. Schreiber, T. W. Mak, and B. R. Bloom. 1995. Tumor necrosis factor-alpha is required in the protective immune response against Mycobacterium tuberculosis in mice. *Immunity* 2: 561-572.

64. Armstrong, J. A., and P. D. Hart. 1971. Response of cultured macrophages to Mycobacterium tuberculosis, with observations on fusion of lysosomes with phagosomes. *J. Exp. Med.* 134: 713-740.

65. Vergne, I., J. Chua, S. B. Singh, and V. Deretic. 2004. Cell biology of mycobacterium tuberculosis phagosome. *Annu. Rev. Cell Dev. Biol.* 20: 367-394.

66. Nguyen, L., and J. Pieters. 2005. The Trojan horse: survival tactics of pathogenic mycobacteria in macrophages. *Trends Cell Biol.* 15: 269-276.

67. Chen, M., H. Gan, and H. G. Remold. 2006. A mechanism of virulence: virulent Mycobacterium tuberculosis strain H37Rv, but not attenuated H37Ra, causes significant mitochondrial inner membrane disruption in macrophages leading to necrosis. *J. Immunol.* 176: 3707-3716.

68. Uetrecht, A. C., and J. E. Bear. 2006. Coronins: the return of the crown. *Trends Cell Biol.* 16: 421-426.

69. Ferrari, G., H. Langen, M. Naito, and J. Pieters. 1999. A coat protein on phagosomes involved in the intracellular survival of mycobacteria. *Cell* 97: 435-447.

70. Jayachandran, R., V. Sundaramurthy, B. Combaluzier, P. Mueller, H. Korf, K. Huygen, T. Miyazaki, I. Albrecht, J. Massner, and J. Pieters. 2007. Survival of mycobacteria in macrophages is mediated by coronin 1-dependent activation of calcineurin. *Cell* 130: 37-50.

71. Sturgill-Koszycki, S., U. E. Schaible, and D. G. Russell. 1996. Mycobacterium-containing phagosomes are accessible to early endosomes and reflect a transitional state in normal phagosome biogenesis. *EMBO J.* 15: 6960-6968.

72. Fratti, R. A., J. Chua, I. Vergne, and V. Deretic. 2003. Mycobacterium tuberculosis glycosylated phosphatidylinositol causes phagosome maturation arrest. *Proc. Natl. Acad. Sci. U.S.A.* 100: 5437-5442.

73. Chua, J., and V. Deretic. 2004. Mycobacterium tuberculosis reprograms waves of phosphatidylinositol 3-phosphate on phagosomal organelles. *J. Biol. Chem.* 279: 36982-36992.

74. Fratti, R. A., J. M. Backer, J. Gruenberg, S. Corvera, and V. Deretic. 2001. Role of phosphatidylinositol 3-kinase and Rab5 effectors in phagosomal biogenesis and mycobacterial phagosome maturation arrest. *J. Cell Biol.* 154: 631-644.

75. Knutson, K. L., Z. Hmama, P. Herrera-Velit, R. Rochford, and N. E. Reiner. 1998. Lipoarabinomannan of Mycobacterium tuberculosis promotes protein tyrosine dephosphorylation and inhibition of mitogen-activated protein kinase in human mononuclear phagocytes. Role of the Src homology 2 containing tyrosine phosphatase 1. *J. Biol. Chem.* 273: 645-652.

76. Chan, E. D., B. W. Winston, S. T. Uh, L. K. Remigio, and D. W. Riches. 1999. Systematic evaluation of the mitogen-activated protein kinases in the induction of iNOS by tumor necrosis factor-alpha and interferon-gamma. *Chest* 116: 91S-92S.

77. Chen, C., Y. H. Chen, and W. W. Lin. 1999. Involvement of p38 mitogen-activated protein kinase in lipopolysaccharide-induced iNOS and COX-2 expression in J774 macrophages. *Immunology* 97: 124-129.

78. Schorey, J. S., and A. M. Cooper. 2003. Macrophage signalling upon mycobacterial infection: the MAP kinases lead the way. *Cell. Microbiol.* 5: 133-142.

79. Keane, J., M. K. Balcewicz-Sablinska, H. G. Remold, G. L. Chupp, B. B. Meek, M. J. Fenton, and H. Kornfeld. 1997. Infection by Mycobacterium tuberculosis promotes human alveolar macrophage apoptosis. *Infect. Immun.* 65: 298-304.

80. Miller, B. H., R. A. Fratti, J. F. Poschet, G. S. Timmins, S. S. Master, M. Burgos, M. A. Marletta, and V. Deretic. 2004. Mycobacteria inhibit nitric oxide synthase recruitment to phagosomes during macrophage infection. *Infect. Immun.* 72: 2872-2878.

81. Darwin, K. H., S. Ehrt, J.-C. Gutierrez-Ramos, N. Weich, and C. F. Nathan. 2003. The proteasome of Mycobacterium tuberculosis is required for resistance to nitric oxide. *Science* 302: 1963-1966.

82. Pieters, J., and H. Ploegh. 2003. Microbiology. Chemical warfare and mycobacterial defense. *Science* 302: 1900-1902.

83. Walburger, A., A. Koul, G. Ferrari, L. Nguyen, C. Prescianotto-Baschong, K. Huygen, B. Klebl, C. Thompson, G. Bacher, and J. Pieters. 2004. Protein kinase G from pathogenic mycobacteria promotes survival within macrophages. *Science* 304: 1800-1804.

84. Scherr, N., P. Müller, D. Perisa, B. Combaluzier, P. Jenö, and J. Pieters. 2009. Survival of pathogenic mycobacteria in macrophages is mediated through autophosphorylation of protein kinase G. *J. Bacteriol.* 191: 4546-4554.

85. Tiwari, D., R. K. Singh, K. Goswami, S. K. Verma, B. Prakash, and V. K. Nandicoori. 2009. Key Residues in Mycobacterium tuberculosis Protein Kinase G Play a Role in Regulating Kinase Activity and Survival in the Host. *J. Biol. Chem.* 284: 27467-27479.

86. Cowley, S., M. Ko, N. Pick, R. Chow, K. J. Downing, B. G. Gordhan, J. C. Betts, V. Mizrahi, D. A. Smith, R. W. Stokes, and Y. Av‐Gay. 2004. The Mycobacterium tuberculosis protein serine/threonine kinase PknG is linked to cellular glutamate/glutamine levels and is important for growth in vivo. *Mol. Microbiol.* 52: 1691-1702.

87. Cho, S.-G., and E.-J. Choi. 2002. Apoptotic signaling pathways: caspases and stress-activated protein kinases. *J. Biochem. Mol. Biol.* 35: 24-27.

88. Strasser, A., L. O'Connor, and V. M. Dixit. 2000. Apoptosis signaling. *Annu. Rev. Biochem.* 69: 217-245.

89. Arends, M. J., and A. H. Wyllie. 1991. Apoptosis: mechanisms and roles in pathology. *Int. Rev. Exp. Pathol.* 32: 223-254.

90. Lauber, K., S. G. Blumenthal, M. Waibel, and S. Wesselborg. 2004. Clearance of apoptotic cells: getting rid of the corpses. *Mol. Cell* 14: 277-287.

91. Devarajan, E., A. A. Sahin, J. S. Chen, R. R. Krishnamurthy, N. Aggarwal, A.-M. Brun, A. Sapino, F. Zhang, D. Sharma, X.-H. Yang, A. D. Tora, and K. Mehta. 2002. Down-regulation of caspase 3 in breast cancer: a possible mechanism for chemoresistance. *Oncogene* 21: 8843-8851.

92. Soung, Y. H., J. W. Lee, S. Y. Kim, J. Jang, Y. G. Park, W. S. Park, S. W. Nam, J. Y. Lee, N. J. Yoo, and S. H. Lee. 2005. CASPASE-8 Gene Is Inactivated by Somatic Mutations in Gastric Carcinomas. *Cancer Research* 65: 815 -821.

93. Rosen, A., and L. Casciola-Rosen. 1999. Autoantigens as substrates for apoptotic proteases: implications for the pathogenesis of systemic autoimmune disease. *Cell Death Differ.* 6: 6-12.

94. Nicholson, D. W., and N. A. Thornberry. 1997. Caspases: killer proteases. *Trends in Biochem. Sci.* 22: 299-306.

95. Thornberry, N. A., and Y. Lazebnik. 1998. Caspases: Enemies Within. *Science* 281: 1312 -1316.

96. Budihardjo, I., H. Oliver, M. Lutter, X. Luo, and X. Wang. 1999. Biochemical pathways of caspase activation during apoptosis. *Annu. Rev. Cell Dev. Biol.* 15: 269-290.

97. Zhang, J.-H., Y. Zhang, and B. Herman. 2003. Caspases, apoptosis and aging. *Ageing Res. Rev.* 2: 357-366.

98. Ashkenazi, A., and V. M. Dixit. 1998. Death Receptors: Signaling and Modulation. *Science* 281: 1305 -1308.

99. Varfolomeev, E. E., M. P. Boldin, T. M. Goncharov, and D. Wallach. 1996. A potential mechanism of "cross-talk" between the p55 tumor necrosis factor receptor and Fas/APO1: proteins binding to the death domains of the two receptors also bind to each other. *J. Exp. Med.* 183: 1271 -1275.

100. MacFarlane, M., and A. C. Williams. 2004. Apoptosis and disease: a life or death decision. *EMBO Rep.* 5: 674-678.

101. Baud, V., and M. Karin. 2001. Signal transduction by tumor necrosis factor and its relatives. *Trends Cell Biol.* 11: 372-377.

102. Yang, X., R. Khosravi-Far, H. Y. Chang, and D. Baltimore. 1997. Daxx, a novel Fas-binding protein that activates JNK and apoptosis. *Cell* 89: 1067-1076.

103. Chang, H. Y., H. Nishitoh, X. Yang, H. Ichijo, and D. Baltimore. 1998. Activation of apoptosis signal-regulating kinase 1 (ASK1) by the adapter protein Daxx. *Science* 281: 1860-1863.

104. Salomoni, P., and A. F. Khelifi. 2006. Daxx: death or survival protein? *Trends Cell Biol.* 16: 97-104.

105. Oberst, A., C. Bender, and D. R. Green. 2008. Living with death: the evolution of the mitochondrial pathway of apoptosis in animals. *Cell Death Differ.* 15: 1139-1146.

106. Garrido, C., L. Galluzzi, M. Brunet, P. E. Puig, C. Didelot, and G. Kroemer. 2006. Mechanisms of cytochrome c release from mitochondria. *Cell Death Differ.* 13: 1423-1433.

107. Li, P., D. Nijhawan, I. Budihardjo, S. M. Srinivasula, M. Ahmad, E. S. Alnemri, and X. Wang. 1997. Cytochrome c and dATP-Dependent Formation of Apaf-1/Caspase-9 Complex Initiates an Apoptotic Protease Cascade. *Cell* 91: 479-489.

108. Schafer, Z. T., and S. Kornbluth. 2006. The apoptosome: physiological, developmental, and pathological modes of regulation. *Dev. Cell* 10: 549-561.

109. Morgenstern, D. E., M. A. C. Gifford, L. L. Li, C. M. Doerschuk, and M. C. Dinauer. 1997. Absence of Respiratory Burst in X-linked Chronic Granulomatous Disease Mice Leads to Abnormalities in Both Host Defense and Inflammatory Response to Aspergillus fumigatus. *J. Exp. Med.*185: 207 -218.

110. Finkel, T. 2011. Signal transduction by reactive oxygen species. *J. Cell Biol.* 194: 7-15.

111. Gonzalez, A., C.-Y. Hung, and G. T. Cole. 2011. Absence of phagocyte NADPH oxidase 2 leads to severe inflammatory response in lungs of mice infected with Coccidioides. *Microb. Pathog.* 51: 432-441.

112. Brown, D. I., and K. K. Griendling. 2009. Nox proteins in signal transduction. *Free Radic. Biol. Med.* 47: 1239-1253.

113. Aguirre, J., and J. D. Lambeth. 2010. Nox enzymes from fungus to fly to fish and what they tell us about Nox function in mammals. *Free Radic. Biol. Med.* 49: 1342-1353.

114. Martin D., B. 2010. The sites and topology of mitochondrial superoxide production. *Exp. Gerontol.* 45: 466-472.

115. Shen, H.-M., and S. Pervaiz. 2006. TNF receptor superfamily-induced cell death: redox-dependent execution. *The FASEB Journal* 20: 1589 -1598.

116. Weinrauch, Y., and A. Zychlinsky. 1999. The induction of apoptosis by bacterial pathogens. *Annu. Rev. Microbiol.* 53: 155-187.

117. Labbé, K., and M. Saleh. 2008. Cell death in the host response to infection. *Cell Death Differ.* 15: 1339-1349.

118. Wahl, C., F. Oswald, U. Simnacher, S. Weiss, R. Marre, and A. Essig. 2001. Survival of Chlamydia pneumoniae-infected Mono Mac 6 cells is dependent on NF-kappaB binding activity. *Infect. Immun.* 69: 7039-7045.

119. Byrne, G. I., and D. M. Ojcius. 2004. Chlamydia and apoptosis: life and death decisions of an intracellular pathogen. *Nat. Rev. Microbiol.* 2: 802-808.

120. Hess, S., J. Peters, G. Bartling, C. Rheinheimer, P. Hegde, M. Magid‐Slav, R. Tal‐Singer, and A. Klos. 2003. More than just innate immunity: comparative analysis of

Chlamydophila pneumoniae and Chlamydia trachomatis effects on host‐cell gene regulation. *Cell. Microbiol.* 5: 785-795.

121. Joshi, S. G., C. W. Francis, D. J. Silverman, and S. K. Sahni. 2003. Nuclear factor kappa B protects against host cell apoptosis during Rickettsia rickettsii infection by inhibiting activation of apical and effector caspases and maintaining mitochondrial integrity. *Infect. Immun.* 71: 4127-4136.

122. Wu, H., R. M. Jones, and A. S. Neish. 2012. The Salmonella effector AvrA mediates bacterial intracellular survival during infection in vivo. *Cell. Microbiol.* 14: 28-39.

123. Jones, R. M., H. Wu, C. Wentworth, L. Luo, L. Collier-Hyams, and A. S. Neish. 2008. Salmonella AvrA Coordinates Suppression of Host Immune and Apoptotic Defenses via JNK Pathway Blockade. *Cell Host Microbe* 3: 233-244.

124. Cornelis, G. R., and H. Wolf-Watz. 1997. The Yersinia Yop virulon: a bacterial system for subverting eukaryotic cells. *Mol. Microbiol.* 23: 861-867.

125. Palmer, L. E., S. Hobbie, J. E. Galán, and J. B. Bliska. 1998. YopJ of Yersinia pseudotuberculosis is required for the inhibition of macrophage TNF-alpha production and downregulation of the MAP kinases p38 and JNK. *Mol. Microbiol.* 27: 953-965.

126. Orth, K., L. E. Palmer, Z. Q. Bao, S. Stewart, A. E. Rudolph, J. B. Bliska, and J. E. Dixon. 1999. Inhibition of the mitogen-activated protein kinase kinase superfamily by a Yersinia effector. *Science* 285: 1920-1923.

127. Zhang, Y., A. T. Ting, K. B. Marcu, and J. B. Bliska. 2005. Inhibition of MAPK and NF-kappa B pathways is necessary for rapid apoptosis in macrophages infected with Yersinia. *J. Immunol.* 174: 7939-7949.

128. Zauberman, A., S. Cohen, E. Mamroud, Y. Flashner, A. Tidhar, R. Ber, E. Elhanany, A. Shafferman, and B. Velan. 2006. Interaction of Yersinia pestis with macrophages: limitations in YopJ-dependent apoptosis. *Infect. Immun.* 74: 3239-3250.

129. Locht, C., R. Antoine, and F. Jacob-Dubuisson. 2001. Bordetella pertussis, molecular pathogenesis under multiple aspects. *Curr. Opin. Microbiol.* 4: 82-89.

130. Khelef, N., A. Zychlinsky, and N. Guiso. 1993. Bordetella pertussis induces apoptosis in macrophages: role of adenylate cyclase-hemolysin. *Infect. Immun.* 61: 4064-4071.

131. Carbonetti, N. H. 2010. Pertussis toxin and adenylate cyclase toxin: key virulence factors of Bordetella pertussis and cell biology tools. *Future Microbiol.* 5: 455-469.

132. Confer, D. L., and J. W. Eaton. 1982. Phagocyte impotence caused by an invasive bacterial adenylate cyclase. *Science* 217: 948-950.

133. Dockrell, D. H., H. M. Marriott, L. R. Prince, V. C. Ridger, P. G. Ince, P. G. Hellewell, and M. K. B. Whyte. 2003. Alveolar macrophage apoptosis contributes to pneumococcal clearance in a resolving model of pulmonary infection. *J. Immunol.* 171: 5380-5388.

134. Marriott, H. M., C. D. Bingle, R. C. Read, K. E. Braley, G. Kroemer, P. G. Hellewell, R. W. Craig, M. K. B. Whyte, and D. H. Dockrell. 2005. Dynamic changes in Mcl-1 expression regulate macrophage viability or commitment to apoptosis during bacterial clearance. *J. Clin. Invest.* 115: 359-368.

135. Keane, J., H. G. Remold, and H. Kornfeld. 2000. Virulent Mycobacterium tuberculosis strains evade apoptosis of infected alveolar macrophages. *J. Immunol.* 164: 2016-2020.

136. Danelishvili, L., J. McGarvey, Y.-J. Li, and L. E. Bermudez. 2003. Mycobacterium tuberculosis infection causes different levels of apoptosis and necrosis in human macrophages and alveolar epithelial cells. *Cell. Microbiol.* 5: 649-660.

137. Oddo, M., T. Renno, A. Attinger, T. Bakker, H. R. MacDonald, and P. R. Meylan. 1998. Fas ligand-induced apoptosis of infected human macrophages reduces the viability of intracellular Mycobacterium tuberculosis. *J. Immunol.* 160: 5448-5454.

138. Schaible, U. E., F. Winau, P. A. Sieling, K. Fischer, H. L. Collins, K. Hagens, R. L. Modlin, V. Brinkmann, and S. H. E. Kaufmann. 2003. Apoptosis facilitates antigen presentation to T lymphocytes through MHC-I and CD1 in tuberculosis. *Nat. Med.* 9: 1039-1046.

139. Winau, F., S. H. E. Kaufmann, and U. E. Schaible. 2004. Apoptosis paves the detour path for CD8 T cell activation against intracellular bacteria. *Cell. Microbiol.* 6: 599-607.

140. Winau, F., S. Weber, S. Sad, J. de Diego, S. L. Hoops, B. Breiden, K. Sandhoff, V. Brinkmann, S. H. E. Kaufmann, and U. E. Schaible. 2006. Apoptotic vesicles crossprime CD8 T cells and protect against tuberculosis. *Immunity* 24: 105-117.

141. Cho, S., V. Mehra, S. Thoma-Uszynski, S. Stenger, N. Serbina, R. J. Mazzaccaro, J. L. Flynn, P. F. Barnes, S. Southwood, E. Celis, B. R. Bloom, R. L. Modlin, and A. Sette. 2000. Antimicrobial activity of MHC class I-restricted CD8+ T cells in human tuberculosis. *Proc. Natl. Acad. Sci. U.S.A.* 97: 12210-12215.

142. Balcewicz-Sablinska, M. K., J. Keane, H. Kornfeld, and H. G. Remold. 1998. Pathogenic Mycobacterium tuberculosis evades apoptosis of host macrophages by release of TNF-R2, resulting in inactivation of TNF-alpha. *J. Immunol.* 161: 2636-2641.

143. Sly, L. M., S. M. Hingley-Wilson, N. E. Reiner, and W. R. McMaster. 2003. Survival of Mycobacterium tuberculosis in host macrophages involves resistance to

apoptosis dependent upon induction of antiapoptotic Bcl-2 family member Mcl-1. *J. Immunol.* 170: 430-437.

144. Kausalya, S., R. Somogyi, A. Orlofsky, and M. B. Prystowsky. 2001. Requirement of A1-a for bacillus Calmette-Guérin-mediated protection of macrophages against nitric oxide-induced apoptosis. *J. Immunol.* 166: 4721-4727.

145. Mogga, S. J., T. Mustafa, L. Sviland, and R. Nilsen. 2002. Increased Bcl-2 and reduced Bax expression in infected macrophages in slowly progressive primary murine Mycobacterium tuberculosis infection. *Scand. J. Immunol.* 56: 383-391.

146. Hinchey, J., S. Lee, B. Y. Jeon, R. J. Basaraba, M. M. Venkataswamy, B. Chen, J. Chan, M. Braunstein, I. M. Orme, S. C. Derrick, S. L. Morris, W. R. Jacobs Jr, and S. A. Porcelli. 2007. Enhanced priming of adaptive immunity by a proapoptotic mutant of Mycobacterium tuberculosis. *J. Clin. Invest.* 117: 2279-2288.

147. Velmurugan, K., B. Chen, J. L. Miller, S. Azogue, S. Gurses, T. Hsu, M. Glickman, W. R. Jacobs, S. A. Porcelli, and V. Briken. 2007. Mycobacterium tuberculosis nuoG Is a Virulence Gene That Inhibits Apoptosis of Infected Host Cells. *PLoS Pathog.* 3: 7.

148. Jayakumar, D., W. R. Jacobs Jr, and S. Narayanan. 2008. Protein kinase E of Mycobacterium tuberculosis has a role in the nitric oxide stress response and apoptosis in a human macrophage model of infection. *Cell. Microbiol.* 10: 365-374.

149. Miller, J. L., K. Velmurugan, M. J. Cowan, and V. Briken. 2010. The type I NADH dehydrogenase of Mycobacterium tuberculosis counters phagosomal NOX2 activity to inhibit TNF-alpha-mediated host cell apoptosis. *PLoS Pathog.* 6: 4.

150. Braunstein, M., B. J. Espinosa, J. Chan, J. T. Belisle, and W. R. Jacobs Jr. 2003. SecA2 functions in the secretion of superoxide dismutase A and in the virulence of Mycobacterium tuberculosis. *Mol. Microbiol.* 48: 453-464.

151. Edwards, K. M., M. H. Cynamon, R. K. Voladri, C. C. Hager, M. S. DeStefano, K. T. Tham, D. L. Lakey, M. R. Bochan, and D. S. Kernodle. 2001. Iron-cofactored superoxide dismutase inhibits host responses to Mycobacterium tuberculosis. *Am. J. Respir. Crit. Care Med.* 164: 2213-2219.

152. Kumar, D., and S. Narayanan. 2011. pknE, a serine/threonine kinase of Mycobacterium tuberculosis modulates multiple apoptotic paradigms. *Infect. Genet. Evol.*

153. Morris, S. M. 2004. Enzymes of Arginine Metabolism. *J. Nutr.* 134: 2743S -2747S.

154. Snapper, S. B., R. E. Melton, S. Mustafa, T. Kieser, and W. R. Jacobs Jr. 1990. Isolation and characterization of efficient plasmid transformation mutants of Mycobacterium smegmatis. *Mol. Microbiol.* 4: 1911-1919.

155. Hatfull, G. F., and W. R. J. (Jr.). 2000. *Molecular genetics of mycobacteria,*. ASM Press.

156. Smith, P. K., R. I. Krohn, G. T. Hermanson, A. K. Mallia, F. H. Gartner, M. D. Provenzano, E. K. Fujimoto, N. M. Goeke, B. J. Olson, and D. C. Klenk. 1985. Measurement of protein using bicinchoninic acid. *Anal. Biochem.* 150: 76-85.

157. Molloy, A., P. Laochumroonvorapong, and G. Kaplan. 1994. Apoptosis, but not necrosis, of infected monocytes is coupled with killing of intracellular bacillus Calmette-Guérin. *J. Exp. Med.* 180: 1499-1509.

158. Vaudaux, P., and F. A. Waldvogel. 1979. Gentamicin antibacterial activity in the presence of human polymorphonuclear leukocytes. *Antimicrob. Agents Chemother.* 16: 743-749.

159. Bonina, L., G. B. Costa, and P. Mastroeni. 1998. Comparative effect of gentamicin and pefloxacin treatment on the late stages of mouse typhoid. *New Microbiol.* 21: 9-14.

160. Riendeau, C. J., and H. Kornfeld. 2003. THP-1 Cell Apoptosis in Response to Mycobacterial Infection. *Infect. Immun.* 71: 254-259.

161. Behar, S., C. Martin, M. Booty, T. Nishimura, X. Zhao, H. Gan, M. Divangahi, and H. Remold. 2011. Apoptosis is an innate defense function of macrophages against Mycobacterium tuberculosis. *Mucosal Immunol* 4: 279-287.

162. Rivero-Lezcano, O. M., C. González-Cortés, D. Reyes-Ruvalcaba, and C. Diez-Tascón. 2010. CCL20 is overexpressed in Mycobacterium tuberculosis-infected monocytes and inhibits the production of reactive oxygen species (ROS). *Clin. Exp. Immunol.* 162: 289-297.

163. Saukkonen, J. J., B. Bazydlo, M. Thomas, R. M. Strieter, J. Keane, and H. Kornfeld. 2002. Beta-chemokines are induced by Mycobacterium tuberculosis and inhibit its growth. *Infect. Immun.* 70: 1684-1693.

164. Wolf, M., I. Clark-Lewis, C. Buri, H. Langen, M. Lis, and L. Mazzucchelli. 2003. Cathepsin D Specifically Cleaves the Chemokines Macrophage Inflammatory Protein-1α, Macrophage Inflammatory Protein-1β, and SLC That Are Expressed in Human Breast Cancer. *Am. J. Pathol.* 162: 1183-1190.

165. Yuan, Z.-M., Y. Huang, T. Ishiko, S. Kharbanda, R. Weichselbaum, and D. Kufe. 1997. Regulation of DNA damage-induced apoptosis by the c-Abl tyrosine kinase. *Proc. Natl. Acad. Sci. U S A.* 94: 1437-1440.

166. Matsuzawa, A., and H. Ichijo. 2008. Redox control of cell fate by MAP kinase: physiological roles of ASK1-MAP kinase pathway in stress signaling. *Biochim. Biophys. Acta.* 1780: 1325-1336.

167. Waas, W. F., H.-H. Lo, and K. N. Dalby. 2001. The Kinetic Mechanism of the Dual Phosphorylation of the ATF2 Transcription Factor by p38 Mitogen-activated Protein (MAP) Kinase α. *J. Biol. Chem.* 276: 5676 -5684.

168. Morton, S., R. J. Davis, and P. Cohen. 2004. Signalling pathways involved in multisite phosphorylation of the transcription factor ATF-2. *FEBS Letters* 572: 177-183.

169. Luo, X., I. Budihardjo, H. Zou, C. Slaughter, and X. Wang. 1998. Bid, a Bcl2 Interacting Protein, Mediates Cytochrome c Release from Mitochondria in Response to Activation of Cell Surface Death Receptors. *Cell* 94: 481-490.

170. Lindsten, T., A. J. Ross, A. King, W.-X. Zong, J. C. Rathmell, H. A. Shiels, E. Ulrich, K. G. Waymire, P. Mahar, K. Frauwirth, Y. Chen, M. Wei, V. M. Eng, D. M. Adelman, M. C. Simon, A. Ma, J. A. Golden, G. Evan, S. J. Korsmeyer, G. R. MacGregor, and C. B. Thompson. 2000. The Combined Functions of Proapoptotic Bcl-2 Family Members Bak and Bax Are Essential for Normal Development of Multiple Tissues. *Mol. Cell* 6: 1389-1399.

171. Mure, H., K. Matsuzaki, K. T. Kitazato, Y. Mizobuchi, K. Kuwayama, T. Kageji, and S. Nagahiro. 2009. Akt2 and Akt3 play a pivotal role in malignant gliomas. *Neuro-Oncology* .

172. Hunter, S., P. Jones, A. Mitchell, R. Apweiler, T. K. Attwood, A. Bateman, T. Bernard, D. Binns, P. Bork, S. Burge, E. de Castro, P. Coggill, M. Corbett, U. Das, L. Daugherty, L. Duquenne, R. D. Finn, M. Fraser, J. Gough, D. Haft, N. Hulo, D. Kahn, E. Kelly, I. Letunic, D. Lonsdale, R. Lopez, M. Madera, J. Maslen, C. McAnulla, J. McDowall, C. McMenamin, H. Mi, P. Mutowo-Muellenet, N. Mulder, D. Natale, C. Orengo, S. Pesseat, M. Punta, A. F. Quinn, C. Rivoire, A. Sangrador-Vegas, J. D. Selengut, C. J. A. Sigrist, M. Scheremetjew, J. Tate, M. Thimmajanarthanan, P. D. Thomas, C. H. Wu, C. Yeats, and S.-Y. Yong. 2012. InterPro in 2011: new developments in the family and domain prediction database. *Nucleic Acids Res.* 40: D306-D312.

173. Yu, Z., S. E. Reichheld, A. Savchenko, J. Parkinson, and A. R. Davidson. 2010. A comprehensive analysis of structural and sequence conservation in the TetR family transcriptional regulators. *J. Mol. Biol.* 400: 847-864.

174. Kloosterman, T. G., M. M. van der Kooi-Pol, J. J. E. Bijlsma, and O. P. Kuipers. 2007. The novel transcriptional regulator SczA mediates protection against Zn2+ stress by activation of the Zn2+-resistance gene czcD in Streptococcus pneumoniae. *Mol. Microbiol.* 65: 1049-1063.

175. Park, H., Y. T. Ro, and Y. M. Kim. 2011. MdoR is a novel positive transcriptional regulator for the oxidation of methanol in Mycobacterium sp. strain JC1. *J. Bacteriol.* 193: 6288-6294.

176. Krogh, A., B. Larsson, G. von Heijne, and E. L. Sonnhammer. 2001. Predicting transmembrane protein topology with a hidden Markov model: application to complete genomes. *J. Mol. Biol.* 305: 567-580.

177. Kelly, D. M., A. M. C. ten Bokum, S. M. O'Leary, M. P. O'Sullivan, and J. Keane. 2008. Bystander macrophage apoptosis after Mycobacterium tuberculosis H37Ra infection. *Infect. Immun.* 76: 351-360.

178. Hartman, M. L., and H. Kornfeld. 2011. Interactions between Naïve and Infected Macrophages Reduce Mycobacterium tuberculosis Viability. *PLoS ONE* 6: e27972.

179. Thorburn, A. 2004. Death receptor-induced cell killing. *Cell. Signal.* 16: 139-144.

180. Zhen, L., A. A. King, Y. Xiao, S. J. Chanock, S. H. Orkin, and M. C. Dinauer. 1993. Gene targeting of X chromosome-linked chronic granulomatous disease locus in a human myeloid leukemia cell line and rescue by expression of recombinant gp91phox. *Proc. Natl. Acad. Sci. U.S.A.* 90: 9832-9836.

181. Pym, A. S., P. Domenech, N. Honoré, J. Song, V. Deretic, and S. T. Cole. 2001. Regulation of catalase–peroxidase (KatG) expression, isoniazid sensitivity and virulence by furA of Mycobacterium tuberculosis. *Mol. Microbiol.* 40: 879-889.

182. Münch, R., K. Hiller, A. Grote, M. Scheer, J. Klein, M. Schobert, and D. Jahn. 2005. Virtual Footprint and PRODORIC: an integrative framework for regulon prediction in prokaryotes. *Bioinformatics* 21: 4187-4189.

183. Dutta, N. K., S. Mehra, A. N. Martinez, X. Alvarez, N. A. Renner, L. A. Morici, B. Pahar, A. G. Maclean, A. A. Lackner, and D. Kaushal. 2012. The Stress-Response Factor SigH Modulates the Interaction between Mycobacterium tuberculosis and Host Phagocytes. *PLoS ONE* 7: e28958.

184. Ng, V. H., J. S. Cox, A. O. Sousa, J. D. MacMicking, and J. D. McKinney. 2004. Role of KatG catalase‐peroxidase in mycobacterial pathogenesis: countering the phagocyte oxidative burst. *Molecular Microbiology* 52: 1291-1302.

185. Pollock, J. D., D. A. Williams, M. A. Gifford, L. L. Li, X. Du, J. Fisherman, S. H. Orkin, C. M. Doerschuk, and M. C. Dinauer. 1995. Mouse model of X-linked chronic granulomatous disease, an inherited defect in phagocyte superoxide production. *Nat. Genet.* 9: 202-209.

186. Ortiz de Orué Lucana, D., I. Wedderhoff, and M. R. Groves. 2012. ROS-Mediated Signalling in Bacteria: Zinc-Containing Cys-X-X-Cys Redox Centres and Iron-Based Oxidative Stress. *J. Signal Transduct.* 2012: 605905.

187. Duarte, V., and J.-M. Latour. 2009. PerR vs OhrR: selective peroxide sensing in Bacillus subtilis. *Mol. BioSyst.* 6: 316-323.

188. Wu, D., and A. I. Cederbaum. 2003. Alcohol, oxidative stress, and free radical damage. *Alcohol. Res. Health.* 27: 277-284.

189. Suto, D., Y. Ikeda, J. Fujii, and Y. Ohba. 2006. Structural Analysis of Amino Acids, Oxidized by Reactive Oxygen Species and an Antibody against N-Formylkynurenine. *J. Clin. Biochem. Nutr.* 38: 107-111.

190. Via, L. E., R. Curcic, M. H. Mudd, S. Dhandayuthapani, R. J. Ulmer, and V. Deretic. 1996. Elements of signal transduction in Mycobacterium tuberculosis: in vitro phosphorylation and in vivo expression of the response regulator MtrA. *J. Bacteriol.* 178: 3314-3321.

191. Supply, P., J. Magdalena, S. Himpens, and C. Locht. 1997. Identification of novel intergenic repetitive units in a mycobacterial two‐component system operon. *Mol. Microbiol.* 26: 991-1003.

192. Haydel, S. E., N. E. Dunlap, and W. H. Benjamin Jr. 1999. In vitroevidence of two-component system phosphorylation between theMycobacterium tuberculosisTrcR/TrcS proteins. *Microb. Pathog.* 26: 195-206.

193. Pérez, E., S. Samper, Y. Bordas, C. Guilhot, B. Gicquel, and C. Martín. 2001. An essential role for phoP in Mycobacterium tuberculosis virulence. *Mol. Microbiol.* 41: 179-187.

194. Zahrt, T. C., and V. Deretic. 2001. Mycobacterium tuberculosis signal transduction system required for persistent infections. *Proc. Natl. Acad. Sci. U.S.A.* 98: 12706-12711.

195. Ewann, F., M. Jackson, K. Pethe, A. Cooper, N. Mielcarek, D. Ensergueix, B. Gicquel, C. Locht, and P. Supply. 2002. Transient Requirement of the PrrA-PrrB Two-Component System for Early Intracellular Multiplication of Mycobacterium tuberculosis. *Infect. Immun.* 70: 2256-2263.

196. Albright, L. M., E. Huala, and F. M. Ausubel. 1989. Prokaryotic Signal Transduction Mediated by Sensor and Regulator Protein Pairs. *Annu. Rev. of Genet.* 23: 311-336.

197. Parkinson, J. S., and E. C. Kofoid. 1992. Communication modules in bacterial signaling proteins. *Annu. Rev. Genet.* 26: 71-112.
198. Ulrich, L. E., E. V. Koonin, and I. B. Zhulin. 2005. One-component systems dominate signal transduction in prokaryotes. *Trends Microbiol.* 13: 52-56.

199. Alber, T. 2009. Signaling mechanisms of the Mycobacterium tuberculosis receptor Ser/Thr protein kinases. *Curr. Opin. Struct. Biol.* 19: 650-657.

200. Padilla-Carlin, D. J., D. N. McMurray, and A. J. Hickey. 2008. The Guinea Pig as a Model of Infectious Diseases. *Comp. Med.* 58: 324-340.

201. Young, D. 2009. Animal models of tuberculosis. *Eur. J. Immunol.* 39: 2011-2014.

202. Blomgran, R., L. Desvignes, V. Briken, and J. D. Ernst. 2012. Mycobacterium tuberculosis Inhibits Neutrophil Apoptosis, Leading to Delayed Activation of Naive CD4 T cells. *Cell Host Microbe* 11: 81-90.